

SYNTHESIS AND REACTIVITY OF SIX-MEMBERED
N-HETEROCYCLIC CHALCOGENONES

by

Jerrod J. Flanagan

A thesis submitted to the faculty of
The University of North Carolina at Charlotte
in partial fulfillment of the requirements
for the degree of Master of Science in
Chemistry

Charlotte

2017

Approved by:

Dr. Daniel Rabinovich

Dr. Thomas A. Schmedake

Dr. Christopher M. Bejger

Dr. Gang Chen

©2017
Jerrod J. Flanagan
ALL RIGHTS RESERVED

ABSTRACT

JERROD J. FLANAGAN. Synthesis and reactivity of six-membered N-heterocyclic chalcogenones (Under the direction of Dr. Daniel Rabinovich)

The synthesis and coordination chemistry of N-heterocyclic thione (NHT) and selone (NHSe) ligands containing a saturated pyrimidine ring and bulky aromatic substituents on the nitrogen atoms is described in this thesis. To further understand the effect that the saturated pyrimidine ring has on the Lewis basicity of the ligands, particularly relative to analogous ligands based on five-membered rings, several closed-shell (d^{10}) metal complexes have been synthesized and fully characterized. For example, mercury(II) complexes $(\text{SpymArE})\text{HgX}_2$, copper(I) compounds $(\text{SpymArE})\text{CuX}$, and gold(I) derivatives $(\text{SpymArE})\text{AuX}$ ($\text{E} = \text{S}, \text{Se}$; $\text{Ar} = 2,6\text{-xylyl}, \text{mesityl}, 2,6\text{-diisopropyl phenyl}$; $\text{X} = \text{Cl}, \text{Br}, \text{I}$) have been isolated and fully characterized. In addition hypervalent iodine adducts $(\text{SpymArE})\text{I}_2$ have also been isolated and structurally characterized. The molecular structures of most of these species have been determined by X-ray crystallography and are compared with those of their corresponding five-membered ring analogues and other related compounds.

ACKNOWLEDGMENTS

I would like to thank everyone who has had a hand in guiding me during my time at the University of North Carolina at Charlotte. I've had the privilege of working under amazing advisors during my college career as a student. The supervision of Dr. Daniel Rabinovich and it would be an understatement to say that he has been a great research advisor and mentor throughout my time working with him. From short and simple to never ending discussions on research, I truly have learned and grown a lot as a chemist. Thank you for your persistence and the quality of work that you always expected from me and that you were always honest with me if I wasn't meeting your expectations. Dr. Carmen Gauthier, I am so lucky to have had you as my undergrad advisor and mentor. I would not have majored in chemistry if you had not been so welcoming during my time as an undergraduate at Florida Southern College and I certainly would not have attained my Masters of Science in Chemistry without you. I couldn't have asked for more from my mentors and advisors.

I would also like to thank the members of the DR group for their support throughout the last couple of years for making it a pleasure to work every day in the lab. Marissa, your commitment to your responsibilities at home and in the lab is admirable and your work ethic everyday has been inspiring. Lizeth, thank you for always being so welcoming when I joined the research group, you were always there when I had a question or needed a snack. Sarah, I am so glad that you joined the DR group and it has been a pleasure to work with you. Thanks to Alex, Ami, Kara, Grace, Hussain, Mustafa, and Kirk for making the lab such an enjoyable place to spend my time. I would be remiss

to not thank both Liliana Moranchel and Brian Park for the exceptional work they contributed to my research during the summer of 2016. You both are much smarter and driven than I was as a high school student and I'm sure you both will reach your career goals. Jessi, you have been my best friend since we met last year and I would not have enjoyed my time at UNC Charlotte nearly as much without you here.

I would like to extend my gratitude to my thesis committee members, Dr. Schmedake, Dr. Bejger, and Dr. Chen for your commitment and time. It is my pleasure to thank Prof. James A. Golen (University of Massachusetts Dartmouth) for his tireless work in solving every crystal structure presented in this thesis.

Additionally, I am grateful to the entire faculty and staff of the chemistry department at UNC Charlotte for making my time here so outstanding. Nancy, thank you for all your assistance with registration and pistachios whenever I needed an afternoon snack. Dr. Jew and Monica thank you for your guidance with teaching. Dr. Merkert for your instruction on the use of instrumentation and your help in resolving any problem I had with an instrument. Finally I would like to thank my family for being as supportive as possible at all times. Mom and Dad, I am blessed to have always been encouraged to challenge myself and not become complacent.

TABLE OF CONTENTS

LIST OF FIGURES	xii
LIST OF TABLES	xvi
LIST OF SCHEMES	xvii
LIST OF ABBREVIATIONS	xviii
CHAPTER 1: INTRODUCTION	1
1.1 Carbene Chemistry	1
1.2 N-Heterocyclic Carbenes	2
1.3 Expanded Ring N-Heterocyclic Carbenes	4
1.4 N-Heterocyclic Thiones (NHT) and Selones (NHSe)	4
1.5 Research Objectives	6
CHAPTER 2: RESULTS AND DISCUSSION	8
2.1 Synthesis of SpymArE	8
2.1.1 Molecular Structures of SpymArE (Ar = Xy, Mes; E = S, Se)	14
2.1.2 SpymArE vs. SIArE	16
2.2 Synthesis and Characterization of Halogen Adducts	18
2.3 Synthesis of Mercury(II) Complexes	22
2.3.1 Molecular Structures of (SpymXyS)HgX ₂	24
2.3.2 Molecular Structures of (SpymXySe)HgX ₂	27
2.3.3 Molecular Structures of (SpymMesS)HgX ₂	30
2.3.4 Molecular Structures of (SpymMesSe)HgX ₂	34
2.3.5 Molecular Structures of [Hg(SpymDippS) ₂][Hg ₂ X ₆]	37
2.3.6 Molecular Structures of [Hg(SpymDippSe) ₂][Hg ₂ X ₆]	39

2.4	Synthesis of Copper(I) Complexes.....	42
2.5	Synthesis of Gold(I) Complexes	45
2.5.1	Molecular Structure of (SpymXyS)AuX	47
2.5.2	Molecular Structure of (SpymXySe)AuBr.....	49
2.5.3	Molecular Structures of (SpymMesS)AuX	51
2.5.4	Molecular Structures of (SpymMesSe)AuX	52
2.5.5	Molecular Structures of (SpymDippS)AuX	54
2.5.6	Molecular Structures of (SpymDippSe)AuX	57
CHAPTER 3: EXPERIMENTALS		60
3.1	General Considerations	60
3.2	Synthesis of SpymArE	61
3.2.1	Synthesis of SpymXyS.....	61
3.2.2	Synthesis of SpymXySe	62
3.2.3	Synthesis of SpymMesS.....	63
3.2.4	Synthesis of SpymMesSe	64
3.2.5	Synthesis of SpymDippS.....	64
3.2.6	Synthesis of SpymDippSe	65
3.3	Synthesis of (SpymArE)I ₂	66
3.3.1	Synthesis of (SpymXyS)I ₂	66
3.3.2	Synthesis of (SpymXySe)I ₂	67
3.3.3	Synthesis of (SpymMesS)I ₂	68
3.3.4	Synthesis of (SpymMesSe)I ₂	68
3.3.5	Synthesis of (SpymDippS)I ₂	69

3.3.6	Synthesis of (SpymDippSe)I ₂	70
3.4	Synthesis of (SpymXyS)HgX ₂	71
3.4.1	Synthesis of (SpymXyS)HgCl ₂	71
3.4.2	Synthesis of (SpymXyS)HgBr ₂	71
3.4.3	Synthesis of (SpymXyS)HgI ₂	72
3.5	Synthesis of (SpymXySe)HgX ₂	73
3.5.1	Synthesis of (SpymXySe)HgCl ₂	73
3.5.2	Synthesis of (SpymXySe)HgBr ₂	73
3.5.3	Synthesis of (SpymXySe)HgI ₂	74
3.6	Synthesis of (SpymMesS)HgX ₂	75
3.6.1	Synthesis of (SpymMesS)HgCl ₂	75
3.6.2	Synthesis of [Hg(SpymMesS) ₂][Hg ₂ Br ₆].....	76
3.6.3	Synthesis of (SpymMesS)HgI ₂	76
3.7	Synthesis of (SpymMesSe)HgX ₂	77
3.7.1	Synthesis of (SpymMesSe)HgCl ₂	77
3.7.2	Synthesis of (SpymMesSe)HgBr ₂	78
3.7.3	Synthesis of (SpymMesSe)HgI ₂	79
3.8	Synthesis of [Hg(SpymDippS) ₂][Hg ₂ X ₆]	79
3.8.1	Synthesis of [Hg(SpymDippS) ₂][Hg ₂ Cl ₆]	79
3.8.2	Synthesis of [Hg(SpymDippS) ₂][Hg ₂ Br ₆].....	80
3.8.3	Synthesis of [Hg(SpymDippS) ₂][Hg ₂ I ₆]	81
3.9	Synthesis of (SpymDippSe)HgX ₂	82
3.9.1	Synthesis of [Hg(SpymDippSe) ₂][Hg ₂ Cl ₆]	82

3.9.2	Synthesis of $[\text{Hg}(\text{SpymDippSe})_2][\text{Hg}_2\text{Br}_6]$	83
3.9.3	Synthesis of $[\text{Hg}(\text{SpymDippSe})_2][\text{Hg}_2\text{I}_6]$	83
3.10	Synthesis of $(\text{SpymXyS})\text{AuX}$	84
3.10.1	Synthesis of $(\text{SpymXyS})\text{AuCl}$	84
3.10.2	Synthesis of $(\text{SpymXyS})\text{AuBr}$	85
3.11	Synthesis of $(\text{SpymXySe})\text{AuX}$	85
3.11.1	Synthesis of $(\text{SpymXySe})\text{AuCl}$	85
3.11.2	Synthesis of $(\text{SpymXySe})\text{AuBr}$	86
3.12	Synthesis of $(\text{SpymMesS})\text{AuX}$	87
3.12.1	Synthesis of $(\text{SpymMesS})\text{AuCl}$	87
3.12.2	Synthesis of $(\text{SpymMesS})\text{AuBr}$	87
3.13	Synthesis of $(\text{SpymMesSe})\text{AuX}$	88
3.13.1	Synthesis of $(\text{SpymMesSe})\text{AuCl}$	88
3.13.2	Synthesis of $(\text{SpymMesSe})\text{AuBr}$	88
3.14	Synthesis of $(\text{SpymDippS})\text{AuX}$	89
3.14.1	Synthesis of $(\text{SpymDippS})\text{AuCl}$	89
3.14.2	Synthesis of $(\text{SpymDippS})\text{AuBr}$	90
3.15	Synthesis of $(\text{SpymDippSe})\text{AuX}$	90
3.15.1	Synthesis of $(\text{SpymDippSe})\text{AuCl}$	90
3.15.2	Synthesis of $(\text{SpymDippSe})\text{AuBr}$	91
CHAPTER 4: CONCLUSIONS AND FUTURE WORK.....		92
4.1	Conclusions.....	92
4.2	Future Work.....	94

REFERENCES.....	100
APPENDIX A: CRYSTAL DATA FOR SpymXyS.....	106
APPENDIX B: CRYSTAL DATA FOR SpymXySe.....	107
APPENDIX C: CRYSTAL DATA FOR SpymMesS.....	108
APPENDIX D: CRYSTAL DATA FOR SpymMesSe.....	109
APPENDIX E: CRYSTAL DATA FOR (SpymMesS)I ₂	110
APPENDIX F: CRYSTAL DATA FOR (SpymDippS)I ₂	111
APPENDIX G: CRYSTAL DATA FOR (SpymXySe)I ₂	112
APPENDIX H: CRYSTAL DATA FOR (SpymMesSe)I ₂	113
APPENDIX I: CRYSTAL DATA FOR (SpymDippSe)I ₂	114
APPENDIX J: CRYSTAL DATA FOR [(SpymXyS) ₂ I][I ₃].....	115
APPENDIX K: CRYSTAL DATA FOR [(SpymXyS) ₂ HgCl][HgCl ₃].....	116
APPENDIX L: CRYSTAL DATA FOR (SpymXyS)HgBr ₂	117
APPENDIX M: CRYSTAL DATA FOR (SpymXyS)HgI ₂	118
APPENDIX N: CRYSTAL DATA FOR (SpymXySe)HgCl ₂	119
APPENDIX O: CRYSTAL DATA FOR (SpymXySe)HgBr ₂	120
APPENDIX P: CRYSTAL DATA FOR (SpymXySe)HgI ₂	121
APPENDIX Q: CRYSTAL DATA FOR [(SpymMesS) ₂ HgCl][HgCl ₃].....	122
APPENDIX R: CRYSTAL DATA FOR [Hg(SpymMesS) ₂][Hg ₂ Br ₆].....	123
APPENDIX S: CRYSTAL DATA FOR (SpymMesS)HgI ₂	124
APPENDIX T: CRYSTAL DATA FOR [(SpymMesSe) ₂ HgCl][HgCl ₃].....	125
APPENDIX U: CRYSTAL DATA FOR (SpymMesSe)HgBr ₂	126
APPENDIX V: CRYSTAL DATA FOR (SpymMesSe)HgI ₂	127

APPENDIX W: CRYSTAL DATA FOR $[\text{Hg}(\text{SpymDippS})_2][\text{Hg}_2\text{Cl}_6]$	128
APPENDIX X: CRYSTAL DATA FOR $[\text{Hg}(\text{SpymDippS})_2][\text{Hg}_2\text{Br}_6]$	129
APPENDIX Y: CRYSTAL DATA FOR $[\text{Hg}(\text{SpymDippS})_2][\text{Hg}_2\text{I}_6]$	130
APPENDIX Z: CRYSTAL DATA FOR $[\text{Hg}(\text{SpymDippSe})_2][\text{Hg}_2\text{Cl}_6]$	131
APPENDIX AA: CRYSTAL DATA FOR $[\text{Hg}(\text{SpymDippSe})_2][\text{Hg}_2\text{Br}_6]$	132
APPENDIX AB: CRYSTAL DATA FOR $[\text{Hg}(\text{SpymDippSe})_2][\text{Hg}_2\text{I}_6]$	133
APPENDIX AC: CRYSTAL DATA FOR $(\text{SpymXyS})\text{CuI}$	134
APPENDIX AD: CRYSTAL DATA FOR $(\text{SpymMesS})\text{CuI}$	135
APPENDIX AE: CRYSTAL DATA FOR $(\text{SpymMesSe})\text{CuI}$	136
APPENDIX AF: CRYSTAL DATA FOR $(\text{SpymXyS})\text{AuCl}$	137
APPENDIX AG: CRYSTAL DATA FOR $(\text{SpymXyS})\text{AuBr}$	138
APPENDIX AH: CRYSTAL DATA FOR $(\text{SpymXySe})\text{AuBr}$	139
APPENDIX AI: CRYSTAL DATA FOR $(\text{SpymMesS})\text{AuCl}$	140
APPENDIX AJ: CRYSTAL DATA FOR $(\text{SpymMesS})\text{AuBr}$	141
APPENDIX AK: CRYSTAL DATA FOR $(\text{SpymMesSe})\text{AuCl}$	142
APPENDIX AL: CRYSTAL DATA FOR $(\text{SpymMesSe})\text{AuBr}$	143
APPENDIX AM: CRYSTAL DATA FOR $(\text{SpymDippS})\text{AuCl}(\text{C}_3\text{H}_6\text{O})_2$	144
APPENDIX AN: CRYSTAL DATA FOR $(\text{SpymDippS})\text{AuBr}(\text{C}_3\text{H}_6\text{O})$	145
APPENDIX AO: CRYSTAL DATA FOR $(\text{SpymDippSe})\text{AuCl}$	146
APPENDIX AP: CRYSTAL DATA FOR $(\text{SpymDippSe})\text{AuBr}$	147

LIST OF FIGURES

Figure 1.1: General representation of a carbene.	1
Figure 1.2: Wanzlick equilibrium between a stable carbene and its dimer.	2
Figure 1.3: Key structural features in NHCs.....	3
Figure 1.4: Bonding in NHT and NHSe ligands.	5
Figure 1.5: Methimazole, carbimazole, and propylthiouracil (PTU).	5
Figure 1.6: SpymArE Proposed ligands.	7
Figure 2.1: ^1H NMR spectrum of SpymXyS in d_6 -acetone.....	9
Figure 2.2: $^{13}\text{C}\{^1\text{H}\}$ NMR spectrum of SpymXyS in d_6 -acetone.....	10
Figure 2.3: ^{13}C NMR spectrum of SpymXyS in d_6 -acetone.	10
Figure 2.4: ^1H NMR spectrum of SpymMesS in d_6 -acetone.	11
Figure 2.5: $^{13}\text{C}\{^1\text{H}\}$ NMR spectrum of SpymMesS in d_6 -acetone.....	11
Figure 2.6: ^{13}C NMR spectrum of SpymMesS in d_6 -acetone.....	12
Figure 2.7: ^1H NMR spectrum of SpymDippS in d_6 -acetone.....	12
Figure 2.8: $^{13}\text{C}\{^1\text{H}\}$ NMR spectrum of SpymDippS in d_6 -DMSO.	13
Figure 2.9: ^{13}C NMR spectrum of SpymDippS in d_6 -DMSO.	13
Figure 2.10: Molecular structure of SpymXyS.	14
Figure 2.11: Molecular structure of SpymXySe.	14
Figure 2.12: Molecular structure of SpymMesS.	15
Figure 2.13: Molecular structure of SpymMesSe.	15
Figure 2.14: SIMesS vs. SpymMesS.	16
Figure 2.15: Space-filling models of SIMesS and SpymMesS.....	17
Figure 2.16: ^{77}Se NMR chemical shifts of SpymArSe and SIArSe	18

Figure 2.17: Molecular structure of (SpymMesS)I ₂	19
Figure 2.18: Molecular structure of (SpymDippS)I ₂	19
Figure 2.19: Molecular structure of (SpymXySe)I ₂	20
Figure 2.20: Molecular structure of (SpymMesSe)I ₂	20
Figure 2.21: Molecular structure of (SpymDippSe)I ₂	21
Figure 2.22: Molecular Structure of [(SpymXyS) ₂ I][I ₃].....	22
Figure 2.23: Molecular structure of the cation in [(SpymXyS) ₂ HgCl][HgCl ₃].....	24
Figure 2.24: Molecular structure of [(SpymXyS) ₂ HgCl][HgCl ₃].....	25
Figure 2.25: Molecular structure of (SpymXyS)HgBr ₂	25
Figure 2.26: Molecular structure of (SpymXyS)HgI ₂	26
Figure 2.27: Molecular structure of (SpymXySe)HgCl ₂	28
Figure 2.28: Molecular structure of (SpymXySe)HgBr ₂	28
Figure 2.29: Molecular structure of (SpymXySe)HgI ₂	29
Figure 2.30: Molecular structure of [(SpymMesS) ₂ HgCl][Hg ₂ Cl ₆].....	30
Figure 2.31: Molecular structure of the cation in [Hg(SpymMesS) ₂][Hg ₂ Br ₆].....	31
Figure 2.32: Molecular structure of (SpymMesS)HgI ₂	31
Figure 2.33: Known NHT ligands of cationic two-coordinate mercury(II) complexes.	33
Figure 2.34: Molecular structure of the cation in [(SpymMesSe) ₂ HgCl][Hg ₂ Cl ₆].....	34
Figure 2.35: Molecular structure of (SpymMesSe)HgBr ₂	35
Figure 2.36: Molecular structure of (SpymMesSe)HgI ₂	35
Figure 2.37: Molecular structure of [Hg(SpymDippS) ₂][Hg ₂ Cl ₆].....	37
Figure 2.38: Molecular structure of [Hg(SpymDippS) ₂][Hg ₂ Br ₆].....	38
Figure 2.39: Molecular structure of [Hg(SpymDippS) ₂][Hg ₂ I ₆].....	38

Figure 2.40: Molecular structure of $[\text{Hg}(\text{SpymDippSe})_2][\text{Hg}_2\text{Cl}_6]$	40
Figure 2.41: Molecular structure of $[\text{Hg}(\text{SpymDippSe})_2][\text{Hg}_2\text{Br}_6]$	40
Figure 2.42: Molecular structure of $[\text{Hg}(\text{SpymDippSe})_2][\text{Hg}_2\text{I}_6]$	41
Figure 2.43: Molecular structure of $(\text{SpymXyS})\text{CuI}$	43
Figure 2.44: Molecular structure of $(\text{SpymMesS})\text{CuI}$	43
Figure 2.45: Molecular structure of $(\text{SpymMesSe})\text{CuI}$	44
Figure 2.46: Two of the $(\text{NHSe})\text{AuCl}$ complexes prepared by Nolan <i>et al.</i>	46
Figure 2.47: Proposed solution state equilibrium of $(\text{SpymArE})\text{AuX}$	46
Figure 2.48: ESI-MS of $(\text{SpymDippS})\text{AuCl}$	47
Figure 2.49: Molecular structure of $(\text{SpymXyS})\text{AuCl}$	48
Figure 2.50: Molecular structure of $(\text{SpymXyS})\text{AuBr}$	48
Figure 2.51: Molecular structure of $(\text{SpymXySe})\text{AuBr}$	50
Figure 2.52: Molecular structure of $(\text{SpymMesS})\text{AuCl}$	51
Figure 2.53: Molecular structure of $(\text{SpymMesS})\text{AuBr}$	51
Figure 2.54: Molecular structure of $(\text{SpymMesSe})\text{AuCl}$	53
Figure 2.55: Molecular structure of $(\text{SpymMesSe})\text{AuBr}$	53
Figure 2.56: Molecular structure of the cation in $[\text{Au}(\text{SpymDippS})][\text{AuCl}_2]$	55
Figure 2.57: Molecular structure of $(\text{SpymDippS})\text{AuBr}$	55
Figure 2.58: ^1H NMR spectrum of $(\text{SpymDippSe})\text{AuCl}$ in d_6 -acetone	57
Figure 2.59: Molecular structure of $(\text{SpymDippSe})\text{AuCl}$	58
Figure 2.60: Molecular structure of the cation in $[\text{Au}(\text{SpymDippSe})_2][\text{AuBr}_2]$	58
Figure 4.1: Proposed new Six-membered NHT and NHSe ligands.	94
Figure 4.2: Proposed water soluble Six-membered NHT and NHSe ligands.	95

Figure 4.3: Proposed seven-membered chalcogenone ligands compared to SpymArE. ...99

LIST OF TABLES

Table 2.1: Selected Bond Lengths (Å) and Angles (°) for SpymArE	15
Table 2.2: Selected Bond Lengths (Å) and Angles (°) for SIMesS and SpymMesS	17
Table 2.3: Selected Bond Lengths (Å) and Angles (°) for (SpymArE)I ₂	21
Table 2.4: Selected Bond Lengths (Å) and Angles (°) for (SpymXyS)HgX ₂	26
Table 2.5: Selected Bond Lengths (Å) and Angles (°) for (SpymXySe)HgX ₂	29
Table 2.6: Selected Bond Lengths (Å) and Angles (°) for (SpymMesS)HgX ₂	32
Table 2.7: Selected Bond Lengths (Å) and Angles (°) for (SpymMesSe)HgX ₂	36
Table 2.8: Selected Bonds Lengths (Å) and Angles (°) for (SpymDippS)HgX ₂	39
Table 2.9: Selected Bond Lengths (Å) and Angles (°) for (SpymDippSe)HgX ₂	41
Table 2.10: Selected Bond Lengths (Å) and Angles (°) for CuI complexes	44
Table 2.11: Selected Bond Lengths (Å) and Angles (°) for (SpymXyS)AuX	49
Table 2.12: Selected Bond Lengths (Å) and Angles (°) for (SpymXySe)AuBr	50
Table 2.13: Selected Bond Lengths (Å) and Angles (°) for (SpymMesS)AuX	52
Table 2.14: Selected Bond Lengths (Å) and Angles (°) for (SpymMesSe)AuX	54
Table 2.15: Selected Bond Lengths (Å) and Angles (°) for (SpymDippS)AuX	56
Table 2.16: Selected Bond Lengths (Å) and Angles (°) for (SpymDippSe)AuX	59

LIST OF SCHEMES

Scheme 2.1: Synthesis of SpymArE	8
Scheme 2.2: Syntheses of (SpymArE) ₂	18
Scheme 2.3: Synthesis of Mercury(II) Complexes	23
Scheme 2.4: Synthesis of Copper(I) Complexes	43
Scheme 2.5: Synthesis of Gold(I) Complexes	46
Scheme 4.1: Proposed Synthesis of SpymArE Iodonium Salts	95
Scheme 4.2: Proposed Synthesis of Bromine and Chlorine Compounds	96
Scheme 4.3: Proposed Synthesis of Copper(I) and Gold(I) Hydroxide Complexes	97
Scheme 4.4: Proposed Synthesis of Copper(I) and Gold(I) Complexes	97
Scheme 4.5: Proposed Synthesis of Dithiocarbamate and Xanthate Metal Complexes	98

LIST OF ABBREVIATIONS

CSD	Cambridge Structural Database
DCM	Dichloromethane
DMSO	Dimethyl sulfoxide
Dipp	2,6-diisopropylphenyl
EA	Elemental analysis
ESI-MS	Electrospray ionization Mass Spectrometry
FT-IR	Fourier Transform Infrared Spectroscopy
h	hour(s)
Mes	2,4,6-trimethylphenyl (mesityl)
MeCN	Acetonitrile
NHC	N-Heterocyclic Carbene
NHT	N-Heterocyclic Thione
NHSe	N-Heterocyclic Selone
NMR	Nuclear Magnetic Resonance
PTU	propylthiouracil
THF	Tetrahydrofuran
ppm	parts per million
Xy	2,6-dimethylphenyl (2,6-xylyl)

CHAPTER 1: INTRODUCTION

1.1 Carbene Chemistry

A carbene is defined as a carbon atom with two substituents that is sp^2 hybridized, leading to the presence of a lone pair on the carbon (Figure 1.1). These divalent carbons are highly reactive due to this electron deficiency, and therefore only were believed to be present as intermediates in some reactions. The two main types of carbenes are classified into Fischer type and Schrock type carbenes.¹ Fischer type carbenes are singlet carbenes that are described as electrophilic and typically stabilized by π -donor substituents (e.g. amino, alkoxy, etc.).¹ These are “L-type” ligands and are most often coordinated to late transition metals with relatively low oxidation states. Schrock type carbenes are triplet carbenes that are more nucleophilic than Fischer type carbenes and are mostly bound to electron donating groups.² These carbenes are “X₂-type” ligands and usually found with early transition metals in higher oxidation states.²

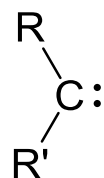


Figure 1.1: General representation of a carbene.

1.2 N-Heterocyclic Carbenes

N-heterocyclic carbenes (NHC) are diaminocarbenes that fall under the classification of Fischer type carbenes, where the carbene is situated between two nitrogens of the heterocycle. The structure of NHCs was originally proposed by Öfele *et al.*, and Wanzlick *et al.*^{3,4}

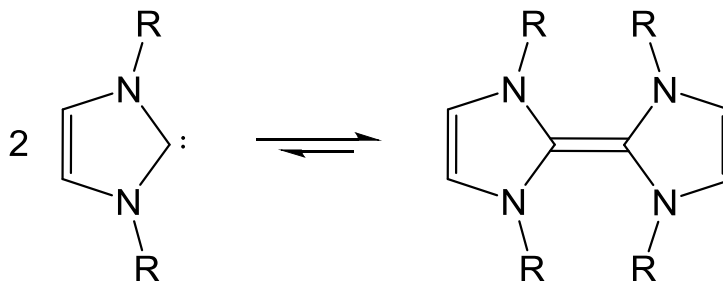


Figure 1.2: Wanzlick equilibrium between a stable carbene and its dimer.

Shown in this Figure 1.3 is the first stable NHC that was isolated by Arduengo, *et al.* in 1991 and its stability is partially dependent on its bulky adamantyl N-substituents, which prevent the dimerization with another NHC species, also known as the Wanzlick equilibrium.^{5,6} The overall stability of this class of NHCs, N-heterocycles composed of two nitrogen atoms, is due to the electronic properties of the nitrogen atoms. These nitrogen atoms are *sigma*-electron-withdrawing and *pi*-electron-donating, leading to inductively stabilizing the carbene through reducing the energy level of the HOMO *sigma*-orbital and mesomerically by the empty *p*-orbital acting as an electron sink to reduce the electron density on the carbene. Unlike acyclic carbenes, the ring structure of an NHC holds the N–C–N bond in a bent geometry, and helps stabilize the *sp*² hybridization of each atom. As a result, the carbon–nitrogen bond lengths are between a single and double bond and further stabilization is achieved through the partial

conjugation of the ring system from the backbone. Figure 1.3 also shows the versatility of NHCs, as a result of the many available variations that the ligand can undergo.

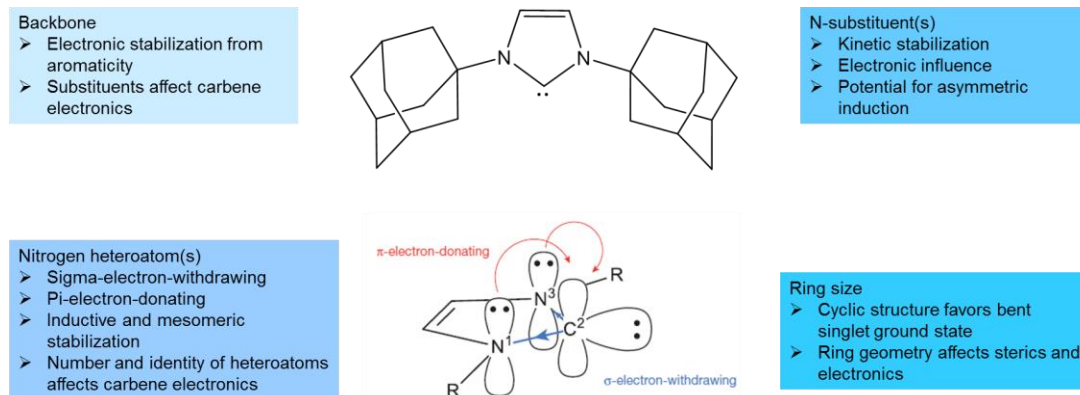


Figure 1.3: Key structural features in NHCs.

The versatility of NHCs begins with the backbone substituents, the most common being hydrogens, however, this can be substituted with electron donating functional groups or more electron withdrawing groups. There are most often two nitrogens in the N-heterocycle, but there has been work done with triazolylidene, containing three nitrogens, thus significantly altering the electron density at the carbene. The most common variations among NHCs are the identity of the N-substituents, their characteristics primarily consisting of steric demand and electronics. A majority can be found to be aromatic, mesityl and diisopropyl phenyl are common, or alkyl substituents of varying size. Arduengo's first isolable carbene was comprised of an imidazole ring and that has been the common N-heterocycle of NHCs, however saturated and expanded ring systems have become more common and thoroughly explored due to their different properties.⁷

1.3 Expanded Ring N-Heterocyclic Carbenes

The ring size of an NHC is one of the many variables that can be changed for this class of ligands. An increasing amount of work has been done recently in this field as the effects of this change in ring size have been studied more thoroughly.⁷⁻¹⁰ The increased ring size of a six- or seven-membered ring has multiple effects on the characteristics of the ligand when compared to those of a five-membered imidazole or saturated imidazole system. These differences can be attributed to the increased N–C–N bond angle which increases the electron density present at the carbene and therefore leads to increased Lewis basicity of the carbene.¹¹ The other effect of this bond angle is the increased steric demand of the N-substituents as they are brought closer to the species that is bonded to the carbene. This increase in steric demand can be shown to lead to increased performance in some NHC metal complex catalyzed reactions.⁸

1.4 N-Heterocyclic Thiones (NHT) and Selones (NHSe)

N-heterocyclic thiones (NHT) and selones (NHSe) are chalcogenone adducts of NHCs where the donor atom is sulfur (NHT) or selenium (NHSe). These compounds retain the *sigma*-donor characteristic of NHCs and are similarly nucleophilic in this regard. The major difference between an NHC and its NHT/NHSe analogues, in terms of their characteristics, is the stability of the ligand. NHT and NHSe ligands are considerably more stable as a result of the loss of the lone pair on the carbene in favor of the chalcogenone. This addition, coupled with the resonance forms shown in Figure 1.4, increase the overall stability of the ligands.¹²⁻¹⁴ The chalcogen also retains much of the sigma donation and π -accepting character of the carbene, allowing for the formation of a wide variety of coordination compounds.¹⁵⁻¹⁷ Another difference between the

coordination of NHCs and chalcogenones deals with the bonding of the donor atom, with NHT and NHSe ligands favoring a bent molecular geometry as a result of the position of the lone pairs on the chalcogen. One of the results of this bent geometry is the proximity of the coordinated species to the N-substituent and it can be hypothesized that there is an increase in the steric effect of the N-substituent when compared to an NHC.

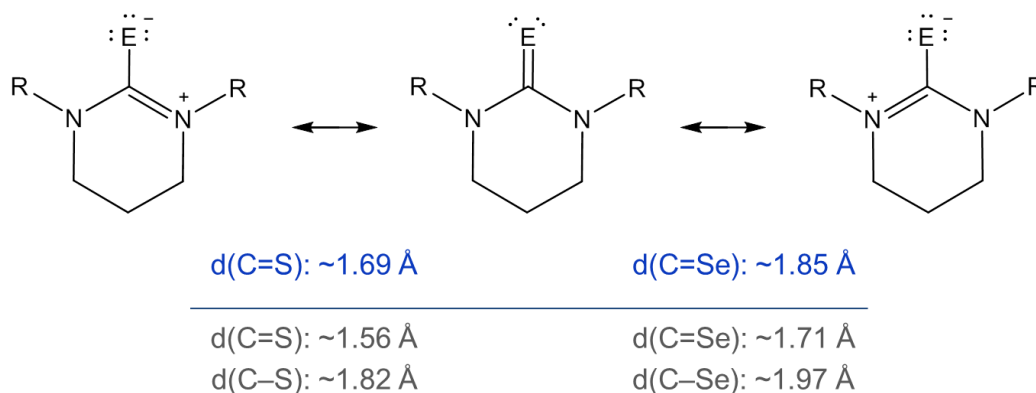


Figure 1.4: Bonding in NHT and NHSe ligands.

Similar to the interest with NHC metal complexes as biologically active compounds, NHT coordination compounds have been found in many relevant biological functions.¹⁸ Figure 1.5 shows three commercially available NHT compounds, methimazole, carbimazole, and propylthiouracil (PTU), which are used to treat hyperthyroidism.

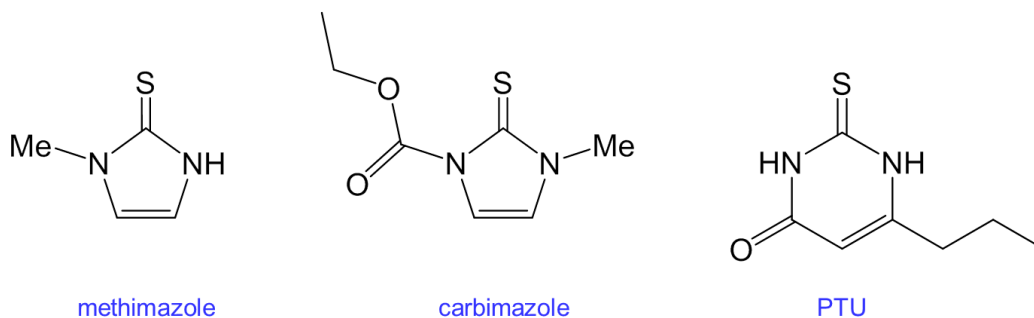


Figure 1.5: Methimazole, carbimazole, and propylthiouracil (PTU).

NHSe compounds have not been as thoroughly studied as NHT ligands, but have shown to possess biological and medicinal function.¹⁹ As a result of these properties and further potential applications, NHSe metal complexes need to be further investigated.

1.5 Research Objectives

The research objectives for this project are to synthesize new six-membered N-Heterocyclic Thione (NHT) and Selone (NHSe) ligands and to assess the reactivity of their metal complexes. There are only a handful of six-membered NHT and NHSe ligands with a saturated backbone in the literature, of which only a fraction of NHT and NHSe ligands have any coordination chemistry explored.^{11,20-30} These known six-membered NHT and NHSe ligands have been investigated as for catalytic activity,²² anticancer agents,²⁷ as well as the coordination to various transition metals to determine ligand properties.^{25,26,29,30} This allows for this project to be the tip of the spear with regard to six-membered NHT and NHSe metal complexes featuring bulky N-substituents. This project will also allow for quantifying how these ligands compare to both six-membered NHCs as well as both saturated and unsaturated five-membered NHT and NHSe ligands in terms of donor ability and steric of the ligands. The exploration into the coordination chemistry of these chalcogenone ligands will include mercury(II), copper(I), gold(I), and potentially other metals. These metals have been chosen due to their closed-shell d^{10} electron states and therefore having soft Lewis-acid character. Shown in Figure 1.6 is the overview of the NHT and NHSe ligands that will be synthesized and coordinated to various metals. The general nomenclature of the ligands is SpymArE. This nomenclature refers to six-membered N-heterocycle, which is known as a pyrimidine, and is saturated thus *Spym*. The *Ar* denotes which of the three aromatic substituents is located on the

nitrogen atoms. This project will explore the 2,6-xylyl (Xy), mesityl (Mes), and the 2,6-diisopropylphenyl (Dipp) substituents. The *E* designates the identity of the chalcogen, sulfur or selenium.

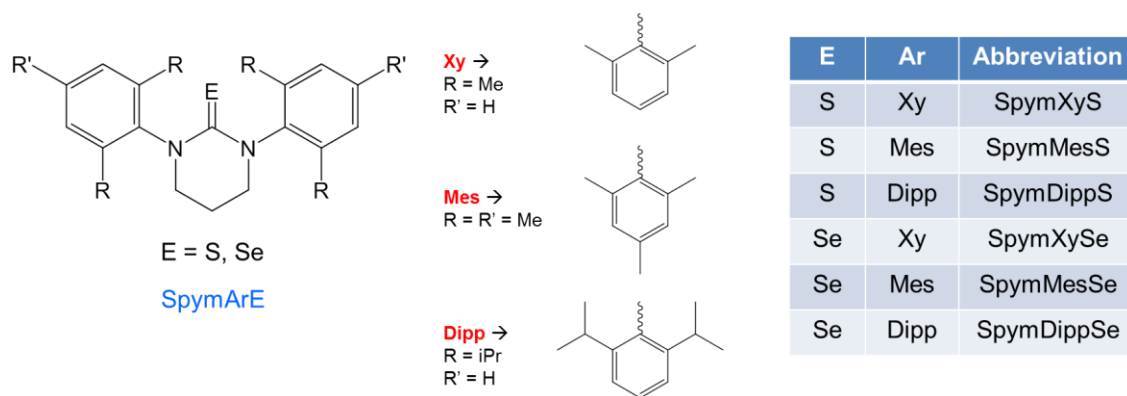


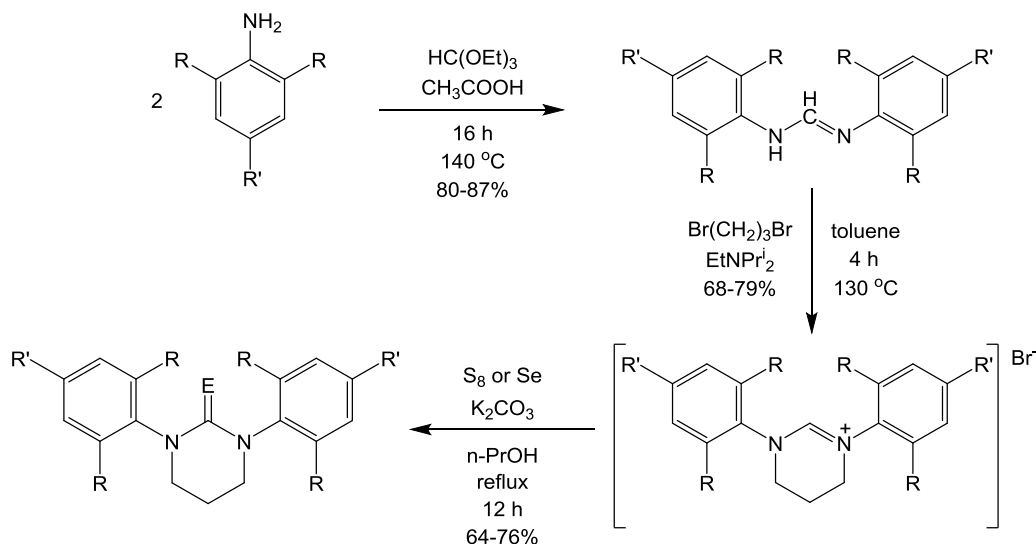
Figure 1.6: SpymArE Proposed ligands.

CHAPTER 2: RESULTS AND DISCUSSION

2.1 Synthesis of SpymArE

The six thione and selone ligands, SpymArE, have been prepared as summarized in Scheme 2.1. The required *N,N'*-diarylamidines are obtained by following the method of Grubbs *et al.*,³¹ and then converted to the corresponding pyrimidinium salts by reacting them with 1,3-dibromopropane in the presence of diisopropylethylamine as a base. The pyrimidinium salts are then reacted with the appropriate elemental chalcogen and potassium carbonate to form the desired ligands.

Scheme 2.1: Synthesis of SpymArE



N,N'-diarylamidines are synthesized through the distillation of ethanol from triethylorthoformate in the presence of the desired aniline via acetic acid catalysis. The

crude product is then purified by trituration with cold hexanes and dried under vacuum. The formamidine reaction for each aryl substituent has a yield comparable to that reported by Grubbs (80–87%). The preparation of the saturated pyrimidine ring system proceeds as the nitrogen atom is deprotonated to allow for the reaction with the 1,3-dibromopropane. This crude product is then isolated by trituration with hot toluene. The final step of the synthesis is the addition of chalcogen to the ring system following the removal of the methine proton with potassium carbonate in n-propanol. The desired product is isolated using a liquid-liquid extraction of dichloromethane and DI water. The ^1H and ^{13}C NMR spectra of each thione ligand are shown in Figures 2.1 through 2.9. The spectra for each corresponding selone are similar and data for these are located in their experimental section.

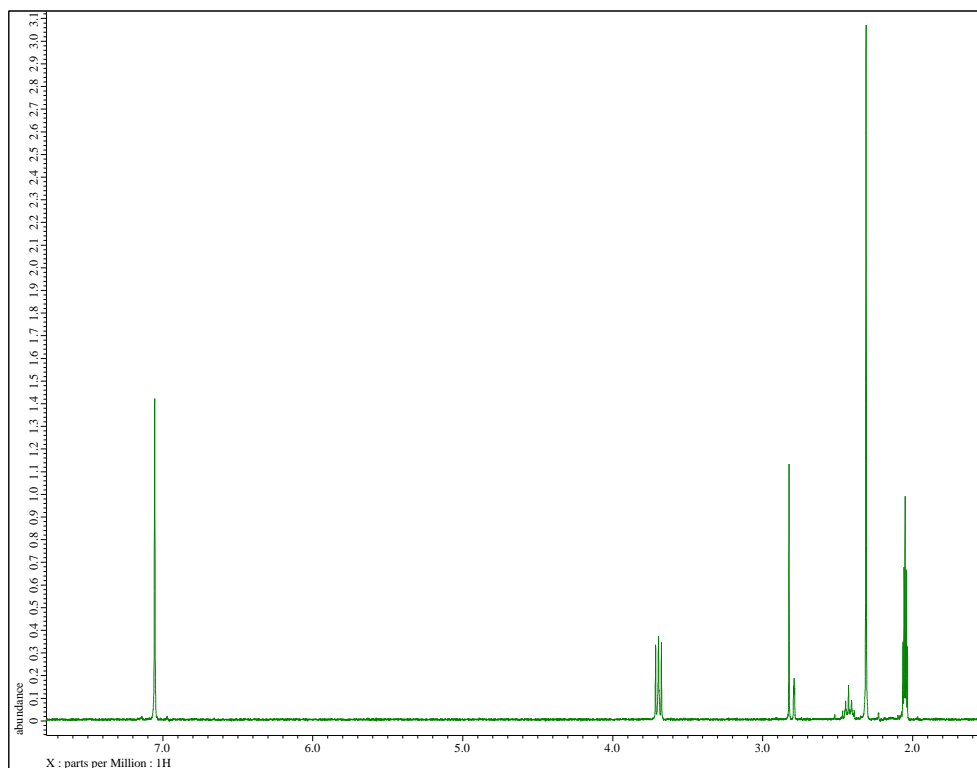


Figure 2.1: ^1H NMR spectrum of SpymXyS in d_6 -acetone.

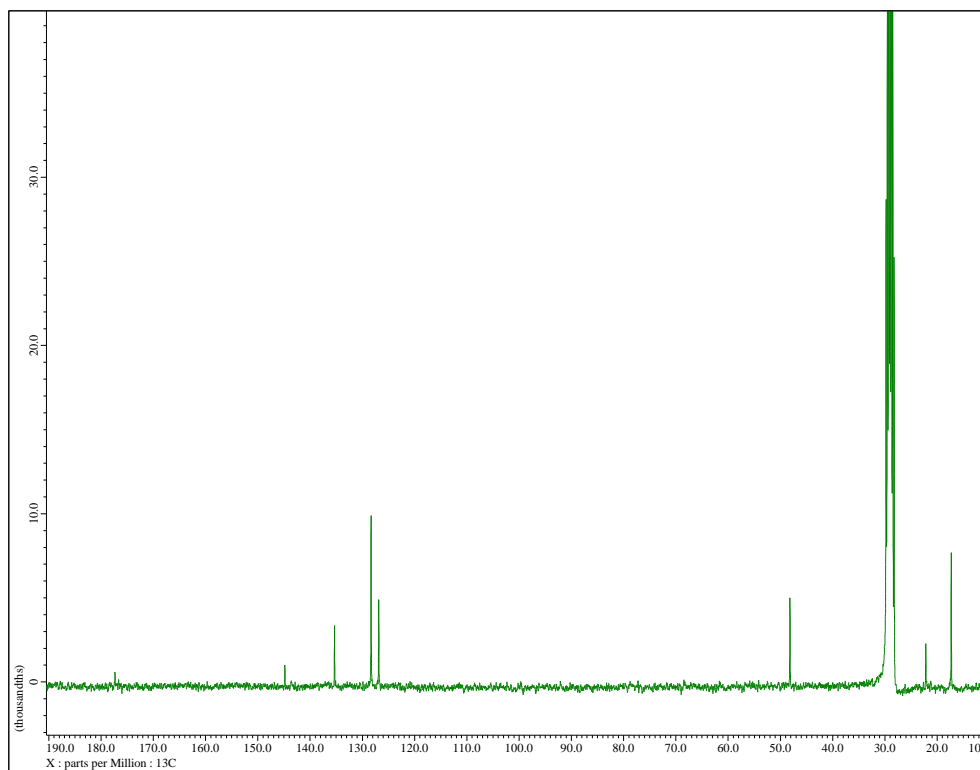


Figure 2.2: $^{13}\text{C}\{^1\text{H}\}$ NMR spectrum of SpymXyS in d_6 -acetone.

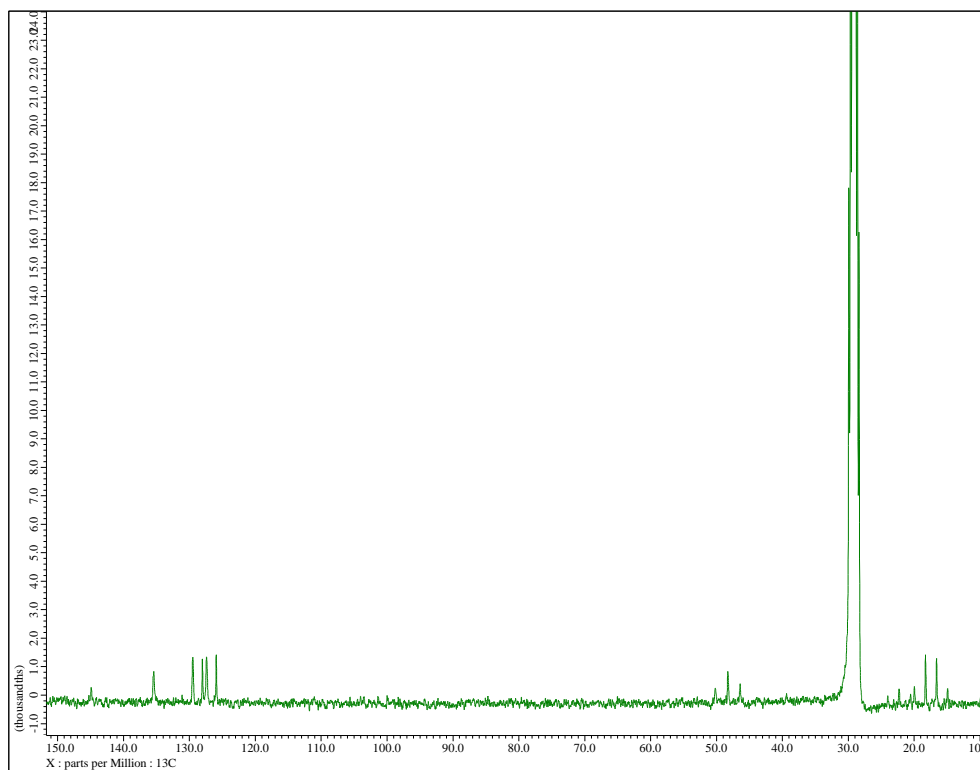


Figure 2.3: ^{13}C NMR spectrum of SpymXyS in d_6 -acetone.

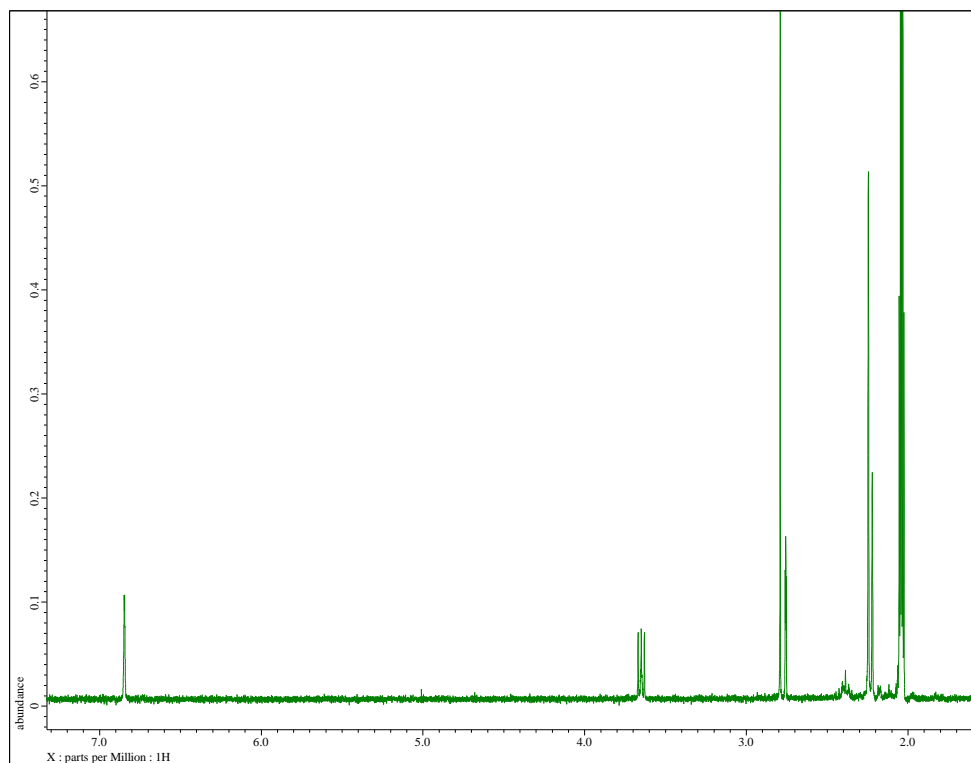


Figure 2.4: ^1H NMR spectrum of SpymMesS in d_6 -acetone.

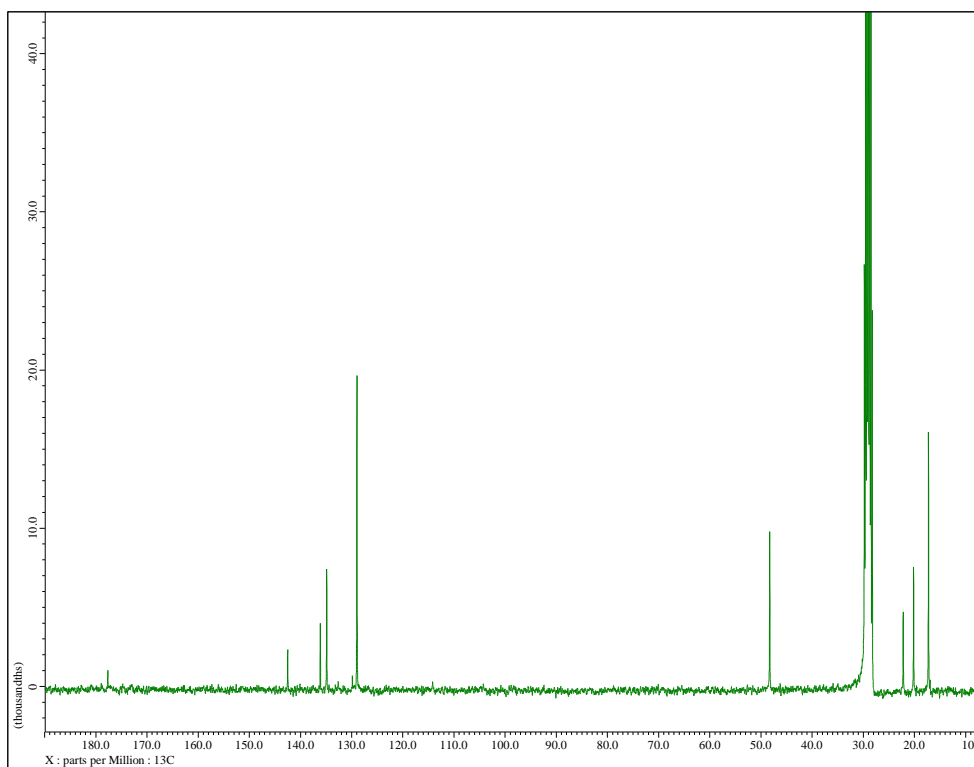


Figure 2.5: $^{13}\text{C}\{^1\text{H}\}$ NMR spectrum of SpymMesS in d_6 -acetone.

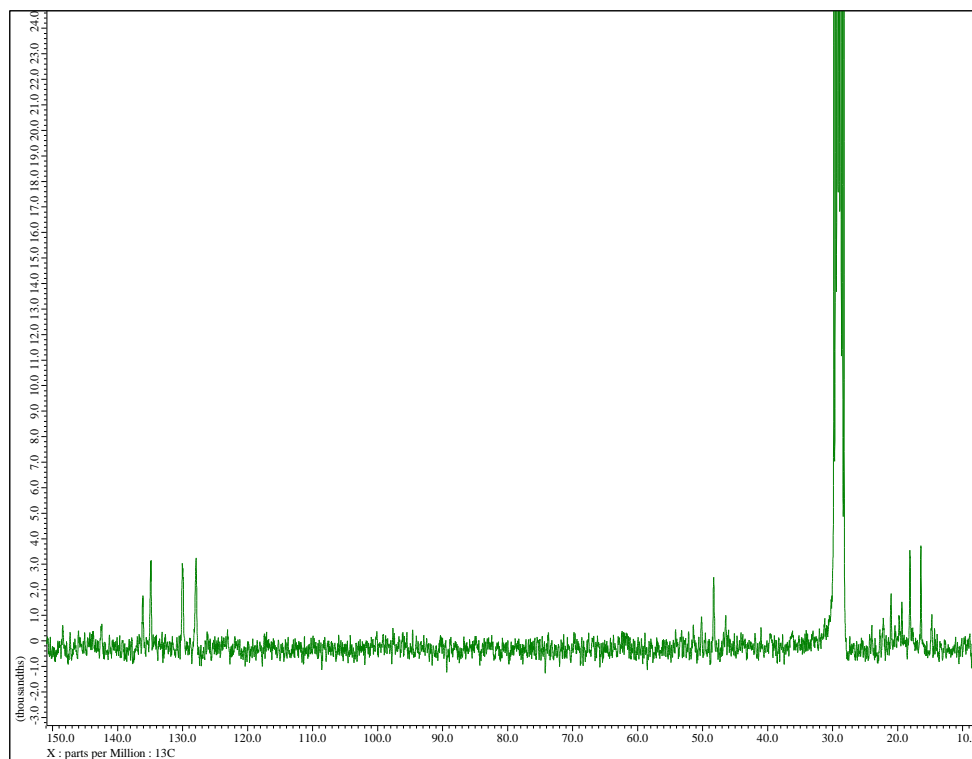


Figure 2.6: ^{13}C NMR spectrum of SpymMesS in d_6 -acetone.

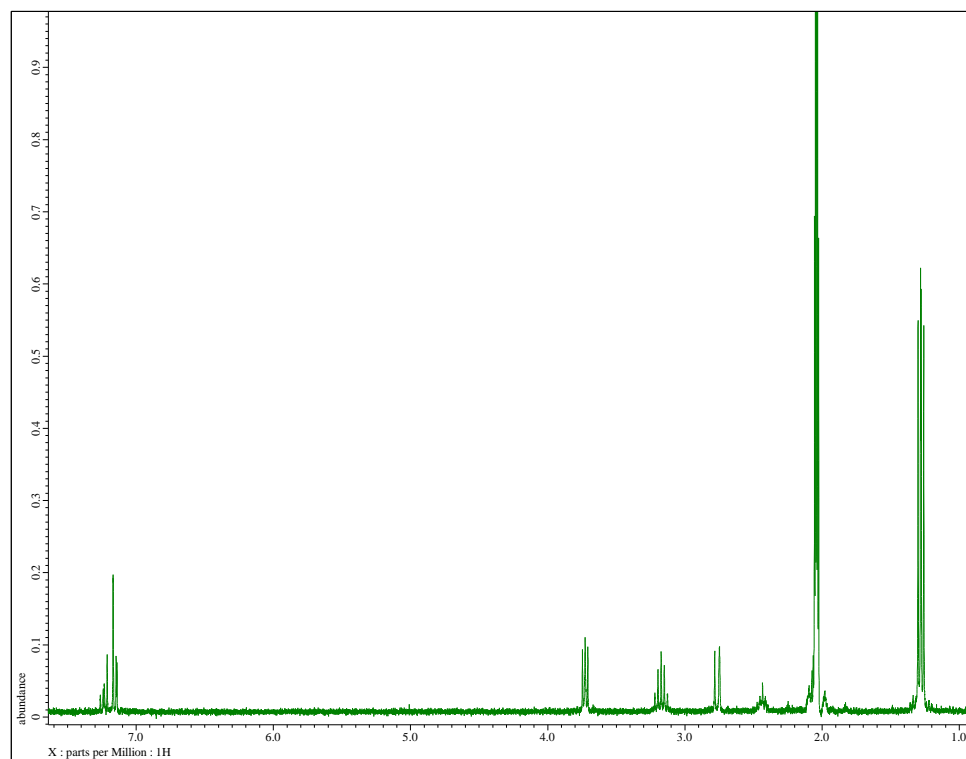


Figure 2.7: ^1H NMR spectrum of SpymDippS in d_6 -acetone.

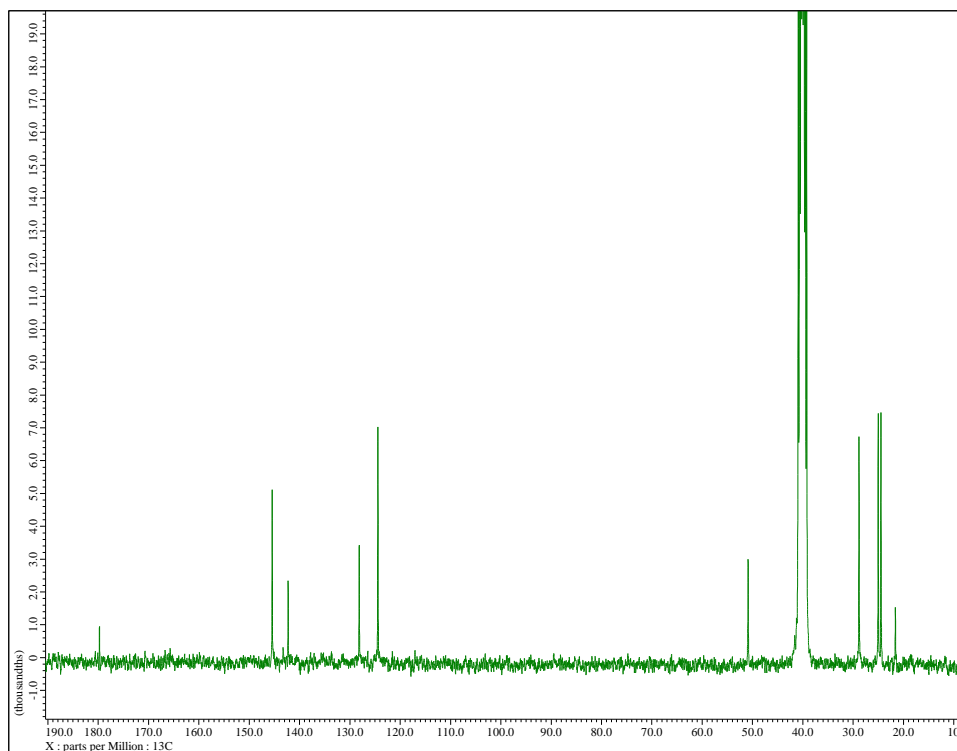


Figure 2.8: $^{13}\text{C}\{^1\text{H}\}$ NMR spectrum of SpymDippS in d_6 -DMSO.

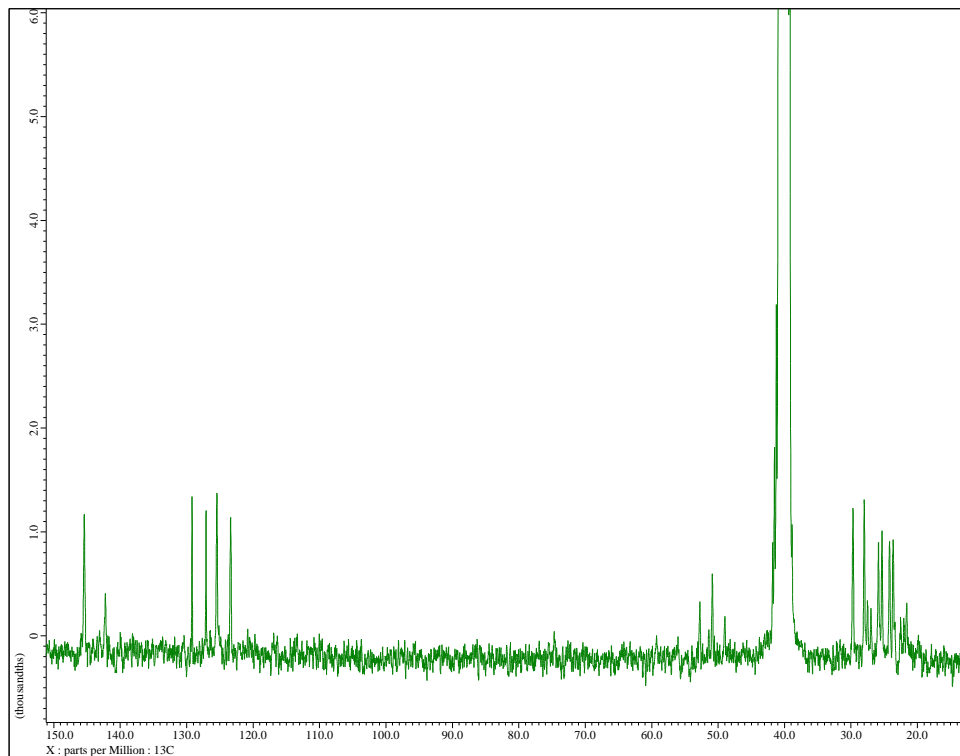


Figure 2.9: ^{13}C NMR spectrum of SpymDippS in d_6 -DMSO.

2.1.1 Molecular Structures of SpymArE (Ar = Xy, Mes; E = S, Se)

The molecular structures of SpymXyE and SpymMesE (E = S, Se) were obtained by X-ray diffraction using single crystals that were obtained by slow evaporation of solutions of the ligands dissolved in acetone.

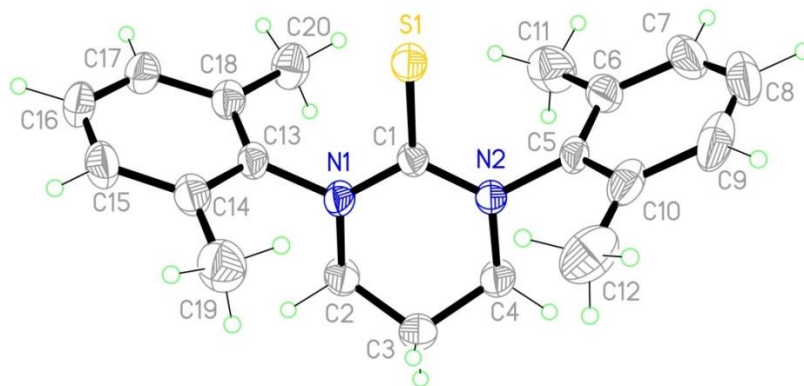


Figure 2.10: Molecular structure of SpymXyS.

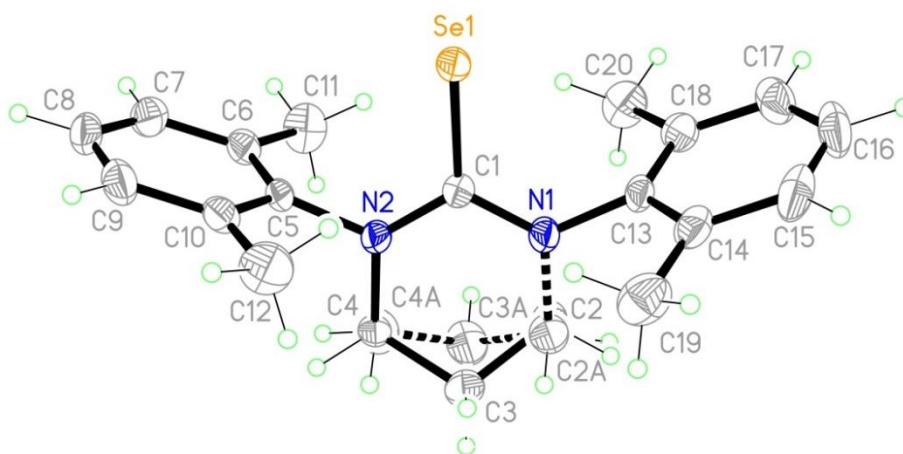


Figure 2.11: Molecular structure of SpymXySe.

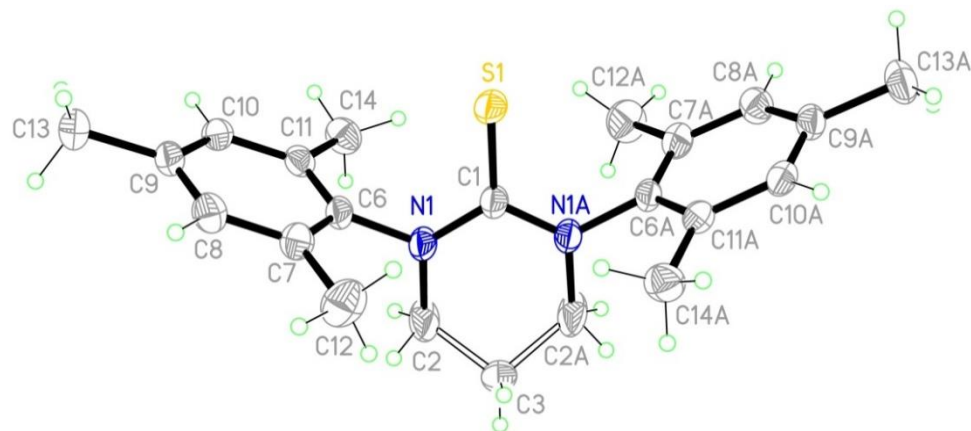


Figure 2.12: Molecular structure of SpymMesS.

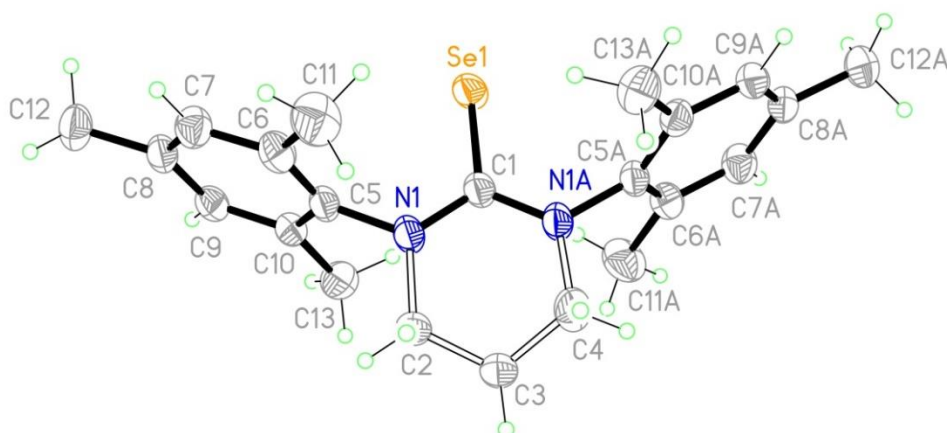


Figure 2.13: Molecular structure of SpymMesSe.

Table 2.1: Selected Bond Lengths (Å) and Angles (°) for SpymArE

	SpymXyS	SpymMesS	SpymXySe	SpymMesSe
C–E (Å)	1.68	1.68	1.86	1.85
N–C–N (°)	118	117	118	118

There is little difference between the molecular structures of the ligands, as the carbon–chalcogen bond lengths are all similar, as are the N–C–N bond angles for each ligand.

2.1.2 SpymArE vs. SIArE

The successful synthesis and characterization by single-crystal X-ray diffraction allowed for the analysis of the SpymArE ligands and the ability to compare them directly with their saturated imidazole analogues, SIArE.³² The mesityl thione ligands, SpymMesS and SIMesS, in Figure 2.14 show similar values for both ligands in terms of bond lengths, most importantly the C–S bonds are 1.67 Å and 1.69 Å for the SIMesS and SpymMesS ligands, respectively. The major difference between these ligands is, as expected, the N–C–N bond angle of the N-heterocyclic ring. The SIMesS ligand's N–C–N bond angle is 107.7°, while the SpymMesS ligand's is 117.4°. While this increased bond angle is the result of the expanded ring, more important is the effects on the sterics of the ligand. Two ways this can be quantitatively compared for these ligands is the distance from the sulfur atom to the ipso carbon of the mesityl ring, 3.17 Å for SIMesS and 2.99 Å for SpymMesS. The angle created by the planes occupied by the mesityl substituents also shows the steric difference between the two ligands. The plane for the SIMesS ligand is 145°, while the SpymMesS ligand is 131° (Figure 2.15).

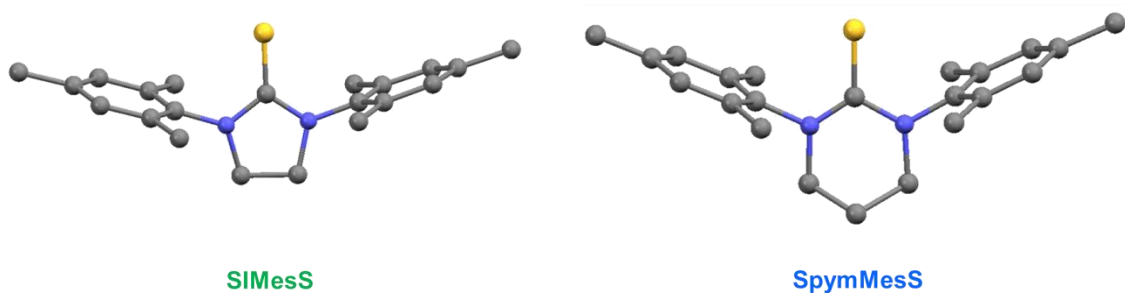


Figure 2.14: SIMesS vs. SpymMesS.

Table 2.2: Selected Bond Lengths (Å) and Angles (°) for SIMesS and SpymMesS

	SIMesS	SpymMesS
C–S (Å)	1.68	1.68
S⋯C _{ipso} (Å)	3.17	2.99
N–C–N (°)	107.7	117.4

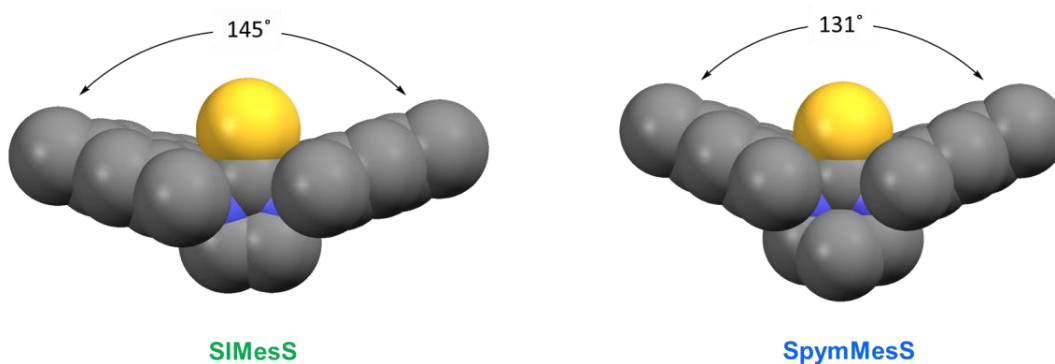


Figure 2.15: Space-filling models of SIMesS and SpymMesS.

The donor abilities of the two ligand types can also be compared by using ^{77}Se NMR spectra of each of the selone ligands for SpymArSe and SIArSe. Shown in Figure 2.16 are the ^{77}Se NMR chemical shift values obtained for each of the SpymArSe and SIArSe ligands. As shown, each of the SpymArSe ligands are downfield of its SIArSe counterparts by at least 154 ppm and at most 206 ppm. ^{77}Se NMR has been utilized by Ganter *et al.* and Nolan *et al.* to quantify the π -acidity of NHC ligands after adding a selenium atom to the NHC.^{11,33} As the signal shifts further downfield, the selenium is less shielded and the NHC is said to be more π -acidic.

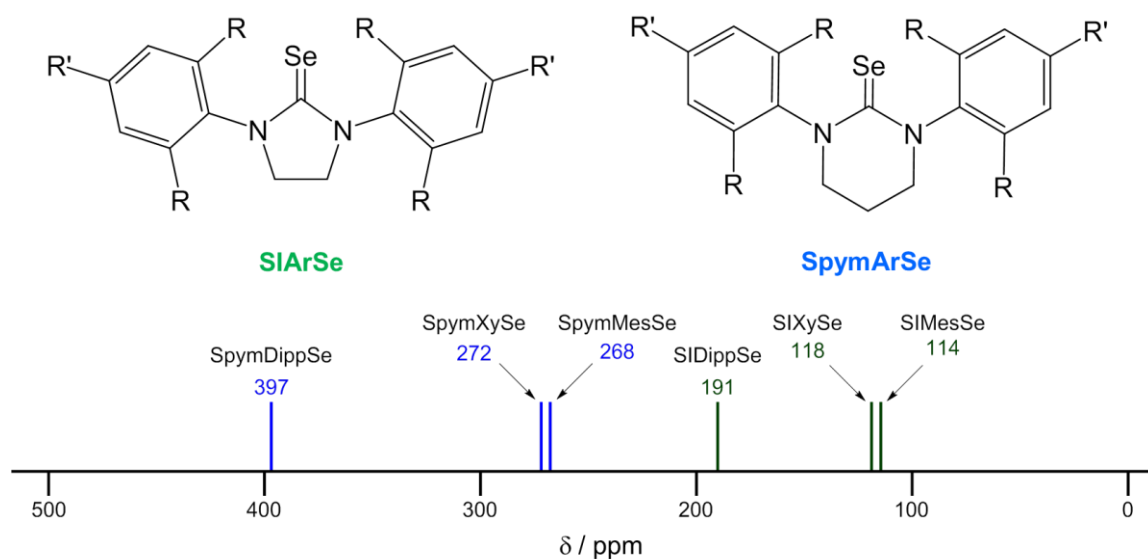
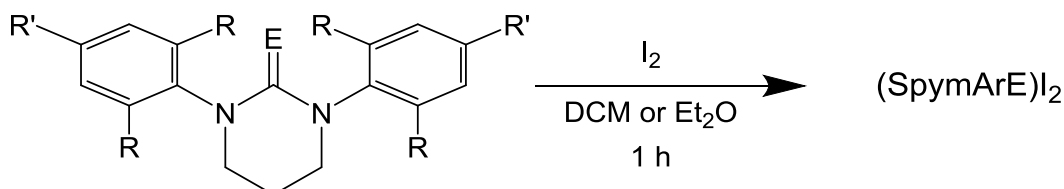


Figure 2.16: ^{77}Se NMR chemical shifts of SpymArSe and SIArSe.

2.2 Synthesis and Characterization of Halogen Adducts

While both sulfur and selenium are good donor atoms to metals, they also can form hypervalent adducts with halogens.^{34,35} Hypervalent halogen compounds have been found to have applications ranging from conductivity to medicinal agents.^{36–38} Iodine compounds, $(\text{SpymArE})\text{I}_2$ (Ar = Xy, Mes, Dipp; E = S, Se), were prepared by reacting the appropriate ligands with I_2 in a 1:1 stoichiometry for 1 hour in dichloromethane or diethyl ether, Scheme 2.2. The resulting compounds are isolated as air-stable brown solids in 80-97% yields.

Scheme 2.2: Syntheses of $(\text{SpymArE})\text{I}_2$



Crystals suitable for single crystal X-ray diffraction were obtained by slow evaporation in dichloromethane, THF, diethyl ether, or chloroform. The structures of five of the (SpymArE)₂ compounds are shown in Figures 2.17 through 2.21 with selected bond lengths and angles data shown in Table 2.3.

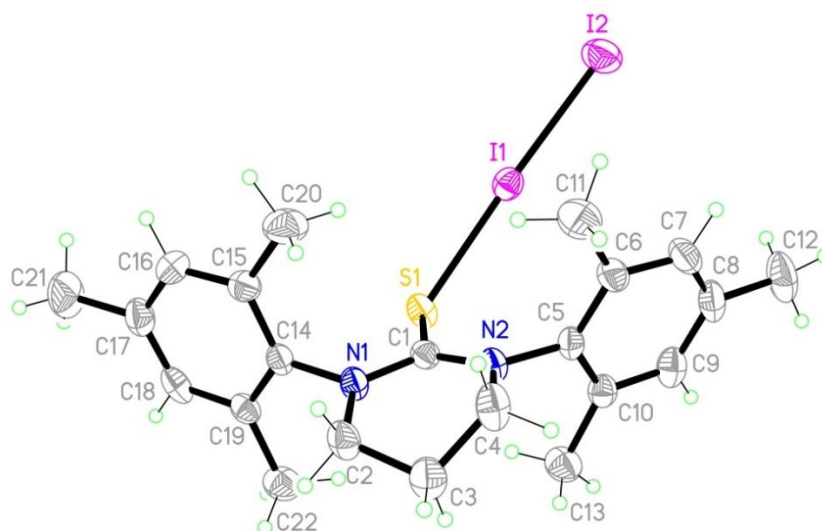


Figure 2.17: Molecular structure of (SpymMesS)₂.

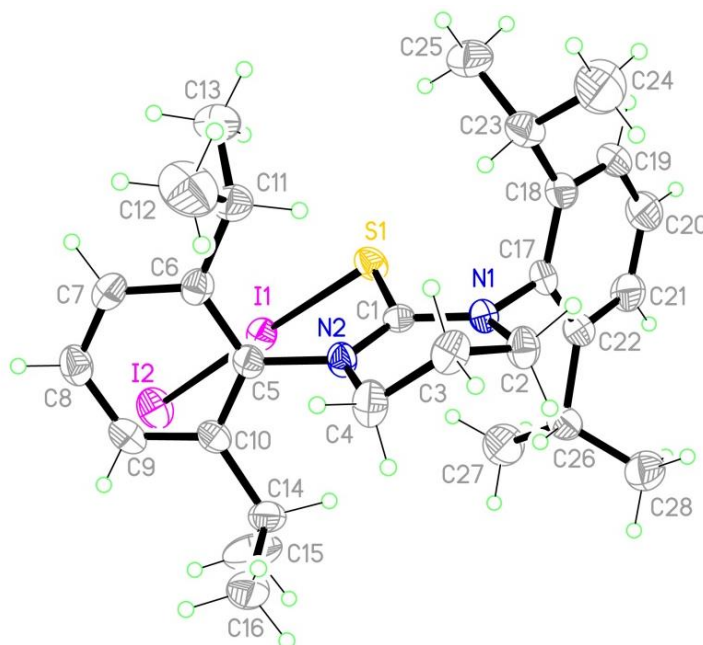


Figure 2.18: Molecular structure of (SpymDippS)₂.

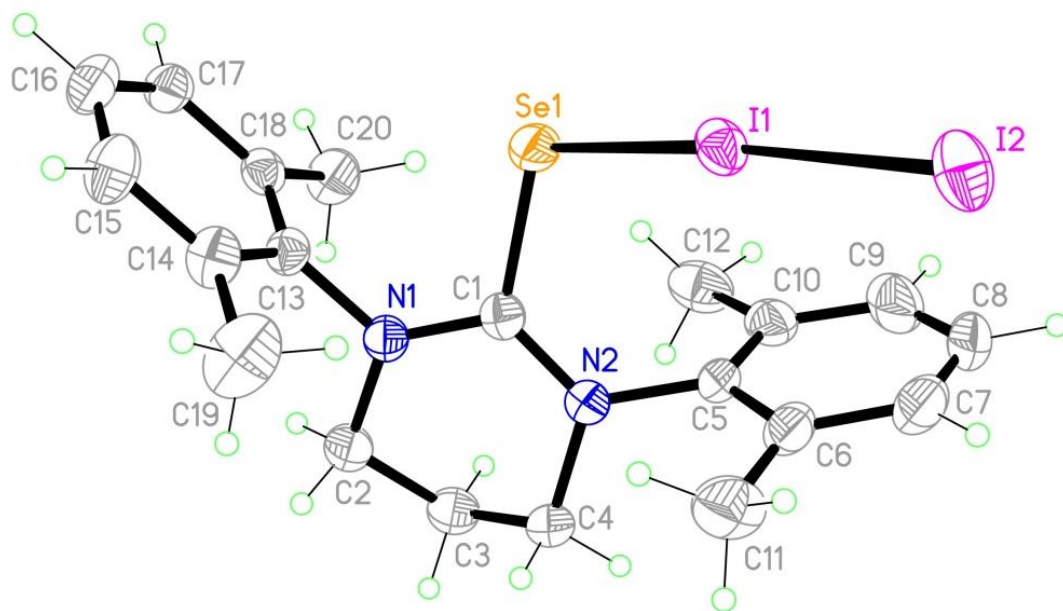


Figure 2.19: Molecular structure of (SpymXySe)I₂.

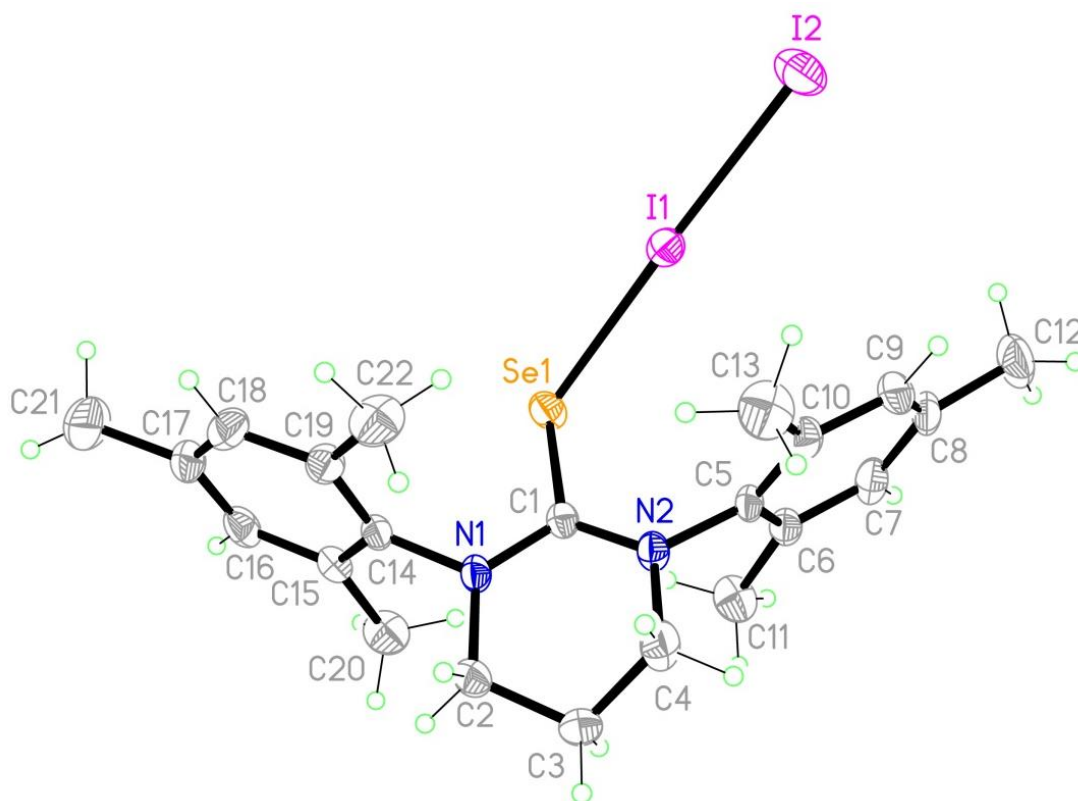


Figure 2.20: Molecular structure of (SpymMesSe)I₂.

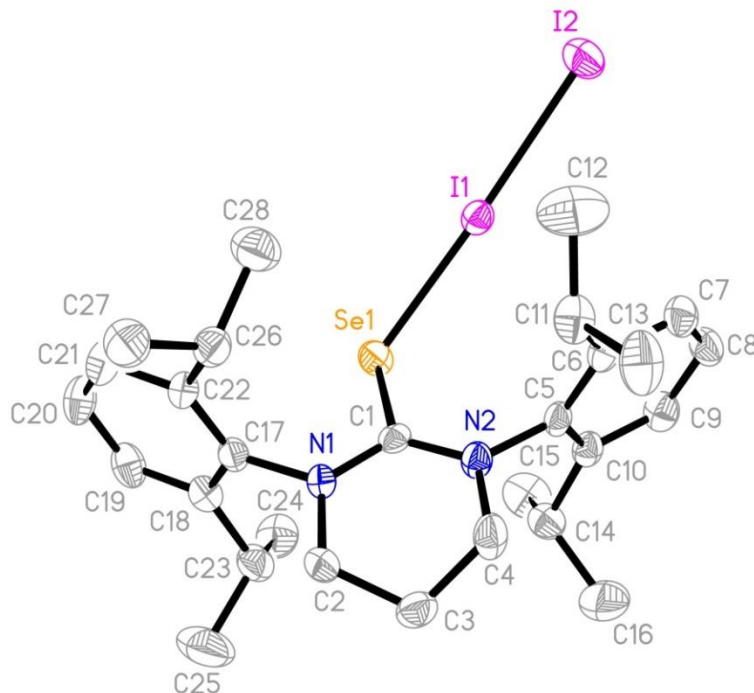


Figure 2.21: Molecular structure of (SpymDippSe) I_2 .

Table 2.3: Selected Bond Lengths (Å) and Angles (°) for (SpymArE) I_2

	SpymMesS	SpymDippS	SpymXySe	SpymMesSe	SpymDippSe
E–I	2.70	2.65	2.72	2.77	2.70
C–E	1.73	1.73	1.92	1.89	1.90
I–I	2.85	2.90	2.99	2.89	2.95
E–I–I	176.5	178.4	176.4	175.2	177.4
C–E–I	112.2	115.1	110.2	107.8	112.6

The carbon–chalcogen bond length for each of the compounds is longer than that of free ligand and is expected as a result of the increased electron density from the iodine. The bond length for the bonded iodine is also longer than that of free iodine (2.72 Å) and can be used to assess the amount of π -back bonding from the chalcogen to the iodine.

The SpymXyS ligand when reacted with an equimolar amount of elemental iodine formed an iodonium compound, Figure 2.22. This molecular structure is composed of a

single iodine atom centered between two sulfur atoms of the SpymXyS ligand. This is unlike the five iodine compounds described in Figures 2.17 to 2.21. Iodonium compounds containing an NHT bonded to the iodonium atom have been prepared previously by Corban *et al.*³⁹ This preparation by Corban *et al.*, however reacted an (NHT)₂I₂ compound with excess iodine to abstract an iodine from the compound and form the iodonium cation and the [I₃]⁻ anion. Iodonium reagents, *e.g.* Barluenga's reagent, are used in organic synthesis for the addition of iodine and a nucleophile to an olefin.^{40,41} Unlike the methods used to synthesize these iodonium compounds, [(SpymXyS)₂I]⁺ was prepared using only SpymXyS ligand and elemental iodine in equimolar amounts.

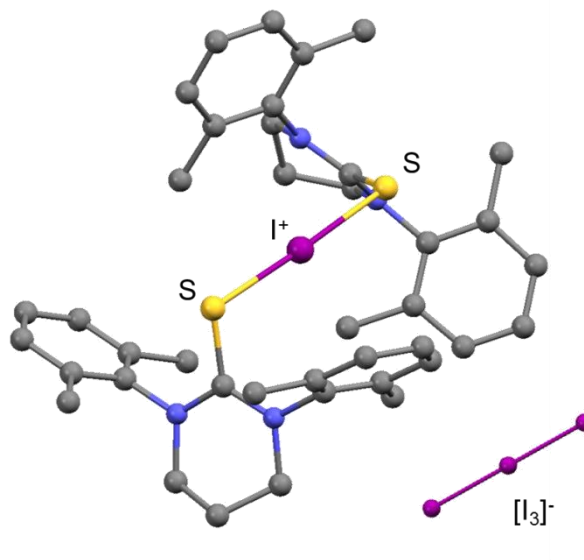


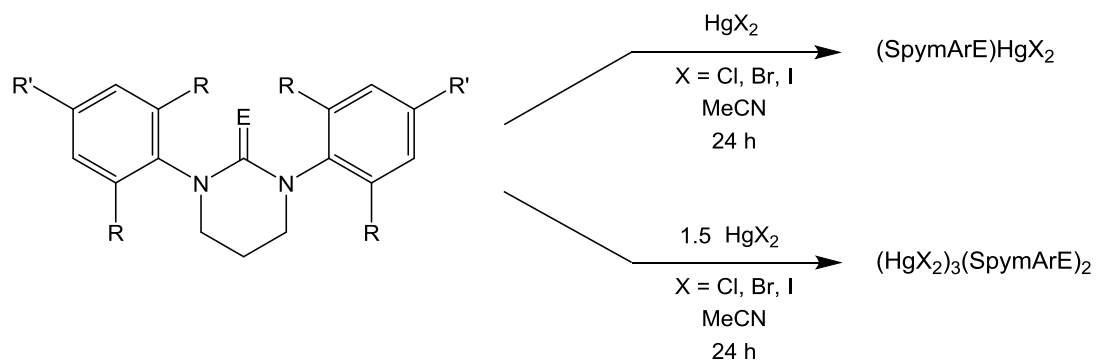
Figure 2.22: Molecular Structure of [(SpymXyS)₂I][I₃].

2.3 Synthesis of Mercury(II) Complexes

To understand these ligands and their binding characteristics, their coordination to closed-shell d¹⁰ metal ions was investigated. Mercury(II) complexes with SpymArE ligands were prepared by reacting mercury(II) halides and ligand. The cytotoxicity of

mercury has often been attributed to its affinity to sulfur, however it has been shown that mercury has even greater selenophilicity.⁴²⁻⁴⁵ These mercury(II) complexes will contain each of these chalcogens and further expand the knowledge of how sulfur and selenium donor ligands coordinate to mercury and provide a facile way to obtain crystallographic data on metal complexes of these chalcogenone ligands. These complexes were synthesized in a 1:1 ratio of metal to ligand, however this did not lead to a 1:1 ratio of metal to ligand in each of the complexes and these varying stoichiometries are shown in Scheme 2.3.

Scheme 2.3: Synthesis of Mercury(II) Complexes



The products, $(\text{SpymArE})\text{HgX}_2$ and $(\text{HgX}_2)_3(\text{SpymArE})_2$, are off-white to yellow solids with solubility significantly less than that of free ligand. Identification of a successful reaction can be seen in the ^1H NMR spectra by a shift in the aromatic methyl proton's peaks. Differentiation between the two metal:ligand stoichiometries in the NMR however is difficult, as there is no additional shift in the ^1H NMR spectra for any of the peaks. These complexes have also been characterized by elemental analysis, melting point, FT-IR analysis, ^{13}C NMR spectroscopy, and single crystal X-ray diffraction.

2.3.1 Molecular Structures of (SpymXyS)HgX₂

The molecular structures of (SpymXyS)HgX₂ (X = Cl, Br, I) were obtained using single crystal X-ray diffraction of crystals that were attained by slow evaporation of solutions of the complexes dissolved in acetonitrile (X = Cl), chloroform (X = Br), or acetone (X = I). Each of the molecular structures contains mononuclear trigonal planar complexes, which can be attributed to the bulky N-substituents; however these three complexes yield two different crystal structures. The mercury(II) chloride complex is a cation, [(SpymXyS)₂HgCl]⁺, which is countered by a polymeric [HgCl₃]⁻ anion, previously reported by Chen *et al.*²⁵ This complex is shown in Figures 2.23 and 2.24.

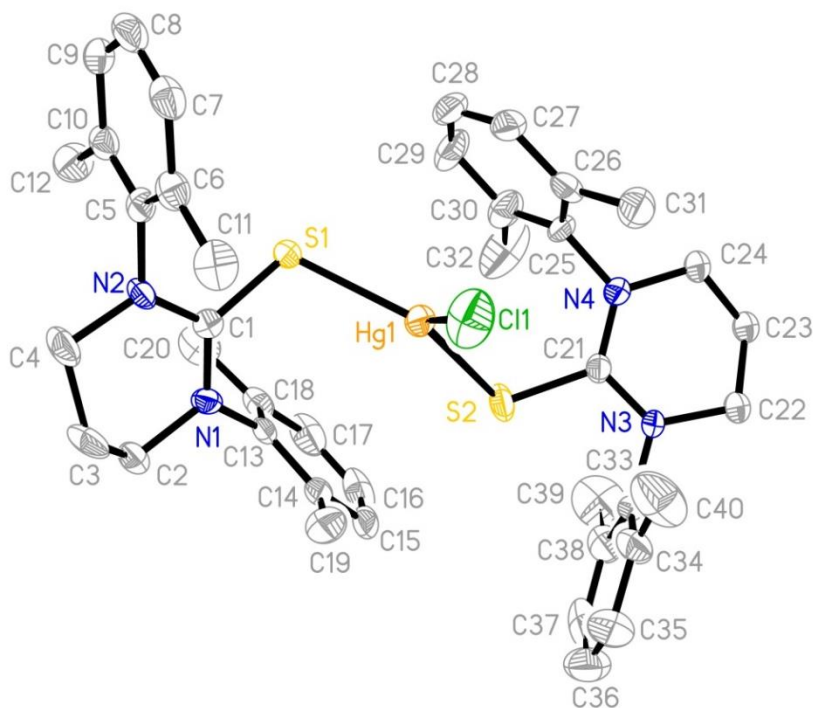


Figure 2.23: Molecular structure of the cation in [(SpymXyS)₂HgCl][HgCl₃].

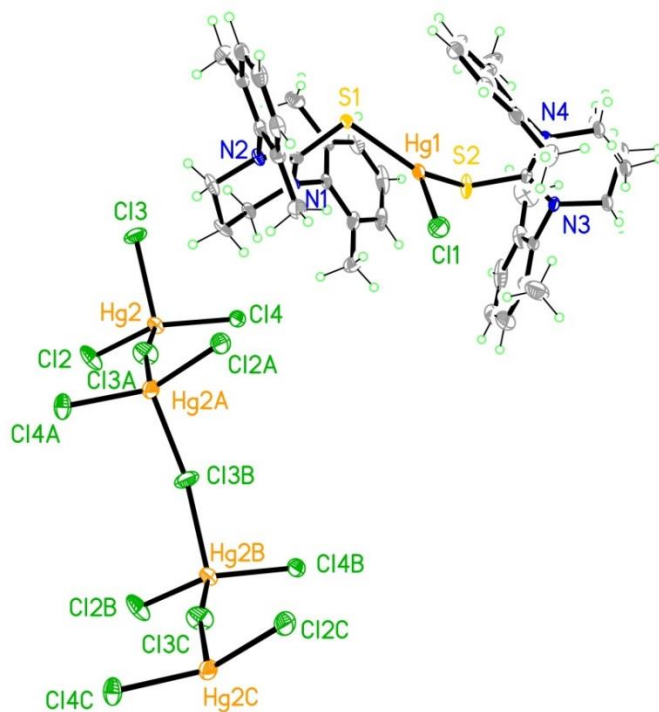


Figure 2.24: Molecular structure of $[(\text{SpymXyS})_2\text{HgCl}][\text{HgCl}_3]$.

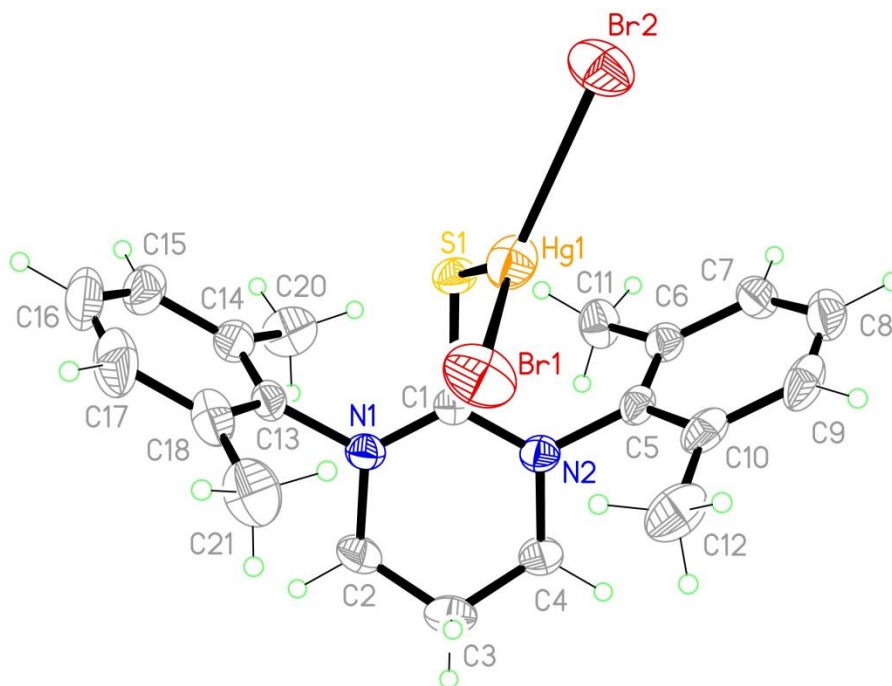


Figure 2.25: Molecular structure of $(\text{SpymXyS})\text{HgBr}_2$.

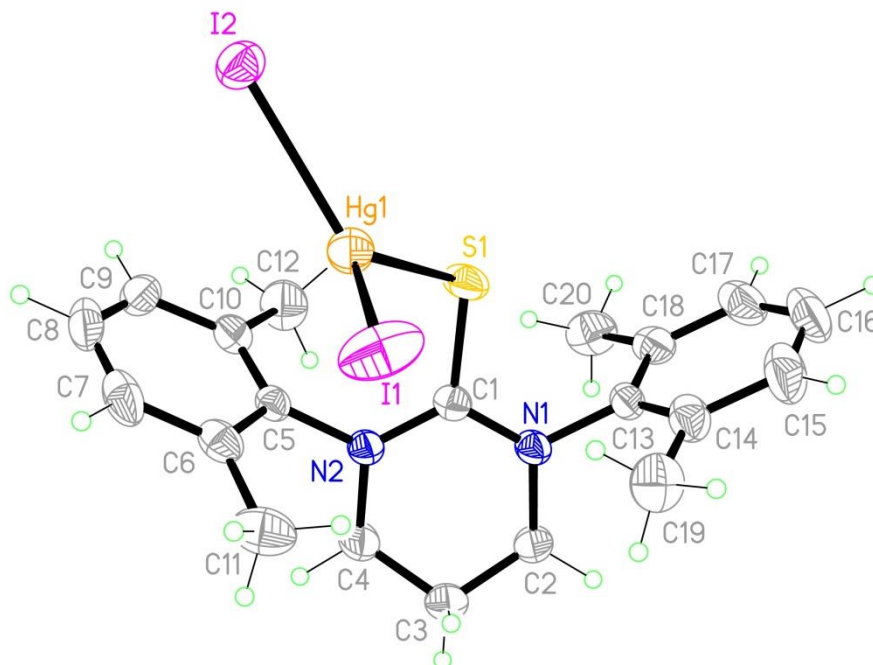


Figure 2.26: Molecular structure of (SpymXyS)HgI₂.

Table 2.4: Selected Bond Lengths (Å) and Angles (°) for (SpymXyS)HgX₂

	X = Cl	X = Br	X = I
C–S	1.74	1.75	1.73
Hg–S	2.42	2.40	2.47
Hg···Cent.*	3.14	4.20	3.35
C–S–Hg	107.5	106.1	109.2
S–Hg–X ₁	113.9	110.6	115.1
S–Hg–X ₂ (or S ₂)	131.4	136.3	121.9
X ₁ –Hg–X ₂ (or S ₂)	114.0	111.9	118.8

*Cent.: Centroid of aromatic ring nearest to the mercury atom

The structures of (SpymXyS)HgX₂ (X = Br, I) are both mononuclear trigonal planar, as is the [(SpymXyS)₂HgCl]⁺ complex, but differ in that they are neutral. These contain one ligand coordinated to the mercury center with two halides. These structures are alike and shown in Figures 2.25 and 2.26. The differences in the values shown in Table 2.4 above are difficult to compare for the mercury(II) chloride and the mercury(II)

bromide and iodide as they are not isostructural. The distance of the mercury atom to the centroid of the nearest aryl ring for the bromide is longer than that of the iodide complex. This would seem to indicate that this is not the result of sterics, but some potential electronic effect from the halide.

The bond distances and angles for the (SpymXyS)HgX₂ complexes are similar to those of the saturated five-membered thione, (SIXyS)HgX₂. There are very few structures of trigonal planar NHT or NHSe mercury(II) halide complexes reported in the literature. Most of these complexes favor tetrahedral geometries around the mercury center.⁴⁶⁻⁴⁸ As a result of the different geometries it is difficult to quantitatively compare crystallographic data between these structures. The only previous example of an NHT mercury halide complex with trigonal planar geometry was reported by Popovic *et al.*⁴⁹ Unlike the SpymArS ligands, the NHT ligand reported is an unsaturated five-membered ring with hydrogen atoms as N-substituents. The C–S (1.72 Å) and the Hg–S (2.46 Å) bond distances are very similar to those for each of the SpymArS ligands. The bond angles, C–S–Hg (99.9°), S–Hg–I₁ (109.0°), S–Hg–I₂ (134.6°), and I₁–Hg–I₂ (108.9°) are each about 10° greater than the trigonal planar SpymArS mercury iodide complexes. The sterics of this NHT and the SpymArS ligands are very different, which is likely the cause of the differences in these bond angles.

2.3.2 Molecular Structures of (SpymXySe)HgX₂

The molecular structures of (SpymXySe)HgX₂ (X = Cl, Br, I) were obtained using single crystal X-ray diffraction of crystals that were attained by slow evaporation of solutions of the complexes dissolved in acetone (X = Cl, Br, I). Each of the molecular

structures contains mononuclear neutral trigonal planar complexes and are the only set of mercury(II) complexes for the SpymArE ligand set to yield the same geometry. The molecular structures of $(\text{SpymXySe})\text{HgX}_2$ ($X = \text{Cl}, \text{Br}, \text{I}$) are shown below along with selected bond values in Table 2.5.

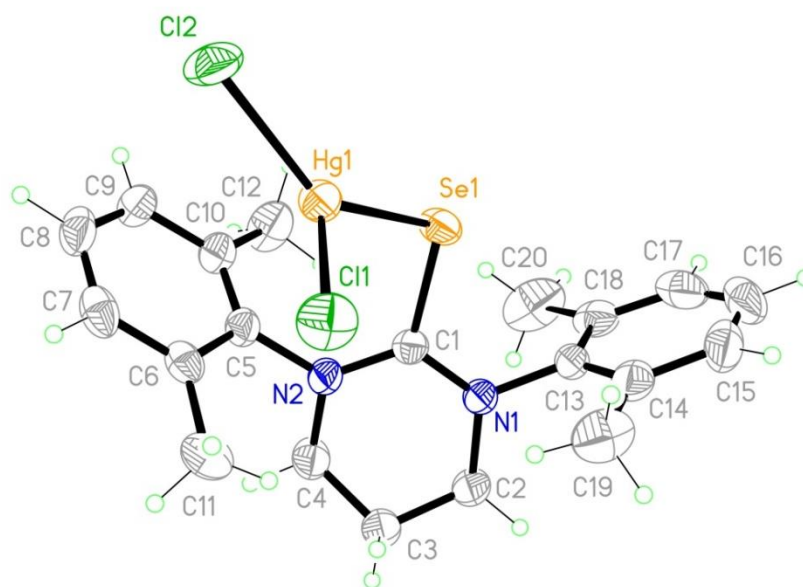


Figure 2.27: Molecular structure of $(\text{SpymXySe})\text{HgCl}_2$.

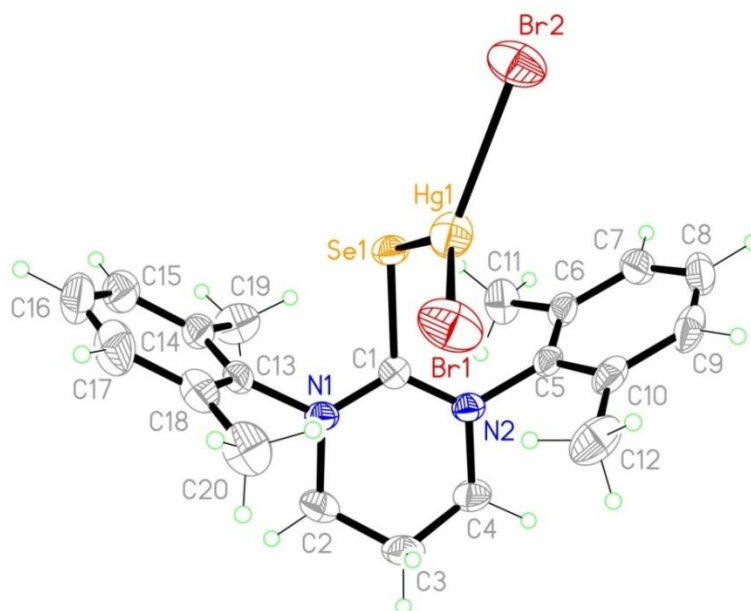


Figure 2.28: Molecular structure of $(\text{SpymXySe})\text{HgBr}_2$.

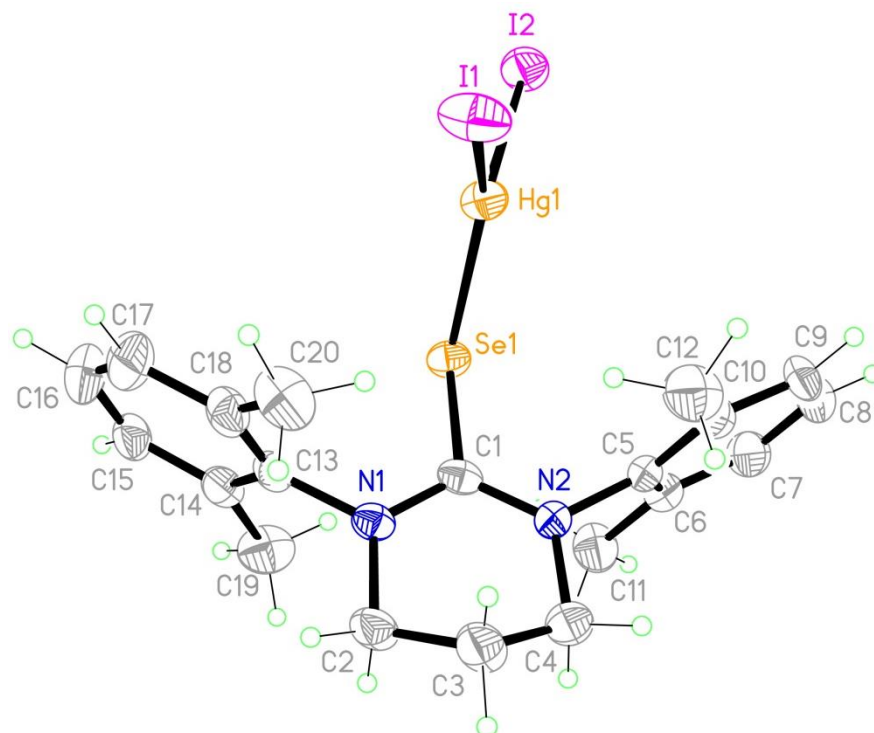


Figure 2.29: Molecular structure of (SpymXySe)HgI₂.

Table 2.5: Selected Bond Lengths (Å) and Angles (°) for (SpymXySe)HgX₂

	X = Cl	X = Br	X = I
C–Se	1.90	1.92	1.91
Hg–Se	2.49	2.49	2.51
Hg··Cent.*	3.23	4.29	4.61
C–Se–Hg	102.7	103.2	107.0
Se–Hg–X ₁	116.7	108.1	102.8
Se–Hg–X ₂	138.0	139.8	139.8
X ₁ –Hg–X ₂	102.4	111.1	117.1

*Cent.: Centroid of aromatic ring nearest to the mercury atom

As a result of the same molecular geometry for each of these mercury(II) halides, the bond length data collected can be used to more accurately draw conclusions from. As seen in table 2.5, the carbon-selenium and mercury-selenium bond distances don't seem to have any significant trend. There does seem to be a correlation between the

distance of the mercury atom to the centroid of the nearest aryl ring and the halides on the mercury. As the electronegativity of the halide increase, the mercury to centroid distance decreases. This inverse proportionality is not likely to be the result of only the electronegativity and it is likely to be the result of multiple factors including sterics and crystal packing. The C–Se–Hg bond angles for each of these complexes would also support this trend as this angle increases from the chloride to the iodide.

2.3.3 Molecular Structures of (SpymMesS)HgX₂ and [Hg(SpymMesS)₂][Hg₂Br₆]

The molecular structures of (SpymMesS)HgX₂ (X = Cl, I) and [Hg(SpymMesS)₂][Hg₂Br₆] were obtained using single crystal X-ray diffraction of crystals that were obtained by slow evaporation of solutions of the complexes in acetone (X = Cl, Br, I). Unlike any of the other SpymArE complexes of mercury(II), the (SpymMesS)HgX₂ complexes are not isostructural and exhibit three different crystal structures. These structures are shown below and selected bond lengths are shown in Table 2.6.

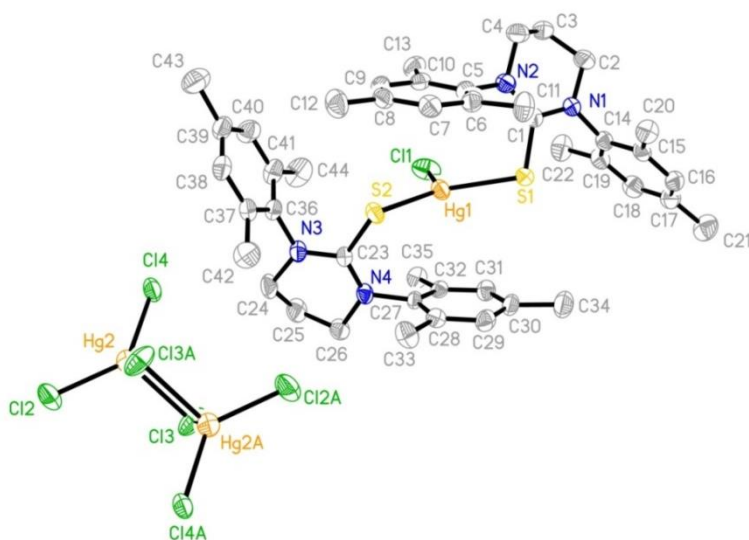


Figure 2.30: Molecular structure of [(SpymMesS)₂HgCl][Hg₂Cl₆].

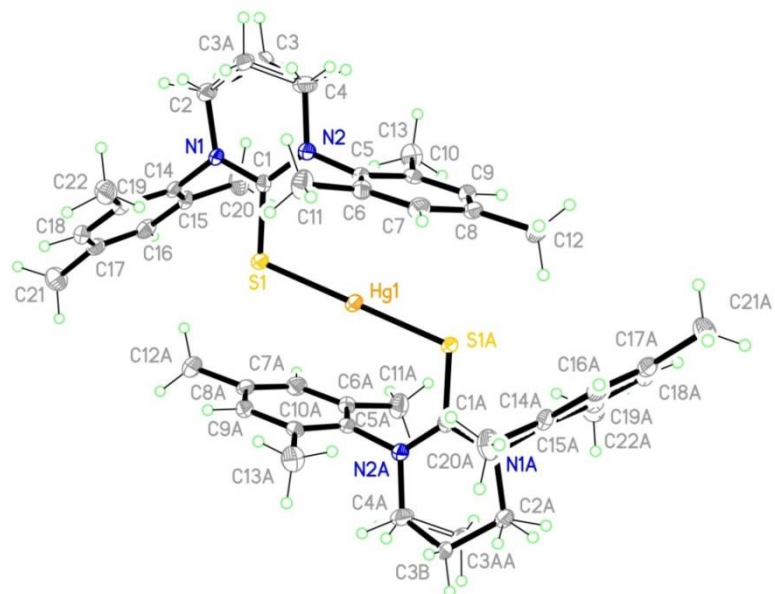


Figure 2.31: Molecular structure of the cation in $[\text{Hg}(\text{SpymMesS})_2][\text{Hg}_2\text{Br}_6]$.

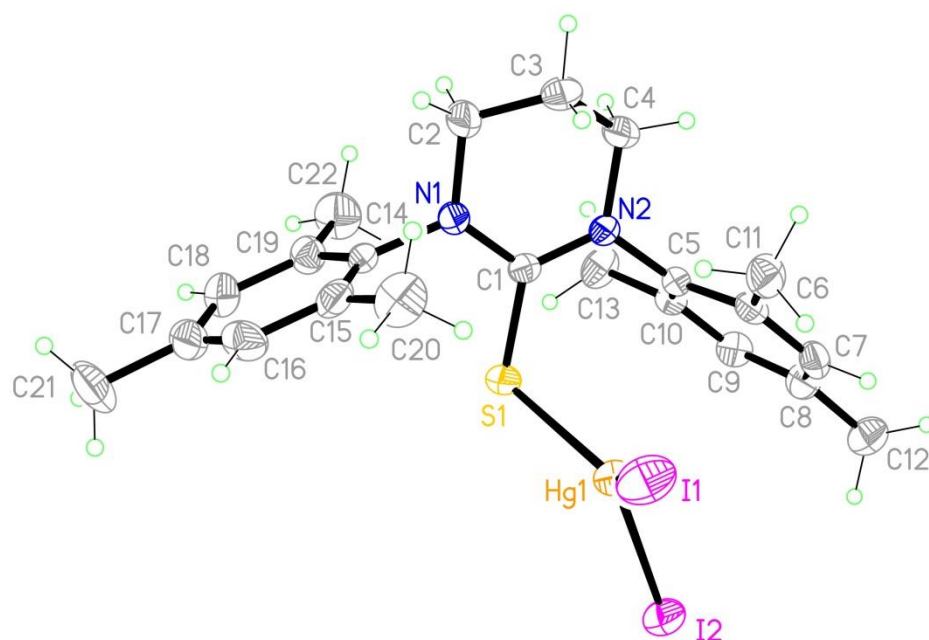


Figure 2.32: Molecular structure of $(\text{SpymMesS})\text{HgI}_2$.

Table 2.6: Selected Bond Lengths (Å) and Angles (°) for (SpymMesS)HgX₂

	X = Cl	X = Br	X = I
C–S	1.75	1.76	1.74
Hg–S	2.45	2.35	2.47
Hg···Cent.*	3.32	3.13	3.64
C–S–Hg	107.2	110.1	106.3
S ₁ –Hg–X ₁	100.95	–	–
S ₂ –Hg–X ₁	119.8	–	–
S ₁ –Hg–S ₂	139.2	180.0	–
S–Hg–X ₁	–	–	112.4
S–Hg–X ₂	–	–	124.0
X ₁ –Hg–X ₂	–	–	120.9

*Cent.: Centroid of aromatic ring nearest to the mercury atom

The [(SpymMesS)₂HgCl]⁺ complex is isostructural to the [(SpymXyS)₂HgCl]⁺ complex, mononuclear charged trigonal planar, having two ligands and one chloride. When comparing these two structures, it can be observed that their C–S bond distances are roughly equivalent, 1.74 Å for [(SpymXyS)₂HgCl]⁺ and 1.75 Å for [(SpymMesS)₂HgCl]⁺, as well as their Hg–S bond distances, 2.42 Å for [(SpymXyS)₂HgCl]⁺ and 2.45 Å for [(SpymMesS)₂HgCl]⁺. There is some difference in the distance of the mercury atom to the centroid of the nearest aryl ring, 3.14 Å for [(SpymXyS)₂HgCl]⁺ and 3.32 Å for [(SpymMesS)₂HgCl]⁺. While this difference is potentially significant, it is most likely a solid state interaction related to the sterics of crystal packing.

The cation in [Hg(SpymMesS)₂][Hg₂Br₆] is a charged linear two-coordinate mercury(II) complex, unlike the trigonal planar metal complexes of mercury(II) chloride and iodide and SpymMesS. Mercury(II) complexes with linear two-coordinate geometries are not unprecedented with N-heterocyclic thiones, but are rare as it has only

been reported with the ligands shown in Figure 2.33.⁵⁰⁻⁵² These previously reported examples of linear two-coordinate mercury(II) complexes vary greatly from the SpymArE ligand set. While there is a six-membered ring present, the N-substituents shown for these ligands have relatively no steric effect when compared to that of a mesityl ring. The mercury(II) bromide complex exhibits some solid state interaction with the mesityl aromatic center with a bond distance of 3.13 Å, the reported literature value for this interaction is 3.19 Å.⁵³

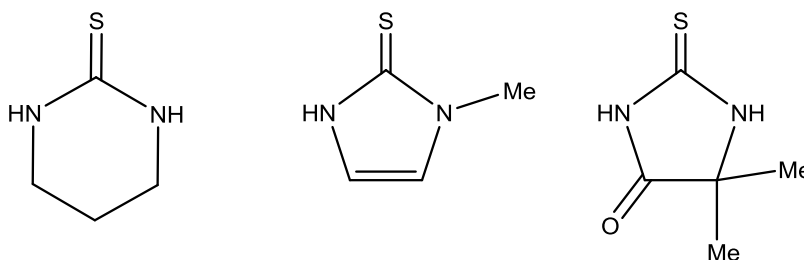


Figure 2.33: Known NHT ligands of cationic two-coordinate mercury(II) complexes.

As shown in Figure 2.32, (SpymMesS)HgI₂ has a trigonal planar geometry around the mercury, similar to that of (SpymXyS)HgI₂. When comparing these two mercury(II) iodide complexes it can be seen that their C–S bond distances are almost equivalent, 1.73 Å for (SpymXyS)HgI₂ and 1.74 Å for (SpymMesS)HgI₂, as well as their Hg–S bond distances, 2.47 Å for both (SpymXyS)HgI₂ and (SpymMesS)HgI₂. There is a sizable difference in the distance of the mercury atom to the centroid of the nearest aryl ring, 3.35 Å for (SpymXyS)HgI₂ and 3.64 Å for (SpymMesS)HgI₂. This difference of about 0.3 Å is possibly significant, as it could indicate the difference in electron density present in the aryl ring for the xylyl and mesityl substituents.

2.3.4 Molecular Structures of (SpymMesSe)HgX₂

The molecular structures of (SpymMesSe)HgX₂ (X = Cl, Br, I) were obtained using single crystal X-ray diffraction of crystals that were attained by slow evaporation of solutions of the complexes dissolved in acetonitrile (X = Cl) or acetone (X = Br, I). Each of the molecular structures contains mononuclear trigonal planar complexes with the mercury(II) chloride complex being charged, [(SpymMesSe)₂HgCl]⁺, and the mercury(II) bromide and iodide complexes being neutral, (SpymMesSe)HgX₂ (X = Br, I).

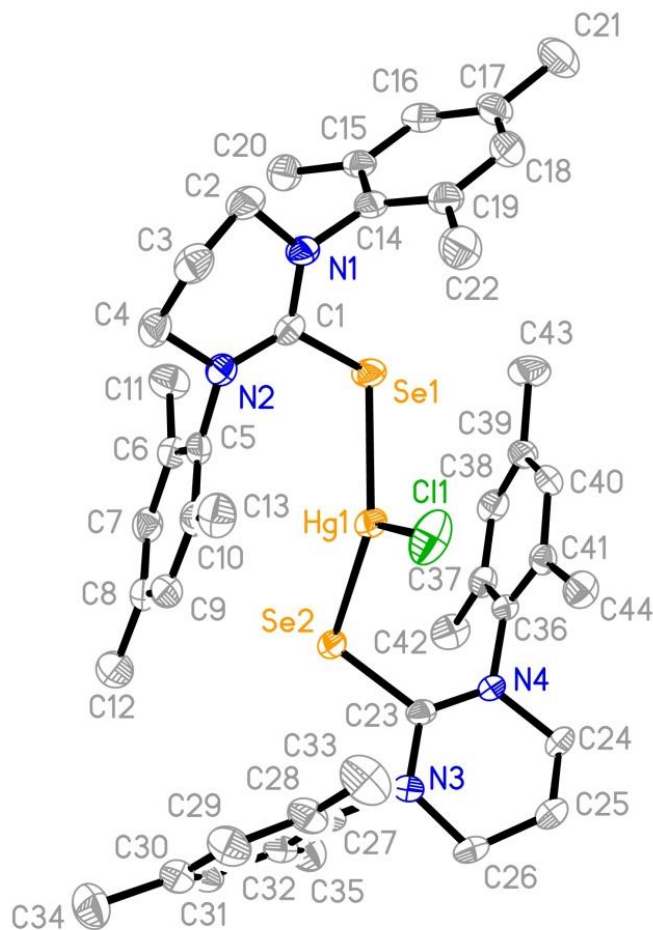


Figure 2.34: Molecular structure of the cation in [(SpymMesSe)₂HgCl][Hg₂Cl₆].

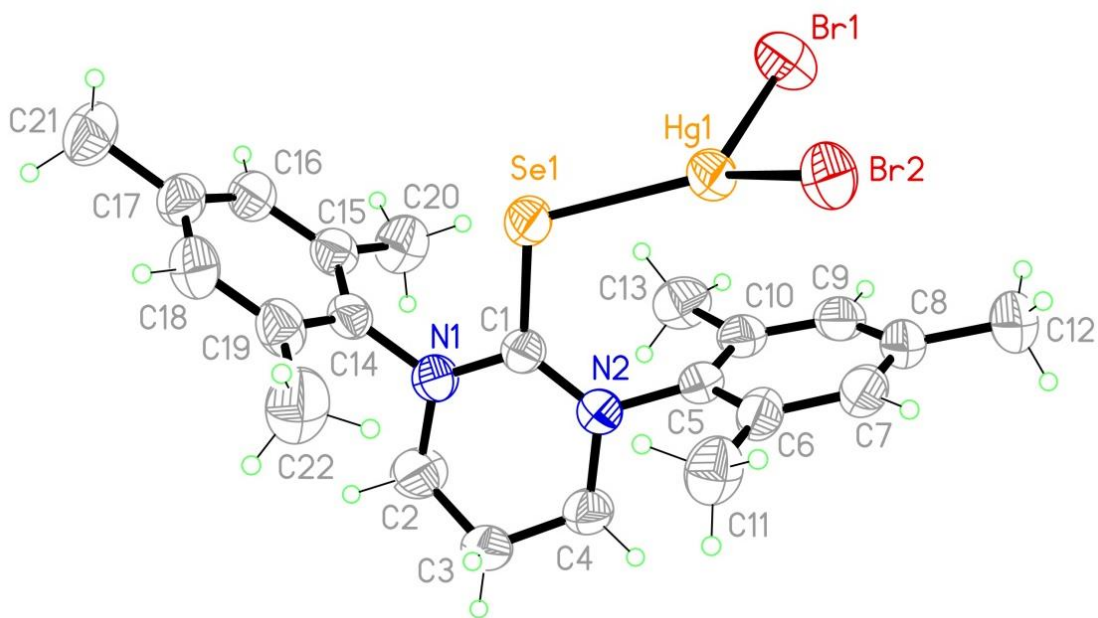


Figure 2.35: Molecular structure of (SpymMesSe)HgBr₂.

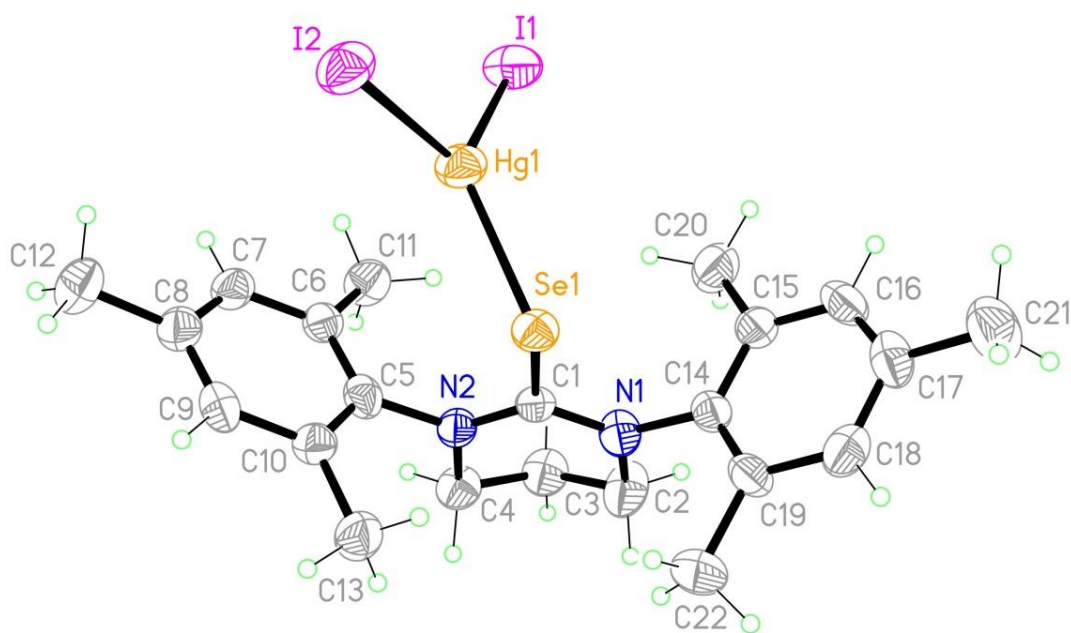


Figure 2.36: Molecular structure of (SpymMesSe)HgI₂.

Table 2.7: Selected Bond Lengths (Å) and Angles (°) for (SpymMesSe)HgX₂

	X = Cl	X = Br	X = I
C–Se	1.90	1.89	1.90
Hg–Se	2.51	2.53	2.55
Hg⋯Cent.*	3.33	3.07	3.79
C–Se–Hg	104.3	109.7	104.0
Se–Hg–X ₁	103.0	114.7	110.9
Se–Hg–X ₂ (or Se ₂)	137.7	131.6	128.3
X ₁ –Hg–X ₂ (or Se ₂)	119.2	110.7	118.4

*Cent.: Centroid of aromatic ring nearest to the mercury atom

The [(SpymMesSe)₂HgCl]⁺ complex is isostructural to the [(SpymMesS)₂HgCl]⁺ complex, mononuclear charged trigonal planar, having two ligands and one chloride. When comparing these two structures, their mercury–chalcogen and carbon–chalcogen bond distances contain different chalcogens and are not of use. The difference in the distance of the mercury atom to the centroid of the nearest aryl ring can be compared to investigate the role of changing the chalcogen to the effects this has on the solid state interaction of the coordinated mercury–arene interaction. The value for [(SpymMesSe)₂HgCl]⁺, 3.33 Å, is almost identical to that of [(SpymMesS)₂HgCl]⁺, 3.32 Å. There is a difference in the carbon–chalcogen–mercury bond angle between [(SpymMesS)₂HgCl]⁺, ~108°, and [(SpymMesSe)₂HgCl]⁺, ~105°. This difference, while the mercury–arene bond distance is similar would seem to indicate the presence of stronger mercury–arene attraction for the selone complex that could be the result of the less electronegativity of the selenium to that of the sulfur donor atom.

The structures of (SpymMesSe)HgX₂ (X = Br, I) are both mononuclear neutral trigonal planar, containing one ligand coordinated to the mercury center with two halides. These structures are alike and their bond distances and angles can be easily compared in

Table 2.7 As shown, the C–Se and Hg–Se for both the mercury(II) bromide and iodide complex are very similar. There is a large difference between the two for their mercury...centroid distance with (SpymMesSe)HgBr₂ at 3.07 Å and (SpymMesSe)HgI₂ at 3.79 Å. As discussed with each of the mercury complexes, the mercury...centroid distance tends to be the only value with significant difference with respect to the halide.

2.3.5 Molecular Structures of [Hg(SpymDippS)₂][Hg₂X₆]

The molecular structures of [Hg(SpymDippS)₂][Hg₂X₆] (X = Cl, Br, I) were obtained using single crystal X-ray diffraction of crystals that were attained by slow evaporation of solutions of the complexes in acetone (X = Br, I) or a mixture of acetone/benzene (X = Cl). Each of the [Hg(SpymDippS)₂]²⁺ cations is linear two-coordinate like the mercury(II) bromide complex for SpymMesS, [Hg(SpymMesS)₂][Hg₂Br₆], with S–Hg–S bond angles of 180° for each of the complexes.

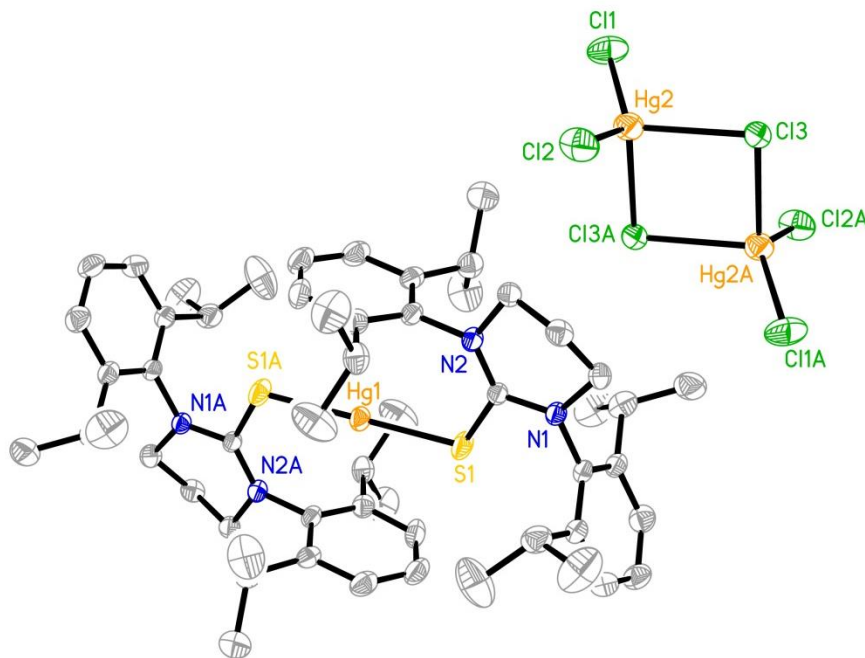


Figure 2.37: Molecular structure of [Hg(SpymDippS)₂][Hg₂Cl₆].

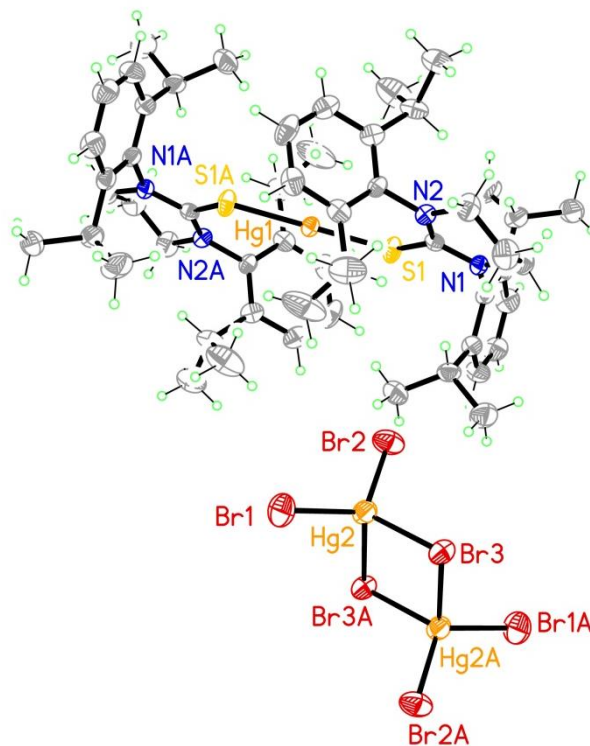


Figure 2.38: Molecular structure of $[\text{Hg}(\text{SpymDippS})_2][\text{Hg}_2\text{Br}_6]$.

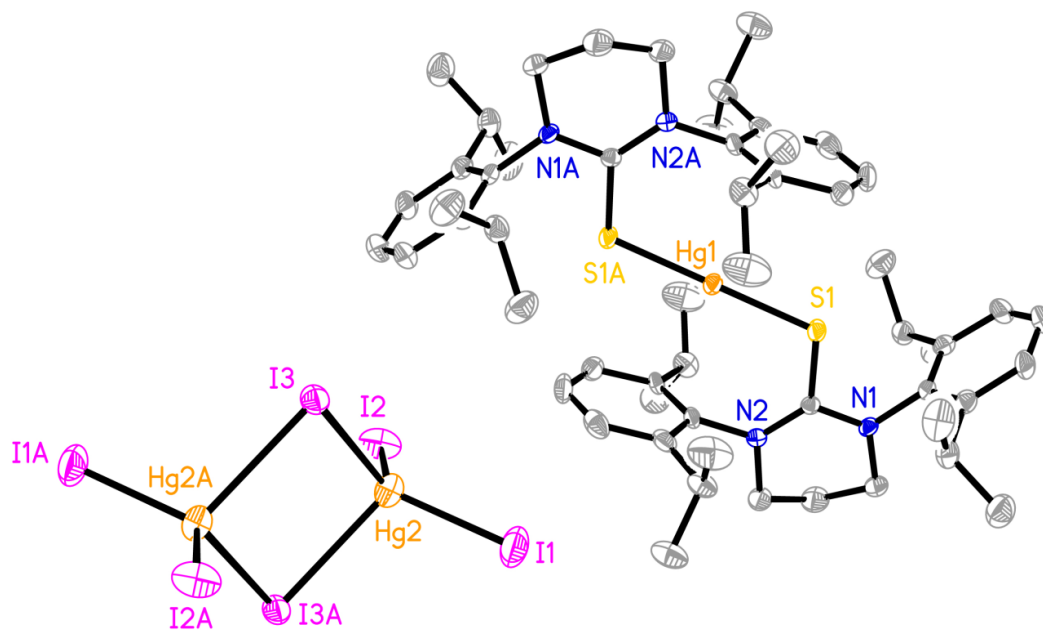


Figure 2.39: Molecular structure of $[\text{Hg}(\text{SpymDippS})_2][\text{Hg}_2\text{I}_6]$.

Table 2.8: Selected Bonds Lengths (Å) and Angles (°) for (SpymDippS)HgX₂

	X = Cl	X = Br	X = I
C–S	1.76	1.76	1.76
Hg–S	2.34	2.33	2.33
Hg···Cent.*	3.08	3.12	3.11
C–S–Hg	111.7	111.0	111.6
S ₁ –Hg–S ₂	180.0	180.0	180.0

*Cent.: Centroid of aromatic ring nearest to the mercury atom

As can be seen in Figures 2.37 through 2.39, each of the SpymDippS mercury(II) halide complexes have the same cation, [Hg(SpymDippS)₂]²⁺. This is reflected in Table 2.8 as each of the bond distances shown is equivalent. This linear two-coordinate geometry of the mercury(II) complex is likely favored despite the identity of the halide as a result of the steric bulk of the 2, 6–diisopropylphenyl substituent.

2.3.6 Molecular Structures of [Hg(SpymDippSe)₂][Hg₂X₆]

The molecular structures of [Hg(SpymDippSe)₂][Hg₂X₆] (X = Cl, Br, I) were obtained using single crystal X-ray diffraction of crystals that were attained by slow evaporation of solutions of the complexes dissolved in acetone (X = Cl, I) or THF (X = Br). Each of the [Hg(SpymDippSe)₂]²⁺ cations is linear two-coordinate like the mercury(II) bromide complex for SpymMesS, [Hg(SpymMesS)₂][Hg₂Br₆], and the each of the mercury(II) halides for SpymDippS, [Hg(SpymDippS)₂][Hg₂X₆] (X = Cl, Br, I), with S–Hg–S bond angles of 180° for each of the complexes.

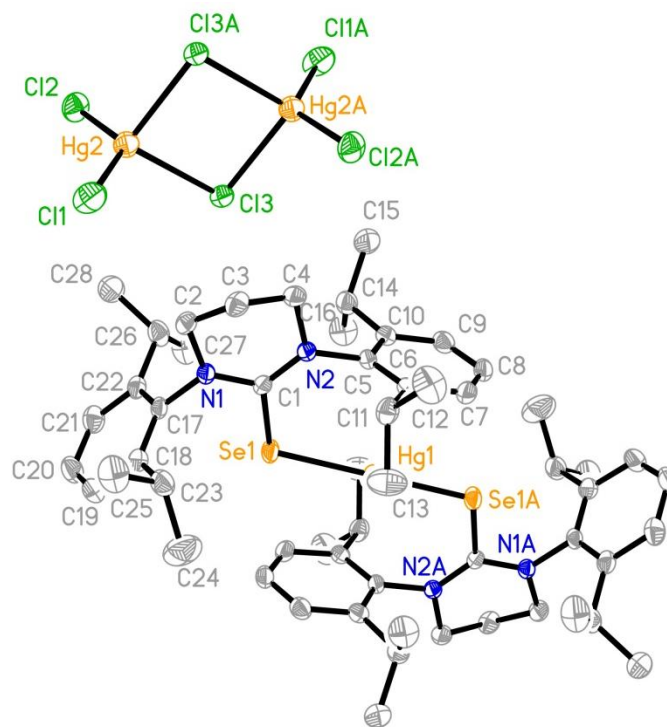


Figure 2.40: Molecular structure of [Hg(SpymDippSe)₂][Hg₂Cl₆].

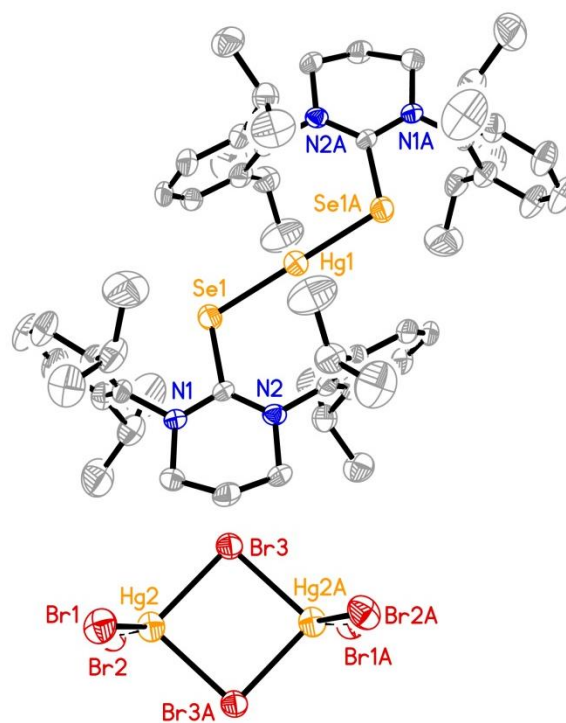


Figure 2.41: Molecular structure of [Hg(SpymDippSe)₂][Hg₂Br₆].

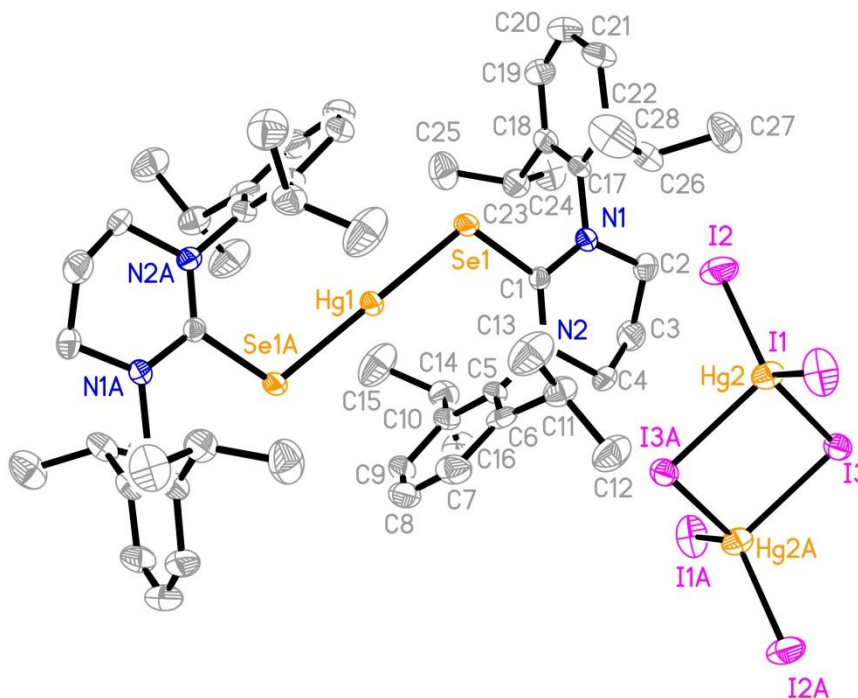


Figure 2.42: Molecular structure of $[\text{Hg}(\text{SpymDippSe})_2][\text{Hg}_2\text{I}_6]$.

Table 2.9: Selected Bond Lengths (Å) and Angles (°) for $(\text{SpymDippSe})\text{HgX}_2$

	X = Cl	X = Br	X = I
C–Se	1.91	1.91	1.92
Hg–Se	2.45	2.43	2.44
Hg \cdots Cent.*	3.06	3.07	3.11
C–Se–Hg	109.0	109.9	108.4
Se ₁ –Hg–Se ₂	180.0	180.0	180.0

*Cent.: Centroid of aromatic ring nearest to the mercury atom

As can be seen in Figures 2.40 through 2.42 each of the SpymDippSe mercury(II) halide complexes have the same cation, $[\text{Hg}(\text{SpymDippSe})_2]^{2+}$. This is reflected in Table 2.9 as each of the bond distances shown is almost identical. As discussed with the SpymDippS mercury(II) halides, each of the cations for the SpymDippSe complexes is same. For both SpymDippS and SpymDippSe, the identity of the halide does not affect the structure of the complex and it can be concluded that this is the result of the steric

demand of the ligand itself, specifically the diisopropyl phenyl N-substituents. The quantitative amount to which the Dipp substituent is sterically demanding when compared to the Xylyl is difficult as there are other factors that play a role in the crystal structures observed.

2.4 Synthesis of Copper(I) Complexes

Copper coordination complexes are abundant in inorganic, organometallic, and biologicals molecules.⁵⁴ The most common oxidation state of copper that is observed is the +2 state, however there are examples of copper(I) complexes that have an important function in the system they are present in.⁵⁵ Copper(I) is a closed-shell d^{10} metal with four-coordinate tetrahedral coordination complexes being most common, with some examples of linear two-coordinate and trigonal planar three-coordinate complexes reported. The closed-shell d^{10} electron configuration leads to the favoring of soft Lewis base donors for coordination, e.g. phosphines.

Copper(I) complexes of SpymArE were synthesized by reacting copper(I) iodide with SpymArE (Ar = Xy, E = S; Ar = Mes, E = S, Se) in a 1:1 stoichiometric ratio, with a slight excess of ligand under inert nitrogen atmosphere (Scheme 2.4). Each compound showed air sensitivity over time and was isolated in 35-55% yields. Each of the structures of the copper(I) complexes is linear two-coordinate with respect to the copper atom having one chalcogen and one iodide bound to the metal.

Scheme 2.4: Synthesis of Copper(I) Complexes

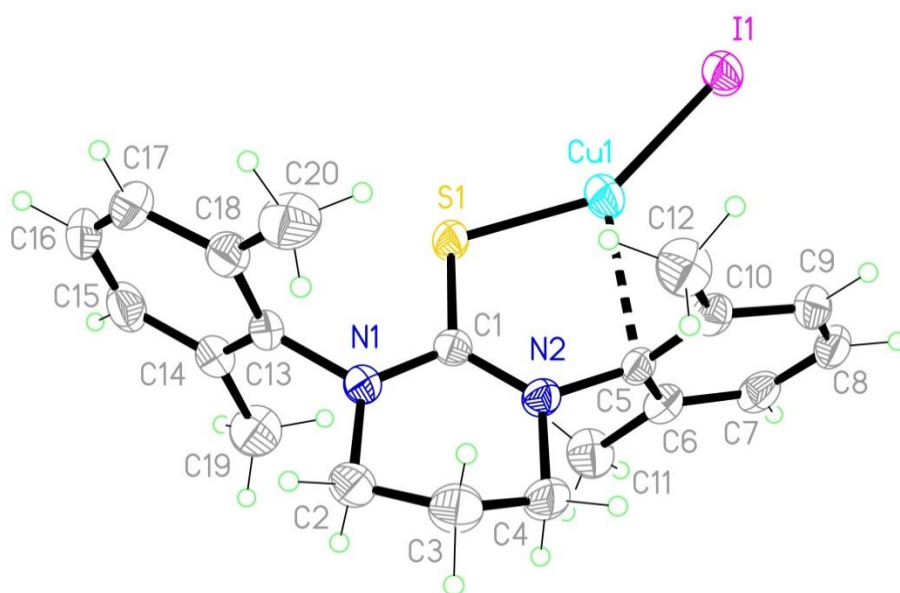
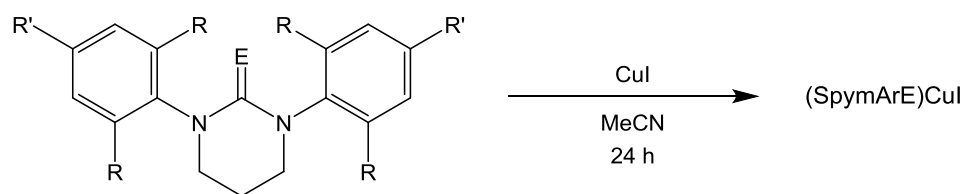


Figure 2.43: Molecular structure of (SpymXyS)CuI.

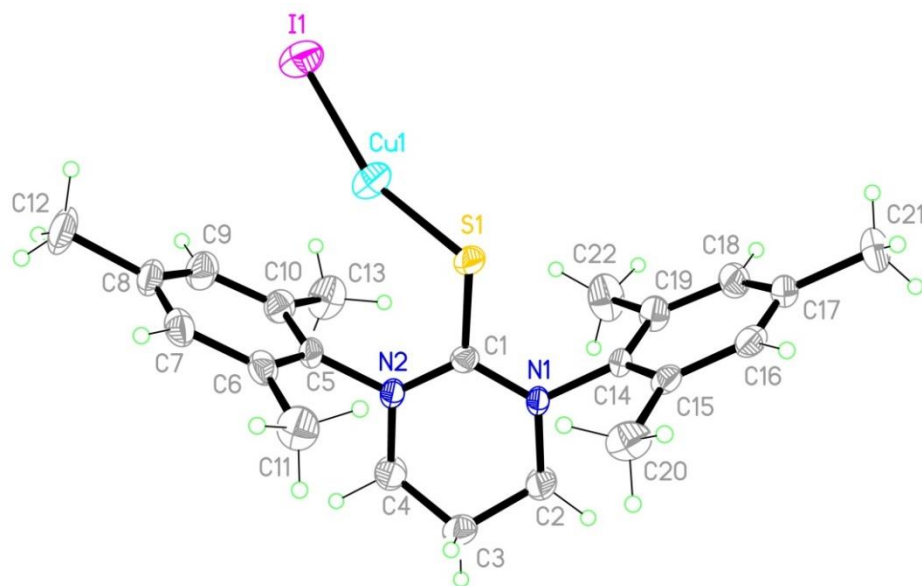


Figure 2.44: Molecular structure of (SpymMesS)CuI.

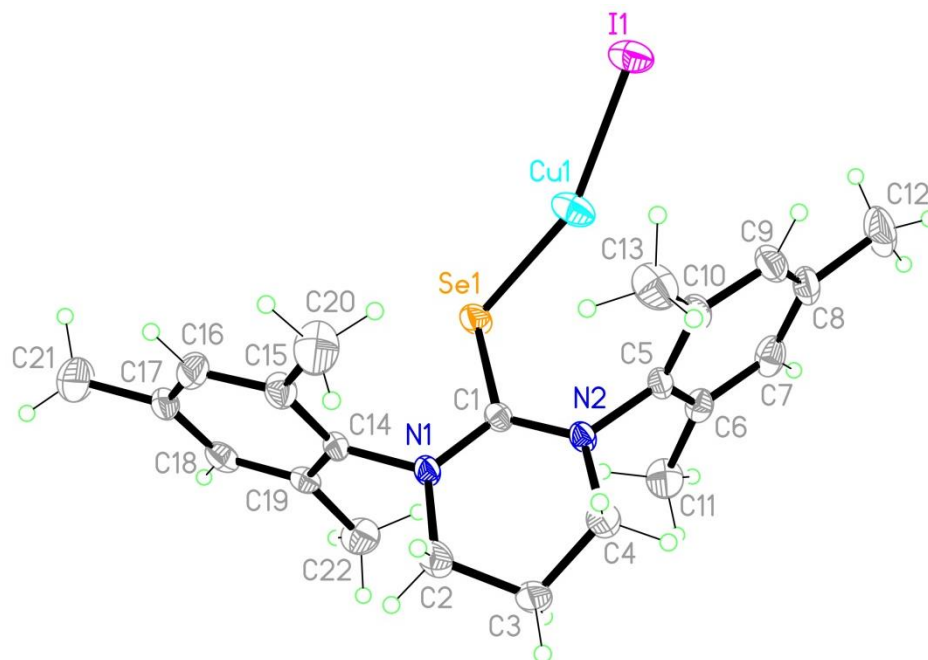


Figure 2.45: Molecular structure of (SpymMesSe)CuI.

Table 2.10: Selected Bond Lengths (Å) and Angles (°) for CuI complexes

	(SpymXyS)CuI	(SpymMesS)CuI	(SpymMesSe)CuI
C–E	1.72	1.73	1.89
Cu–E	2.17	2.17	2.28
Cu \cdots Cent.*	2.79	3.06	3.05
C–E–Cu	104.2	108.2	105.7
E–Cu–I	149.3	160.2	157.2

*Cent.: Centroid of aromatic ring nearest to the copper atom

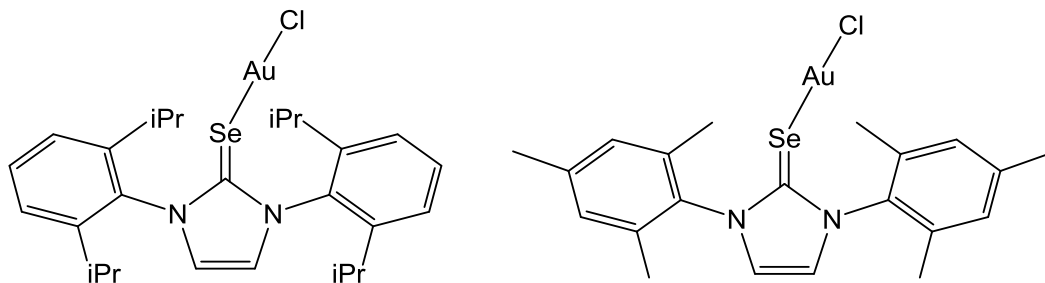
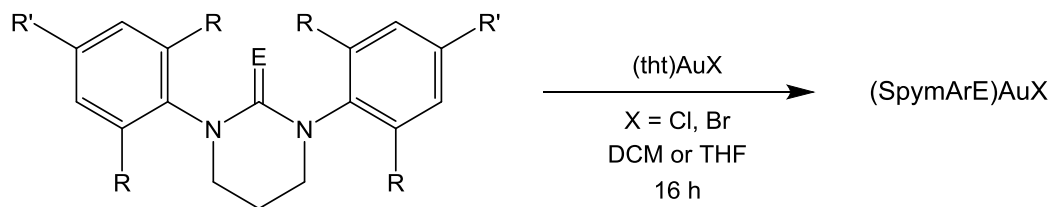
The molecular structures of the copper(I) iodide complexes are neutral linear two-coordinate. These copper(I) complexes exhibit some solid state interaction with the aromatic substituent and the (SpymXyS)CuI complex shows evidence of weak bonding interaction between the copper and ipso carbon of the phenyl ring. This bond distance of 2.46 Å is within the known bond distances for copper–carbon bonds. There is little evidence in the solution state for this interaction and further work must be done to define

this as a true interaction for this complex or a possible pathway for decomposition. The copper(I) iodide complexes of SpymMesS and SpymMesSe are suitable for the understanding of how altering the donor atom from sulfur to selenium effect the bonding of the species. As expected the bonds associated with coordination are longer for the selenone than the thione with the exception of the distance for the copper...centroid interaction being approximately equivalent. This equivalent copper...centroid distance supports the hypothesis of interaction for the aromatic substituent and the copper atom.

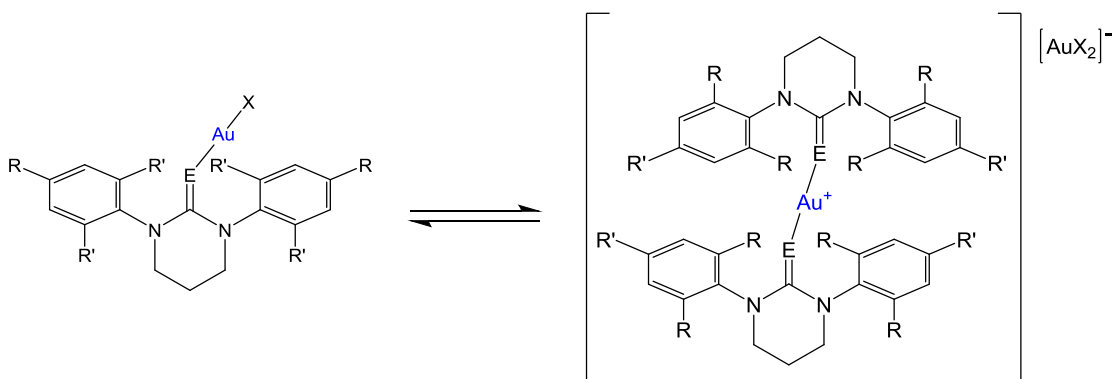
2.5 Synthesis of Gold(I) Complexes

To further expand the coordination chemistry of the SpymArE (Ar = Xy, Mes, Dipp; E = S, Se) ligands, they have been coordinated to gold(I). These complexes, (SpymArE)AuX (Ar = Xy, Mes, Dipp; E = S, Se; X = Cl, Br), were prepared by treating the ligands with (tht)AuX (X = Cl, Br) in a equimolar ratio with a slight excess of ligand, Scheme 2.5.⁵⁶ All twelve compounds are air-stable and have been isolated in 68-89% yields. The structures of these gold(I) complexes in the solid state are shown to be linear two-coordinate neutral, with the gold atom bonded to one ligand and one halide, or charged, with the gold atom bonded to two ligands and an anion composed of [AuX₂]⁻. Linear two-coordinate gold(I) complexes with chalcogen donor atoms are preceded in the literature.⁵⁷ Nolan *et al.* reported the preparation of linear gold(I) complexes with various NHSe ligands by reacting them with (Me₂S)AuCl in THF (Figure 2.46).

Scheme 2.5: Synthesis of Gold(I) Complexes

Figure 2.46: Two of the $(\text{NHSe})\text{AuCl}$ complexes prepared by Nolan *et al.*

While the crystal structures of these complexes are shown below, it was evident from the ^1H NMR, ^{13}C NMR, and ESI-MS that these complexes existed in a solution state equilibrium between the neutral and charged species (Figures 2.47 and 2.48). This observation was previously reported by Nolan *et al.* with their gold(I) NHSe complexes and Cavell *et al.* with silver(I) NHC complexes as well.^{7,57}

Figure 2.47: Proposed solution state equilibrium of $(\text{SpymArE})\text{AuX}$.

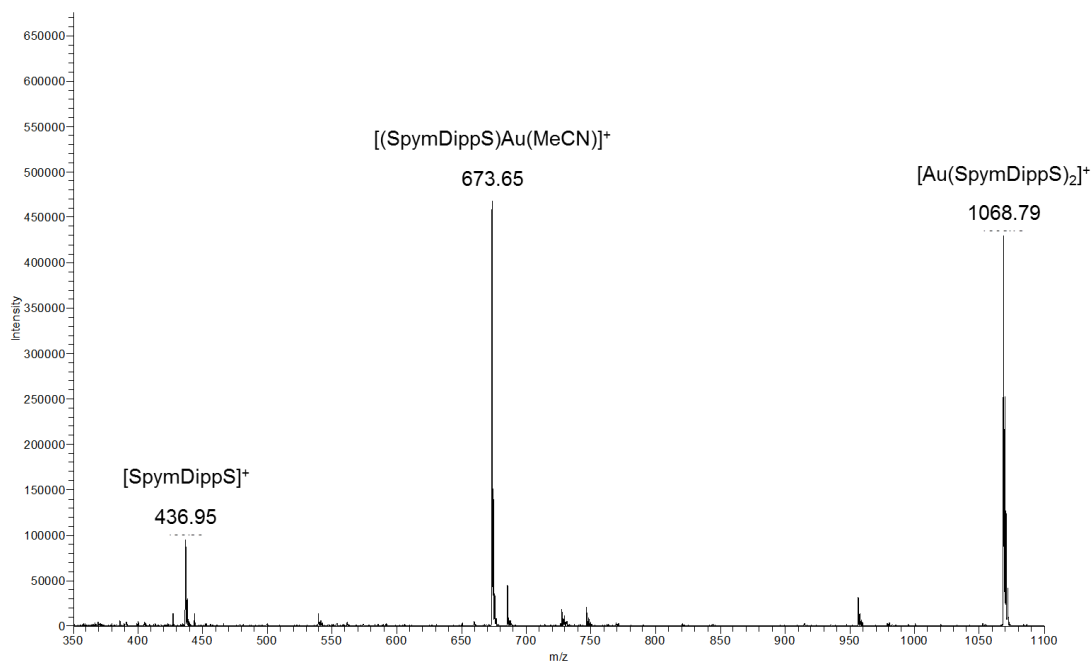


Figure 2.48: ESI-MS of (SpymDippS)AuCl.

2.5.1 Molecular Structures of (SpymXyS)AuX

The molecular structures of (SpymXyS)AuX (X = Cl, Br) were obtained using single crystal X-ray diffraction of suitable crystals that were attained by slow evaporation of solutions of the complexes dissolved in acetonitrile (X = Cl, Br). These structures are shown below in Figures 2.49 and 2.50 with selected bond lengths are shown in Table 2.11.

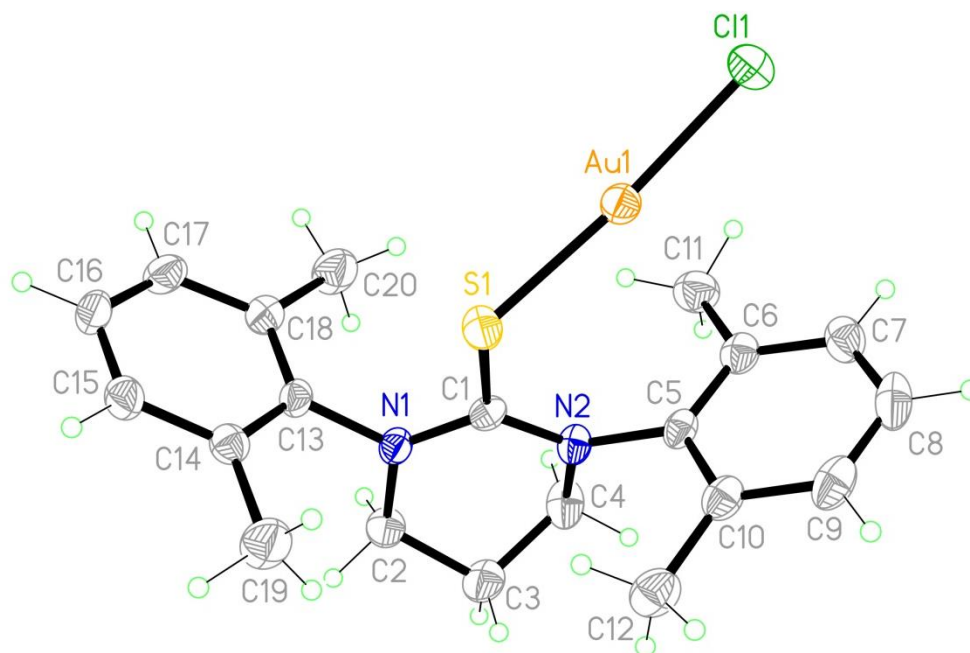


Figure 2.49: Molecular structure of (SpymXyS)AuCl.

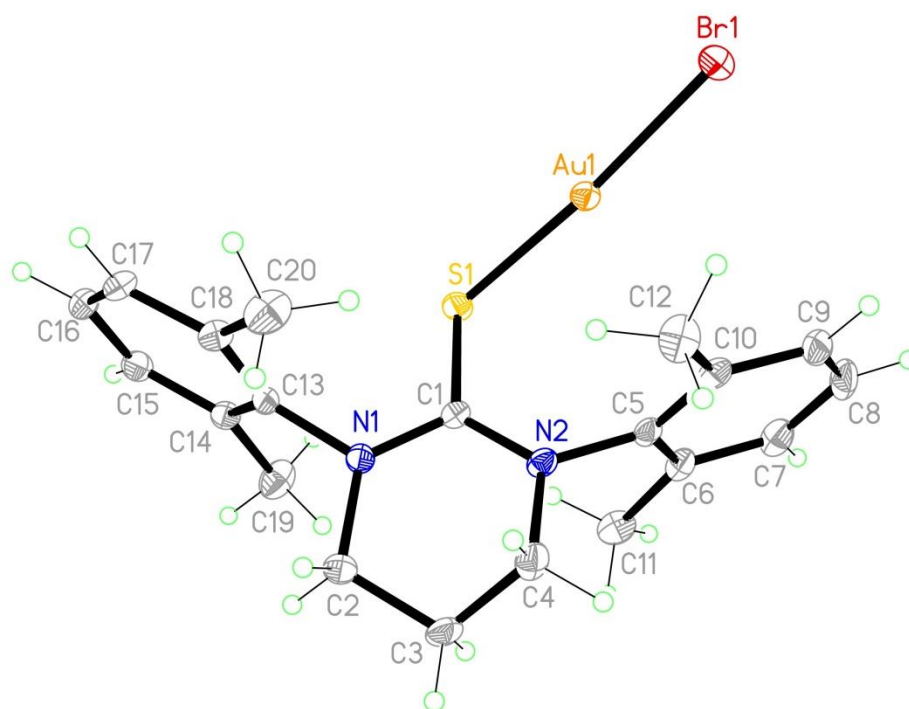


Figure 2.50: Molecular structure of (SpymXyS)AuBr.

Table 2.11: Selected Bond Lengths (Å) and Angles (°) for (SpymXyS)AuX

	X = Cl	X = Br
C–S	1.75	1.74
Au–S	2.25	2.26
Au⋯Cent.*	3.44	3.41
C–S–Au	110.2	110.0
S–Au–X	175.1	175.3

*Cent.: Centroid of aromatic ring nearest to the gold atom

The gold(I) complexes of SpymXyS are both neutral species with distorted linear geometry with S–Au–X bond angles of 175.1° (X = Cl) and 175.3° (X = Br) respectively. The sulfur donor atom exhibits a bent geometry with C–S–Au bond angles of 110.2° (X = Cl) and 110.0° (X = Br). The gold⋯centroid distances for the SpymXyS ligand are roughly equivalent (3.44 Å for X = Cl and 3.41 Å for X = Br) and unlike the mercury(II) halides for SpymXyS, the gold(I) complexes of SpymXyS are isostructural.

2.5.2 Molecular Structure of (SpymXySe)AuBr

The molecular structure of (SpymXySe)AuBr was obtained using single crystal X-ray diffraction of suitable crystals that were attained by slow evaporation of a solution of the complex dissolved in acetonitrile. This structure is shown below in Figure 2.51 with selected bond lengths and angles are shown in Table 2.12.

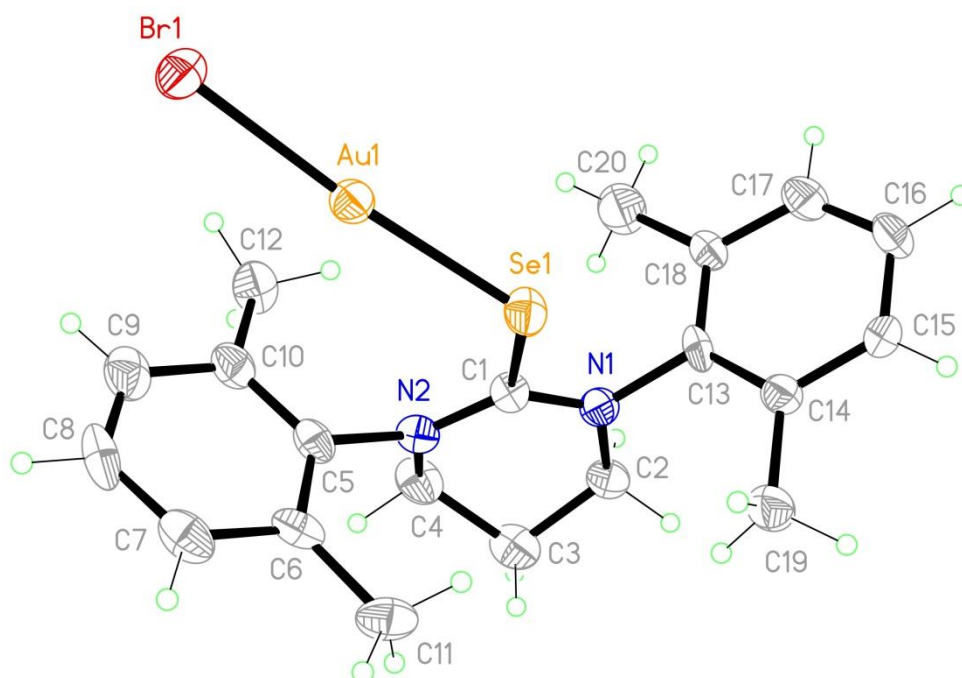


Figure 2.51: Molecular structure of (SpymXySe)AuBr.

Table 2.12: Selected Bond Lengths (Å) and Angles (°) for (SpymXySe)AuBr

(SpymXySe)AuBr	
C–Se	1.91
Au–Se	2.43
Au···Cent.*	3.07
C–Se–Au	107.1
Se–Au–Br	175.4

*Cent.: Centroid of aromatic ring nearest to the gold atom

The bond distances for the SpymXySe gold(I) bromide are similar to the reported values of SIMesSe gold(I) chloride by Nolan *et al.*⁵⁷ This structure is a good analogue for comparison as it is also a linear two-coordinate neutral complex. The C–Se bond distance (1.87 Å) and the Au–Se bond distance (2.36 Å) are both within 0.05 Å of the values found in this complex. These small differences are likely due to the different halide present on the gold(I) atom.

2.5.3 Molecular Structures of (SpymMesS)AuX

The molecular structures of (SpymMesS)AuX (X = Cl, Br) were obtained using single crystal X-ray diffraction of suitable crystals that were attained by slow evaporation of solutions of the complexes dissolved in acetone (X = Cl) and THF (X = Br). These structures are shown below in Figures 2.52 and 2.53 with selected bond lengths are shown in Table 2.13.

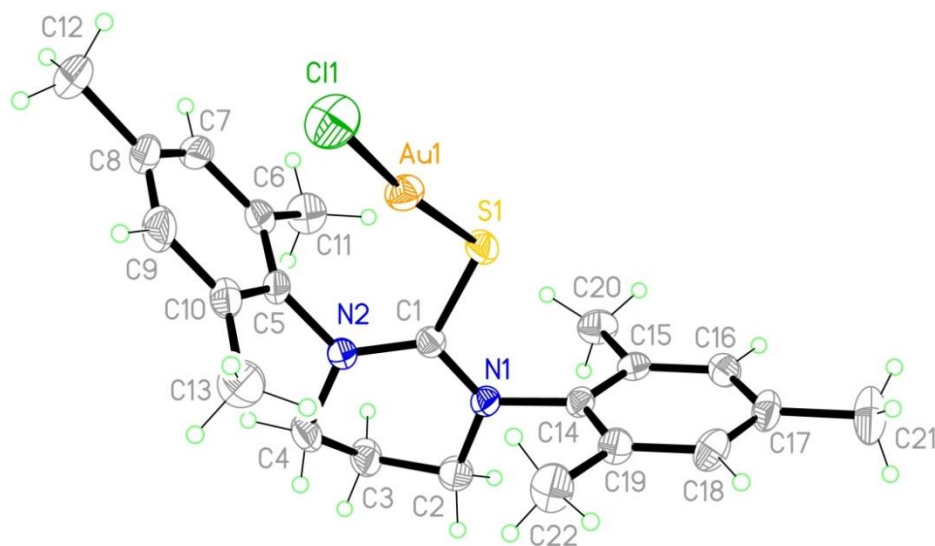


Figure 2.52: Molecular structure of (SpymMesS)AuCl.

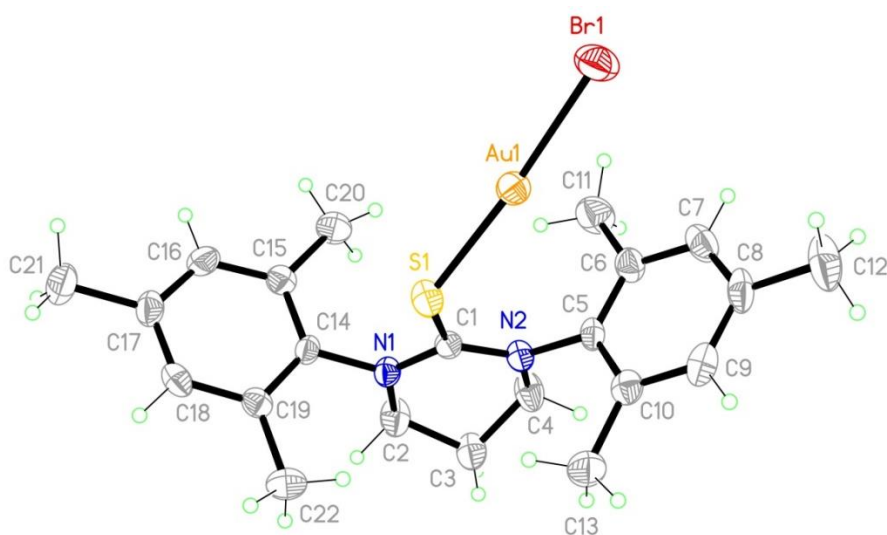


Figure 2.53: Molecular structure of (SpymMesS)AuBr.

Table 2.13: Selected Bond Lengths (Å) and Angles (°) for (SpymMesS)AuX

	X = Cl	X = Br
C–S	1.74	1.72
Au–S	2.26	2.17
Au⋯Cent.*	3.37	3.36
C–S–Au	111.6	111.2
S–Au–X	173.8	174.1

*Cent.: Centroid of aromatic ring nearest to the gold atom

The gold(I) complexes of SpymMesS are both neutral species with distorted linear geometry with S–Au–X bond angles of 173.8° (X = Cl) and 174.1° (X = Br) respectively. The sulfur donor atom exhibits a bent geometry with C–S–Au bond angles of 111.6° (X = Cl) and 111.2° (X = Br). The gold⋯centroid distances for the SpymMesS ligand are roughly equivalent (3.37 Å for X = Cl and 3.36 Å for X = Br) and, unlike the mercury(II) halides for SpymMesS, this distance does not vary with respect to the identity of the halide. These Au–arene interactions are more than an angstrom longer than that reported by Echavarren *et al* (2.20-2.44 Å) and therefore any weak interaction between these would likely exist in the solid state only.^{58,59}

2.5.4 Molecular Structures of (SpymMesSe)AuX

The molecular structures of (SpymMesSe)AuX (X = Cl, Br) were obtained using single crystal X-ray diffraction of suitable crystals that were attained by slow evaporation of solutions of the complexes dissolved in acetone (X = Cl) and THF (X = Br). These structures are shown below in Figures 2.54 and 2.55 with selected bond lengths and angles are shown in Table 2.14.

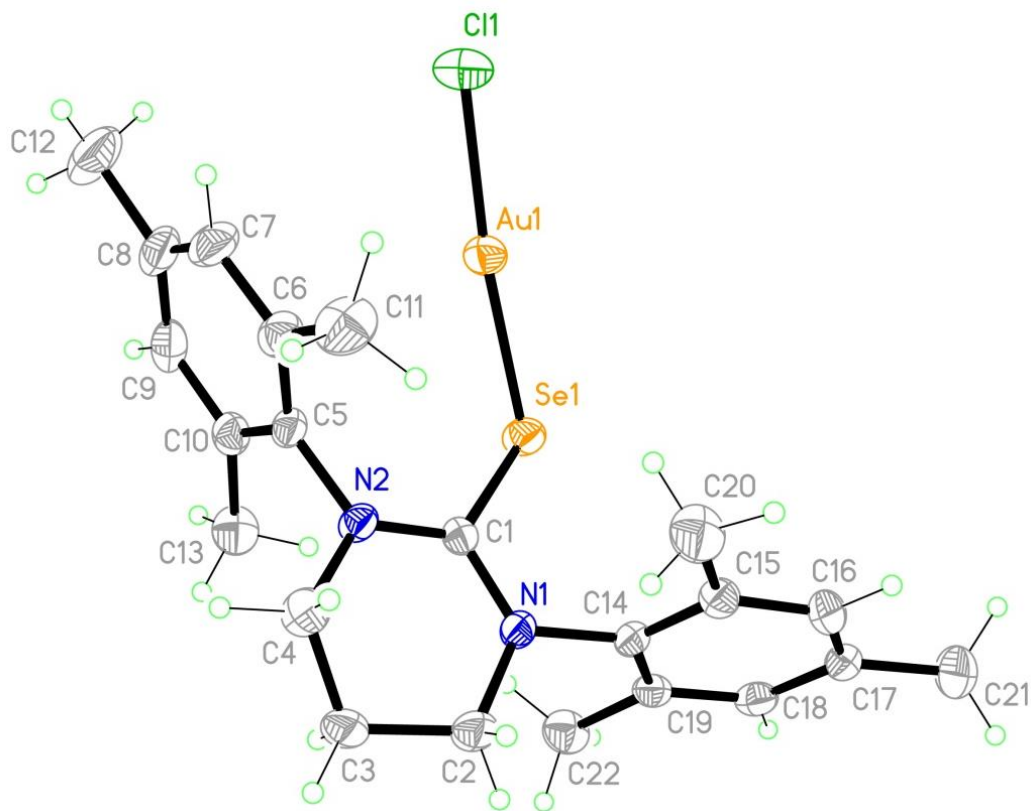


Figure 2.54: Molecular structure of (SpymMesSe)AuCl.

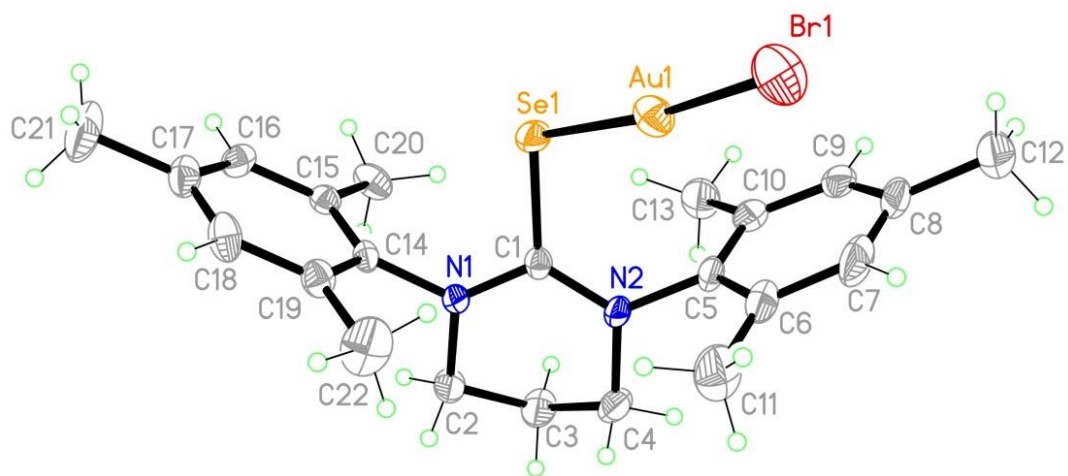


Figure 2.55: Molecular structure of (SpymMesSe)AuBr.

Table 2.14: Selected Bond Lengths (Å) and Angles (°) for (SpymMesSe)AuX

	X = Cl	X = Br
C–Se	1.90	1.89
Au–Se	2.37	2.37
Au···Cent.*	3.38	3.38
C–Se–Au	109.5	109.4
Se–Au–X	173.3	173.5

*Cent.: Centroid of aromatic ring nearest to the gold atom

The gold(I) complexes of SpymMesSe are both neutral compounds with distorted linear geometry with Se–Au–X bond angles of 173.3° (X = Cl) and 173.5° (X = Br) respectively. The selenium donor atom exhibits a bent geometry with C–Se–Au bond angles of 109.5° (X = Cl) and 109.4° (X = Br). The gold···centroid distances for the SpymMesSe ligand are equivalent (3.38 Å) and just like the gold(I) complexes for SpymMesS, this distance does not vary with respect to the identity of the halide. The C–Se–Au bond angles are more bent for each of the SpymMesSe gold(I) complexes than both of the SpymMesS gold(I) complexes while have roughly equivalent gold···centroid distances.

2.5.5 Molecular Structures of (SpymDippS)AuX

The molecular structures of (SpymDippS)AuX (X = Cl, Br) were obtained using single crystal X-ray diffraction of suitable crystals that were attained by slow evaporation of solutions of the complexes dissolved in acetone (X = Cl, Br). These structures are shown below in Figures 2.56 and 2.57 with selected bond lengths are shown in table 2.15. The SpymDippS gold(I) halides are the only compounds with different structures as the

identity of the halide is changed as the gold(I) chloride compound is linear charged two-coordinate and the gold(I) bromide compound is linear neutral two-coordinate.

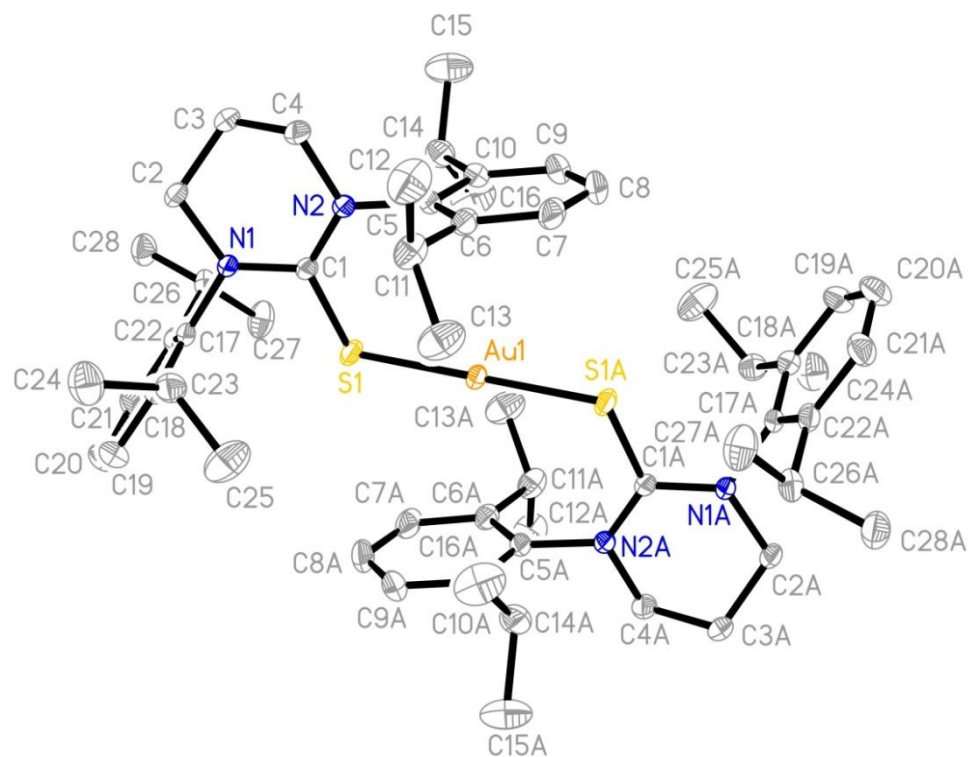


Figure 2.56: Molecular structure of the cation in $[\text{Au}(\text{SpymDippS})][\text{AuCl}_2]$.

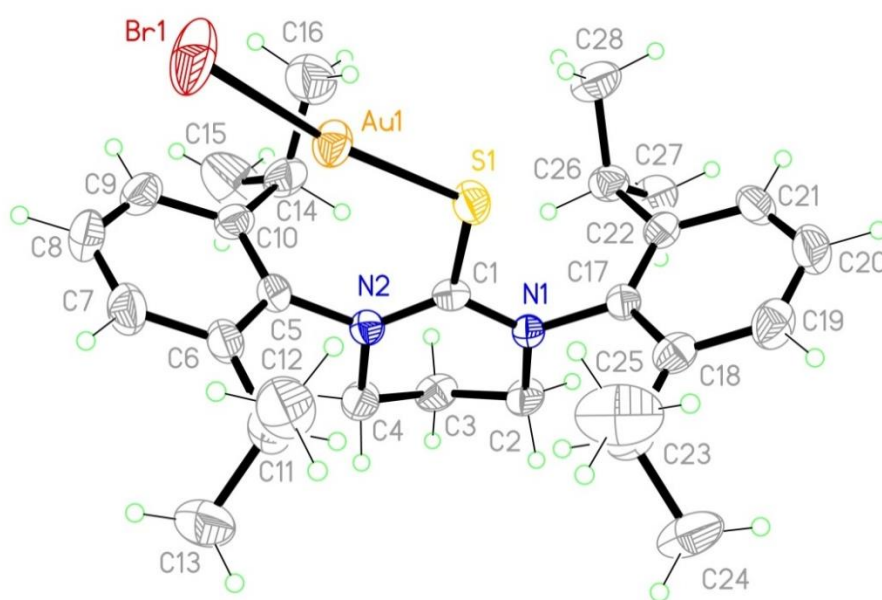


Figure 2.57: Molecular structure of $(\text{SpymDippS})\text{AuBr}$.

Table 2.15: Selected Bond Lengths (Å) and Angles (°) for (SpymDippS)AuX

	X = Cl	X = Br
C–S	1.73	1.73
Au–S	2.28	2.26
Au \cdots Cent.*	3.20	3.20
C–S–Au	114.7	115.6
S–Au–X (or S ₂)	180.0	170.0

*Cent.: Centroid of aromatic ring nearest to the gold atom

As a result of the different structures, the bond distance and angle values are not as simple to compare. However, it can be seen in Table 2.15 that despite the difference in structure there is little difference in these values for these complexes. The only value with significant difference is the bond angle around the Au metal atom. For the gold(I) chloride compound the bond angle (S–Au–S) is exactly linear at 180.0°, while the bond angle for the gold(I) bromide compound (S–Au–Br) is distorted linear at 170.0°. One of the reasons for this distortion could be related to the gold \cdots centroid interaction distance being identical and the electron density of the bromide atom repelling against the electron density of the arene. The SpymDippS gold(I) chloride complex is the only linear two-coordinate charged complex of gold(I) that has been obtained for these ligands. Nolan *et al.* reported a similar linear two-coordinate charged complex for the SpymDippSe gold(I) chloride complex. The donor atom is not the same for these complexes and while they are isostructural, the bond distances and angles are difficult to compare.

As mentioned in section 2.5, there is solution state equilibrium and the crystal structures of the SpymDippS and SpymDippSe gold(I) complexes support this hypothesis. Figure 2.58 is the ¹H NMR spectrum of SpymDippS gold(I) chloride complex

and the solution state behavior can be observed as there are an addition set of peaks present for each proton signal.

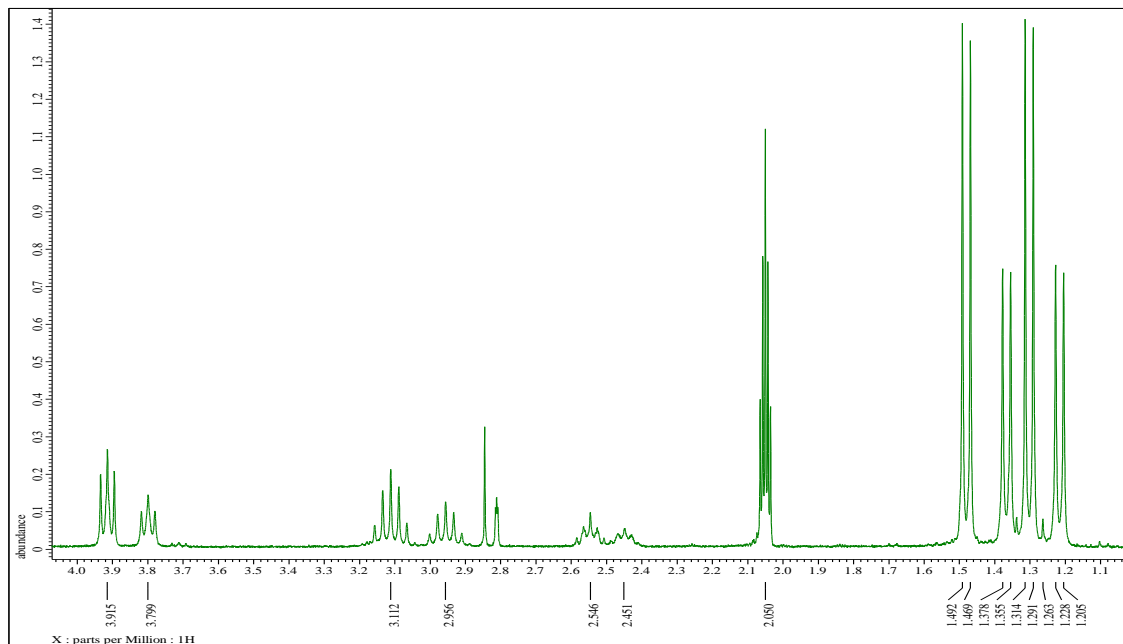


Figure 2.58: ^1H NMR spectrum of $(\text{SpymDippSe})\text{AuCl}$ in d_6 -acetone

2.5.6 Molecular Structures of $(\text{SpymDippSe})\text{AuX}$

The molecular structure of $(\text{SpymDippSe})\text{AuX}$ ($X = \text{Cl}, \text{Br}$) was obtained using single crystal X-ray diffraction of suitable crystals that were attained by slow evaporation of solutions of the complex dissolved in acetone ($X = \text{Cl}$) and acetonitrile ($X = \text{Br}$). These structures are shown below in Figures 2.59 and 2.60 with selected bond lengths and angles are shown in table 2.16.

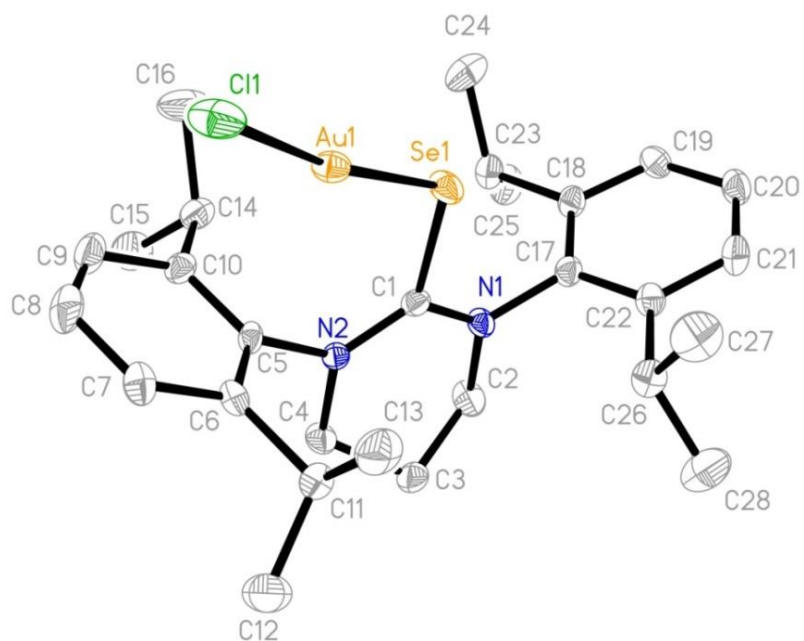


Figure 2.59: Molecular structure of (SpymDippSe)AuCl.

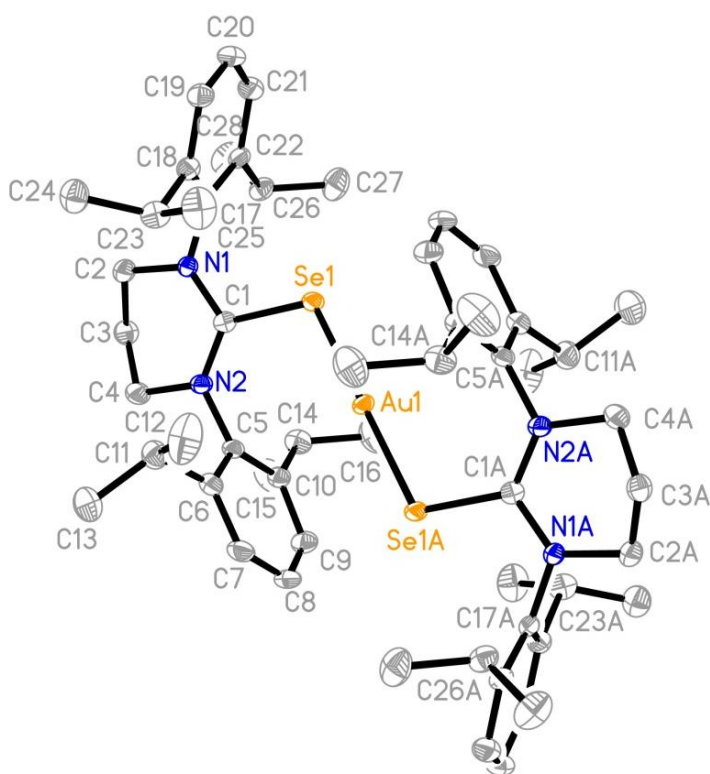


Figure 2.60: Molecular structure of the cation in [Au(SpymDippSe)₂][AuBr₂].

Table 2.16: Selected Bond Lengths (Å) and Angles (°) for (SpymDippSe)AuX

	X = Cl	X = Br
C–Se	1.90	1.89
Au–Se	2.36	2.38
Au···Cent.*	3.20	3.21
C–Se–Au	110.9	110.9
S–Au–X (or S ₂)	171.6	180.0

*Cent.: Centroid of aromatic ring nearest to the gold atom

The gold(I) chloride complexes for the SpymDippS and SpymDippSe are unfortunately not isostructural and not easily comparable. The SpymDippSe gold(I) chloride and SpymDippS gold(I) bromide are linear two-coordinate neutral complexes, while the SpymDippSe gold(I) bromide and SpymDippS gold(I) chloride are linear two-coordinate charged complexes. Their chalcogen–gold bond distances differ as expected, while the Au–arene interactions are almost identical, 3.20 and 3.21 Å. This equivalence is the result of weak solid state interaction between the gold(I) atom and aryl substituent.

As shown by the structures of SpymArE gold(I) complexes, there exist both neutral and charged species that when in solution favor an equilibrium between the linear two-coordinate neutral and charged complexes that can be observed in the NMR and ESI-MS (Figures 2.47, 2.48, and 2.58). The gold–sulfur and gold–selenium bond distances are similar for each ligand, as are the gold···centroid distances. The effect that each ligand has on its gold(I) complex will be further explored with reactivity studies.

CHAPTER 3: EXPERIMENTALS

3.1 General Considerations

All reactions were performed under aerobic conditions or under dry oxygen-free nitrogen in an Innovative Technology System One-M-DC glove box where indicated. Solvents were purified and degassed by standard procedures and all commercially available reagents were used as received. ^1H , ^{13}C , and ^{77}Se NMR spectra were obtained on a JEOL ECX-300 (300 MHz) or a JEOL ECX-500 (500 MHz). NMR chemical shifts reported in ppm relative to TMS ($\delta = 0$ ppm) for ^1H , and ^{13}C NMR and relative to Me_2Se ($\delta = 0$ ppm) for ^{77}Se NMR. Ph_2Se_2 ($\delta = 463$ ppm) was used as an external standard for ^{77}Se NMR data. The solvents were referenced internally with respect to the solvent peaks (^1H : δ 2.05 ppm for d_6 -acetone, 2.50 ppm for d_6 -DMSO, 5.32 ppm for CD_2Cl_2 , 7.26 ppm for CDCl_3 ; ^{13}C : 29.84 for d_6 -acetone, 39.52 ppm for d_6 -DMSO, 53.84 ppm for CD_2Cl_2 , 77.16 ppm for CDCl_3).⁶⁰ FT-IR spectra data obtained using a Perkin-Elmer Spectrum 100 FT-IR spectrometer with relative intensities of the absorptions indicated in parentheses (vs = very strong, s = strong, m = medium, w = weak). Electrospray ionization mass spectrometry performed on a Thermo Scientific MSQ Plus in a 50/50 acetonitrile:water mixture at a flow rate of 10 mL/min. Elemental analyses performed by Atlantic Microlab, Inc. (Norcross, GA).

3.2 Synthesis of SpymArE

The formamidines ArN=CHNHAr (Ar = Mes, Dipp)³¹ and their corresponding pyrimidinium bromide derivatives⁶¹ were prepared as reported. The Xylyl (2, 6-diisopropylphenyl) compound was prepared similarly. Each of the pyrimidinium bromide derivatives [SpymArH]Br was obtained in spectroscopically pure form after trituration with hot toluene and washing the resulting solid with diethyl ether.

3.2.1 Synthesis of SpymXyS

A stirred mixture of [SpymXyH]Br (1.000 g, 2.678 mmol), elemental sulfur (0.103 g, 3.214 mmol), and potassium carbonate (0.481 g, 3.482 mmol) in n-propanol (25 mL) was heated to reflux for 12 h. The resulting orange suspension was concentrated under reduced pressure to *ca.* 1 mL and triturated with pentane (10 mL). Removal of the volatiles under reduced pressure gives an orange solid residue. The product was extracted into dichloromethane (30 mL) and the pale orange extract was washed with DI water (3 x 30 mL). The organic phase was separated, concentrated under vacuum to *ca.* 1 mL, and treated with pentane (10 mL), leading to the precipitation of the off-white product, which was isolated by filtration and dried *in vacuo* for 14 h (0.608 g, 70%). The ligand is spectroscopically pure and can be used for further reactions but analytically pure samples can be obtained by recrystallization from dichloromethane/pentane. Mp = 196-198 °C (dec.). NMR data (in d₆-acetone): ¹H δ 2.31 (s, 12 H, CH₃), 2.43 (quintet, ³J_{H-H} = 5.9, 2 H, CH₂), 3.69 (t, ³J_{H-H} = 5.9, 4 H, CH₂), 7.05 (s, 6 H, C₆H₃); ¹³C δ 18.1 (q, ¹J_{C-H} = 127, 4 C, CH₃), 23.0 (t, ¹J_{C-H} = 131, 1 C, CH₂), 49.0 (t, ¹J_{C-H} = 143, 2 C, CH₂), 127.7 (d, ¹J_{C-H} =

160, 2 C, Cp in C_6H_3), 129.2 (d, $^1J_{C-H} = 157$, 4 C, C_m in C_6H_3), 136.1 (s, 4 C, C_o in C_6H_3), 145.7 (s, 2 C, C_{ipso} in C_6H_3), 178.1 (s, 1 C, C=S). IR data: 3020 (w), 2972 (w), 2937 (w), 2859 (w), 1663 (w), 1594 (w), 1490 (s), 1470 (s), 1443 (m), 1390 (m), 1372 (w), 1318 (s), 1299 (vs), 1262 (m), 1225 (w), 1201 (s), 1164 (w), 1107 (w), 1094 (w), 1081 (w), 1063 (w), 1031 (w), 985 (w), 917 (w), 883 (w), 855 (w), 780 (m), 765 (s), 743 (w), 669 (w), 646 (w), 591 (s), 549 (w), 529 (m). Anal. Calc. for $C_{20}H_{24}N_2S$: C, 74.0; H, 7.5; N, 8.6. Found: C, 73.5; H, 7.4; N, 8.6%.

3.2.2 Synthesis of SpymXySe

A stirred mixture of [SpymXyH]Br (1.005 g, 2.797 mmol), elemental selenium (0.499 g, 3.618 mmol), and potassium carbonate (0.484 g, 3.502 mmol) in n-propanol (40 mL) was heated to reflux for 12 h. The resulting dark grey suspension was concentrated under reduced pressure to *ca.* 1 mL and triturated with pentane (10 mL). Removal of the volatiles under reduced pressure gives a grey solid residue. The product was extracted into dichloromethane (30 mL) and the light grey extract was washed with DI water (3 x 30 mL). The organic phase was separated, concentrated under vacuum to *ca.* 1 mL, and treated with pentane (10 mL), leading to the precipitation of the off-white product, which was isolated by filtration and dried *in vacuo* for 14 h (0.706 g, 68%). Mp = 284-286 °C (dec.). NMR data (in d_6 -acetone): 1H δ 2.32 (s, 12 H, CH_3), 2.46 (quintet, $^3J_{H-H} = 5.9$, 2 H, CH_2), 3.67 (t, $^3J_{H-H} = 5.9$, 4 H, CH_2), 7.06 (s, 6 H, C_6H_3); ^{13}C δ 18.3 (q, $^1J_{C-H} = 127$, 4 C, CH_3), 22.7 (t, $^1J_{C-H} = 132$, 1 C, CH_2), 48.8 (t, $^1J_{C-H} = 142$, 2 C, CH_2), 127.8 (d, $^1J_{C-H} =$

159, 2 C, C_p in C₆H₃), 129.2 (d, ¹J_{C-H} = 161, 4 C, C_m in C₆H₃), 135.9 (s, 4 C, C_o in C₆H₃), 146.7 (s, 2 C, C_{ipso} in C₆H₃), 177.3 (s, 1 C, C=Se). IR data: 2963 (w), 2943 (w), 2905 (w), 2867 (w), 1592 (w), 1495 (s), 1470 (m), 1446 (m), 1393 (w), 1370 (w), 1352 (w), 1301 (vs), 1263 (m), 1243 (w), 1208 (m), 1185 (w), 1166 (w), 1158 (w), 1082 (m), 1033 (m), 990 (w), 917 (w), 887 (w), 865 (w), 794 (s), 773 (s), 743 (w), 669 (w), 621 (w), 576 (w), 557 (m), 529 (m). Anal. Calc. for C₂₀H₂₄N₂Se: C, 64.7; H, 6.5; N, 7.5. Found: C, 64.2; H, 6.8; N, 7.4%.

3.2.3 Synthesis of SpymMesS

A stirred mixture of [SpymMesH]Br (1.006 g, 2.506 mmol), elemental sulfur (0.096 g, 2.994 mmol), and potassium carbonate (0.450 g, 3.256 mmol) in n-propanol (25 mL) was heated to reflux for 12 h. The resulting orange suspension was concentrated under reduced pressure to *ca.* 1 mL and triturated with pentane (10 mL). Removal of the volatiles under reduced pressure gives an orange solid residue. The product was extracted into dichloromethane (30 mL) and the pale orange extract was washed with DI water (3 x 30 mL). The organic phase was separated, concentrated under vacuum to *ca.* 1 mL, and treated with pentane (10 mL), leading to the precipitation of the off-white product, which was isolated by filtration and dried *in vacuo* for 14 h (0.671 g, 76%). ¹H NMR spectroscopic data match those previously reported.²³

3.2.4 Synthesis of SpymMesSe

A stirred mixture of [SpymMesH]Br (1.000 g, 2.491 mmol), elemental selenium (0.235 g, 2.976 mmol), and potassium carbonate (0.455 g, 3.292 mmol) in n-propanol (40 mL) was heated to reflux for 12 h. The resulting dark grey suspension was concentrated under reduced pressure to *ca.* 1 mL and triturated with pentane (10 mL). Removal of the volatiles under reduced pressure gives an grey solid residue. The product was extracted into dichloromethane (30 mL) and the light grey extract was washed with DI water (3 x 30 mL). The organic phase was separated, concentrated under vacuum to *ca.* 1 mL, and treated with pentane (10 mL), leading to the precipitation of the off-white product, which was isolated by filtration and dried *in vacuo* for 14 h (0.741 g, 75%). ¹H NMR spectroscopic data match those previously reported.¹¹

3.2.5 Synthesis of SpymDippS

A stirred mixture of [SpymDippH]Br (1.004 g, 2.068 mmol), elemental sulfur (0.084 g, 2.620 mmol), and potassium carbonate (0.450 g, 2.685 mmol) in n-propanol (25 mL) was heated to reflux for 12 h. The resulting orange suspension was concentrated under reduced pressure to *ca.* 1 mL and triturated with pentane (10 mL). Removal of the volatiles under reduced pressure gives an orange solid residue. The product was extracted into dichloromethane (30 mL) and the pale orange extract was washed with DI water (3 x 30 mL). The organic phase was separated, concentrated under vacuum to *ca.* 1 mL, and treated with pentane (10 mL), leading to the precipitation of the off-white product, which was isolated by filtration and dried *in vacuo* for 14 h (0.596 g, 66%). Mp

= 300-302 °C (dec.). ¹H NMR data (in d₆-acetone): δ 1.27 [d, ³J_{H-H} = 6.9, 12 H, CH(CH₃)₂], 1.28 [d, ³J_{H-H} = 6.9, 12 H, CH(CH₃)₂], 2.44 (quintet, ³J_{H-H} = 5.6, 1 H, CH₂), 3.18 [septet, ³J_{H-H} = 6.9, 4 H, CH(CH₃)₂], 3.73 (t, ³J_{H-H} = 5.8, 2 H, CH₂), 7.14-7.28 (m, 6 H, C₆H₃); ¹³C NMR data (in d₆-DMSO): δ 21.1 (t, ¹J_{C-H} = 134, 1 C, CH₂), 23.9 [q, ¹J_{C-H} = 129, 4 C, CH(CH₃)₂], 24.5 [q, ¹J_{C-H} = 126, 4 C, CH(CH₃)₂], 28.3 [d, ¹J_{C-H} = 129, 4 C, CH(CH₃)₂], 50.3 (t, ¹J_{C-H} = 143, 2 C, CH₂), 123.9 (d, ¹J_{C-H} = 156, 4 C, C_m in C₆H₃), 127.6 (d, ¹J_{C-H} = 158, 2 C, C_p in C₆H₃), 141.7 (s, 4 C, C_o in C₆H₃), 144.9 (s, 2 C, C_{ipso} in C₆H₃), 179.2 (s, 1 C, C=S). IR data: 2958 (m), 2927 (w), 2865 (m), 1588 (w), 1489 (s), 1474 (m), 1463 (m), 1450 (m), 1391 (w), 1381 (w), 1347 (m), 1314 (vs), 1297 (vs), 1256 (w), 1200 (s), 1162 (w), 1148 (w), 1102 (w), 1089 (w), 1057 (m), 936 (m), 884 (w), 856 (w), 800 (s), 763 (m), 751 (s), 725 (w), 670 (w), 648 (w), 616 (w), 588 (m).

3.2.6 Synthesis of SpymDippSe

A stirred mixture of [SpymDippH]Br (1.005 g, 2.070 mmol), elemental selenium (0.195 g, 2.475 mmol), and potassium carbonate (0.378 g, 2.735 mmol) in n-propanol (40 mL) was heated to reflux for 12 h. The resulting dark grey suspension was concentrated under reduced pressure to *ca.* 1 mL and triturated with pentane (10 mL). Removal of the volatiles under reduced pressure gives a grey solid residue. The product was extracted into dichloromethane (30 mL) and the light grey extract was washed with DI water (3 x 30 mL). The organic phase was separated, concentrated under vacuum to *ca.* 1 mL, and treated with pentane (10 mL), leading to the precipitation of the off-white product, which

was isolated by filtration and dried *in vacuo* for 14 h (0.641 g, 64%). Mp = 296-298 °C (dec.). ¹H NMR data (in d₆-acetone): δ 1.28 [d, ³J_{H-H} = 6.9, 12 H, CH(CH₃)₂], 1.35 [d, ³J_{H-H} = 6.9, 12 H, CH(CH₃)₂], 2.47 (quintet, ³J_{H-H} = 5.9, 1 H, CH₂), 3.17 [septet, ³J_{H-H} = 6.8, 4 H, CH(CH₃)₂], 3.71 (t, ³J_{H-H} = 5.8, 2 H, CH₂), 7.14-7.30 (m, 6 H, C₆H₃); ¹³C NMR data (in d₆-DMSO): δ 20.7 (t, ¹J_{C-H} = 132, 1 C, CH₂), 23.8 [q, ¹J_{C-H} = 125, 4 C, CH(CH₃)₂], 24.7 [q, ¹J_{C-H} = 125, 4 C, CH(CH₃)₂], 28.4 [d, ¹J_{C-H} = 129, 4 C, CH(CH₃)₂], 50.1 (t, ¹J_{C-H} = 144, 2 C, CH₂), 124.0 (d, ¹J_{C-H} = 155, 4 C, C_m in C₆H₃), 127.7 (d, ¹J_{C-H} = 159, 2 C, C_p in C₆H₃), 142.9 (s, 4 C, C_o in C₆H₃), 144.6 (s, 2 C, C_{ipso} in C₆H₃), 178.6 (s, 1 C, C=Se). IR data: 2959 (m), 2926 (w), 2865 (w), 1590 (w), 1493 (s), 1474 (w), 1463 (m), 1451 (m), 1390 (w), 1381 (w), 1343 (w), 1297 (vs), 1256 (w), 1201 (m), 1178 (w), 1162 (w), 1147 (w), 1103 (w), 1086 (w), 1057 (m), 984 (w), 937 (w), 884 (w), 799 (m), 763 (w), 750 (m), 612 (w), 590 (w), 554 (m).

3.3 Synthesis of (SpymArE)I₂

3.3.1 Synthesis of (SpymXyS)I₂

Dichloromethane (10 mL) was added to a mixture of elemental iodine (0.058 g, 0.229 mmol) and SpymXyS (0.083 g, 0.256 mmol), resulting in the formation of a dark brown solution. After stirring for 1 h, the solution was concentrated under reduced pressure to *ca.* 1 mL and treated with pentane (10 mL), leading to the separation of the brown product, which was isolated by filtration and dried *in vacuo* for 20 h (0.125 g, 94%). Mp = 190-192 °C (dec.). NMR data (in CD₂Cl₂): ¹H δ 2.36 (s, 12 H, CH₃), 2.41 (quintet, ³J_{H-H} = 5.9, 2 H, CH₂), 3.67 (t, ³J_{H-H} = 5.9, 4 H, CH₂), 7.13-7.25 (m, 6 H, C₆H₃); ¹³C δ

18.7 (q, $^1J_{C-H} = 127$, 4 C, CH_3), 21.4 (t, $^1J_{C-H} = 133$, 1 C, CH_2), 50.0 (t, $^1J_{C-H} = 144$, 2 C, CH_2), 128.8 (d, $^1J_{C-H} = 161$, 2 C, C_p in C_6H_3), 129.5 (d, $^1J_{C-H} = 163$, 4 C, C_m in C_6H_3), 135.1 (s, 4 C, C_o in C_6H_3), 143.0 (s, 2 C, C_{ipso} in C_6H_3), 171.4 (s, 1 C, $C=S$). IR data: 2962 (w), 2941 (w), 2912 (w), 2860 (w), 1590 (w), 1525 (s), 1468 (m), 1441 (m), 1396 (m), 1376 (w), 1315 (s), 1302 (vs), 1265 (w), 1241 (w), 1204 (m), 1184 (w), 1165 (m), 1105 (w), 1095 (w), 1078 (w), 1038 (m), 1001 (w), 986 (w), 887 (w), 835 (m), 774 (vs), 740 (m), 669 (w). Anal. Calc. for $C_{20}H_{24}I_2N_2S$: C, 41.5; H, 4.2; N, 4.8. Found: C, 41.8; H, 4.2; N, 4.8%.

3.3.2 Synthesis of (SpymXySe)I₂

Dichloromethane (10 mL) was added to a mixture of elemental iodine (0.051 g, 0.201 mmol) and SpymXySe (0.081 g, 0.218 mmol), resulting in the formation of a dark brown solution. After stirring for 1 h, the solution was concentrated under reduced pressure to *ca.* 1 mL and treated with pentane (10 mL), leading to the separation of the brown product, which was isolated by filtration and dried *in vacuo* for 20 h (0.089 g, 71%). Mp = 209-211 °C (dec.). NMR data (in CD_2Cl_2): 1H δ 2.36 (s, 12 H, CH_3), 2.46 (quintet, $^3J_{H-H} = 5.8$, 2 H, CH_2), 3.70 (t, $^3J_{H-H} = 5.8$, 4 H, CH_2), 7.16-7.26 (m, 6 H, C_6H_3); ^{13}C δ 18.8 (q, $^1J_{C-H} = 130$, 4 C, CH_3), 21.1 (t, $^1J_{C-H} = 133$, 1 C, CH_2), 50.2 (t, $^1J_{C-H} = 145$, 2 C, CH_2), 129.5 (d, $^1J_{C-H} = 161$, 2 C, C_p in C_6H_3), 129.7 (d, $^1J_{C-H} = 164$, 4 C, C_m in C_6H_3), 135.0 (s, 4 C, C_o in C_6H_3), 143.5 (s, 2 C, C_{ipso} in C_6H_3), 165.5 (s, 1 C, $C=Se$). IR data: 2969 (w), 2935 (w), 2911 (w), 1590 (w), 1532 (s), 1467 (m), 1452 (w), 1442 (w), 1397 (m), 1372 (w), 1349 (w), 1319 (s), 1302 (vs), 1266 (w), 1242 (w), 1224 (w), 1207 (m), 1182 (w), 1161 (m), 1110 (w), 1097 (w), 1076 (m), 1022 (m), 995 (m), 907 (w), 889 (w),

812 (m), 780 (vs), 743 (m), 670 (w). Anal. Calc. for $C_{20}H_{24}I_2N_2Se$: C, 38.4; H, 3.9; N, 4.5. Found: C, 38.3; H, 3.8; N, 4.6%.

3.3.3 Synthesis of (SpymMesS)I₂

Dichloromethane (10 mL) was added to a mixture of elemental iodine (0.049 g, 0.193 mmol) and SpymMesS (0.079 g, 0.224 mmol), resulting in the formation of a dark brown solution. After stirring for 1 h, the solution was concentrated under reduced pressure to *ca.* 1 mL and treated with pentane (10 mL), leading to the separation of the brown product, which was isolated by filtration and dried *in vacuo* for 16 h (0.078 g, 67%). Mp = 208-210 °C (dec.). NMR data (in CD_2Cl_2): 1H δ 2.31 (s, 12 H, CH_3), 2.31 (s, 6 H, CH_3), 2.39 (quintet, $^3J_{H-H} = 5.9$, 2 H, CH_2), 3.64 (t, $^3J_{H-H} = 5.9$, 4 H, CH_2), 6.98 (s, 4 H, C_6H_2); ^{13}C δ 18.6 (q, $^1J_{C-H} = 127$, 4 C, CH_3), 21.2 (q, $^1J_{C-H} = 127$, 2 C, CH_2), 21.3 (t, $^1J_{C-H} = 136$, 1 C, CH_2), 50.2 (t, $^1J_{C-H} = 144$, 2 C, CH_2), 130.1 (d, $^1J_{C-H} = 160$, 4 C, C_m in C_6H_2), 134.6 (s, 4 C, C_o in C_6H_2), 138.9 (s, 2 C, C_p in C_6H_2), 140.5 (s, 2 C, C_{ipso} in C_6H_2), 170.9 (s, 1 C, $C=S$). IR data: 2967 (w), 2909 (w), 2847 (w), 2726 (w), 1608 (w), 1523 (s), 1475 (m), 1438 (w), 1396 (m), 1371 (w), 1349 (w), 1321 (vs), 1302 (vs), 1256 (w), 1229 (w), 1208 (s), 1155 (w), 1105 (w), 1088 (w), 1045 (m), 1013 (w), 989 (w), 952 (w), 892 (w), 850 (m), 833 (s), 758 (w), 723 (w). Anal. Calc. for $C_{22}H_{28}I_2N_2S$: C, 43.6; H, 4.7; N, 4.6. Found: C, 43.8; H, 4.8; N, 4.6%.

3.3.4 Synthesis of (SpymMesSe)I₂

Dichloromethane (10 mL) was added to a mixture of elemental iodine (0.043 g, 0.169 mmol) and SpymMesSe (0.085 g, 0.213 mmol), resulting in the formation of a dark brown solution. After stirring for 1 h, the solution was concentrated under reduced

pressure to *ca.* 1 mL and treated with pentane (10 mL), leading to the separation of the brown product, which was isolated by filtration and dried *in vacuo* for 16 h (0.106 g, 96%). Mp = 224-227 °C (dec.). NMR data (in CD₂Cl₂): ¹H δ 2.31 (s, 12 H, CH₃), 2.32 (s, 6 H, CH₃), 2.42 (quintet, ³J_{H-H} = 5.8, 2 H, CH₂), 3.67 (t, ³J_{H-H} = 5.8, 4 H, CH₂), 6.99 (s, 4 H, C₆H₂); ¹³C δ 18.7 (q, ¹J_{C-H} = 128, 4 C, CH₃), 21.1 (t, ¹J_{C-H} = 135, 1 C, CH₂), 21.2 (q, ¹J_{C-H} = 128, 2 C, CH₂), 50.3 (t, ¹J_{C-H} = 145, 2 C, CH₂), 130.3 (d, ¹J_{C-H} = 162, 4 C, C_m in C₆H₂), 134.6 (s, 4 C, C_o in C₆H₂), 139.6 (s, 2 C, C_p in C₆H₂), 141.2 (s, 2 C, C_{ipso} in C₆H₂), C=Se not observed. IR data: 2966 (w), 2908 (w), 2845 (w), 2725 (w), 1607 (m), 1532 (s), 1474 (m), 1446 (m), 1397 (m), 1371 (m), 1321 (m), 1304 (vs), 1253 (m), 1228 (w), 1208 (s), 1165 (w), 1106 (w), 1082 (w), 1026 (m), 996 (w), 982 (w), 950 (w), 892 (w), 851 (m), 810 (m), 721 (w). Anal. Calc. for C₂₂H₂₈I₂N₂Se: C, 40.5; H, 4.3; N, 4.3. Found: C, 40.3; H, 4.2; N, 4.3%.

3.3.5 Synthesis of (SpymDippS)I₂

Diethyl ether (10 mL) was added to a mixture of elemental iodine (0.040 g, 0.158 mmol) and SpymDippS (0.080 g, 0.183 mmol), resulting in the formation of a dark brown solution. After stirring for 8 h, the solution was concentrated under reduced pressure to *ca.* 1 mL and treated with pentane (10 mL), leading to the separation of the brown product, which was isolated by filtration and dried *in vacuo* for 16 h (0.088 g, 81%). Mp = 148-150 °C (dec.). NMR data (in CD₂Cl₂): ¹H δ 1.28 [d, ³J_{H-H} = 6.9, 12 H, CH(CH₃)₂], 1.33 [d, ³J_{H-H} = 6.9, 12 H, CH(CH₃)₂], 2.36 (quintet, ³J_{H-H} = 5.6, 2 H, CH₂), 2.98 [septet, ³J_{H-H} = 6.9, 4 H, CH(CH₃)₂], 3.66 (t, ³J_{H-H} = 5.8, 4 H, CH₂), 7.20 (d, ³J_{H-H} = 8.0, 4 H, C₆H₃), 7.35 (t, ³J_{H-H} = 8.0, 2 H, C₆H₃); ¹³C δ 21.2 (t, ¹J_{C-H} = 133, 1 C, CH₂), 24.1 [q, ¹J_{C-H} = 131, 4 C, CH(CH₃)₂], 25.3 [q, ¹J_{C-H} = 126, 4 C, CH(CH₃)₂], 29.6 [d, ¹J_{C-H} = 126, 4 C,

CH(CH₃)₂], 51.9 (t, ¹J_{C-H} = 144, 2 C, CH₂), 125.2 (d, ¹J_{C-H} = 155, 4 C, C_m in C₆H₃), 129.6 (d, ¹J_{C-H} = 161, 2 C, C_p in C₆H₃), 140.6 (s, 4 C, C_{ipso} in C₆H₃), 145.7 (s, 2 C, C_o in C₆H₃), 174.7 (s, 1 C, C=S). IR data: 2960 (w), 2925 (w), 2865 (w), 1656 (w), 1589 (w), 1548 (w), 1517 (m), 1459 (w), 1439 (w), 1396 (w), 1381 (w), 1308 (s), 1262 (w), 1222 (w), 1206 (w), 1177 (w), 1160 (w), 1099 (w), 1081 (m), 1055 (m), 1042 (s), 934 (w), 884 (w), 837 (m), 793 (m), 752 (s), 725 (m), 673 (w). Anal. Calc. for C₂₈H₄₀I₂N₂S: C, 48.7; H, 5.8; N, 4.1. Found: C, 48.0; H, 5.6; N, 4.0%.

3.3.6 Synthesis of (SpymDippSe)I₂

Dichloromethane (10 mL) was added to a mixture of elemental iodine (0.038 g, 0.142 mmol) and SpymDippSe (0.081 g, 0.167 mmol), resulting in the formation of a dark brown solution. After stirring for 1 h, the solution was concentrated under reduced pressure to *ca.* 1 mL and treated with pentane (10 mL), leading to the separation of the brown product, which was isolated by filtration and dried *in vacuo* for 18 h (0.065 g, 62%). Mp = 168-170 °C (dec.). IR data: 2962 (m), 2923 (w), 2864 (w), 1660 (w), 1588 (w), 1529 (s), 1458 (w), 1450 (w), 1397 (w), 1380 (w), 1361 (w), 1353 (w), 1317 (s), 1308 (vs), 1258(w), 1219 (w), 1206 (m), 1177 (w), 1146 (w), 1101 (w), 1078 (w), 1054 (w), 1043 (m), 1028 (w), 996 (w), 933 (w), 883 (w), 815 (w), 798 (s), 793 (s), 752 (s), 724 (w), 694 (w), 673 (w).

3.4 Synthesis of (SpymXyS)HgX₂

3.4.1 Synthesis of (SpymXyS)HgCl₂

Acetonitrile (8 mL) was added to a mixture of HgCl₂ (0.061 g, 0.225 mmol) and SpymXyS (0.080 g, 0.247 mmol), resulting in the formation of a pale yellow solution, which was stirred for 24 h. Concentration of the solution under reduced pressure to *ca.* 1 mL and addition of diethyl ether (10 mL) led to the separation of the off-white product, which was isolated by filtration and dried *in vacuo* for 18 h (0.111 g, 83%). Mp = 242-244 °C (dec.). NMR data (in d₆-acetone): ¹H δ 2.38 (s, 12 H, CH₃), 2.53 (quintet, ³J_{H-H} = 5.9, 2 H, CH₂), 3.91 (t, ³J_{H-H} = 5.9, 4 H, CH₂), 7.15-7.19 (m, 6 H, C₆H₃); ¹³C δ 18.3 (q, ¹J_{C-H} = 127, 4 C, CH₃), 21.9 (t, ¹J_{C-H} = 133, 1 C, CH₂), 50.6 (t, ¹J_{C-H} = 144, 2 C, CH₂), 129.8 (d, ¹J_{C-H} = 161, 2 C, C_p in C₆H₃), 130.5 (d, ¹J_{C-H} = 159, 4 C, C_m in C₆H₃), 135.8 (s, 2 C, C_o in C₆H₃), 143.5 (s, 4 C, C_{ipso} in C₆H₃), C=S not observed. IR data: 2918 (w), 1591 (w), 1535 (s), 1468 (m), 1445 (w), 1400 (m), 1379 (w), 1329 (s), 1308 (s), 1266 (w), 1244 (w), 1211 (m), 1186 (w), 1162 (w), 1078 (w), 1032 (w), 999 (w), 833 (m), 800 (w), 774 (s), 670 (w). Anal. Calc. for C₂₀H₂₄Cl₂HgN₂S: C, 40.3; H, 4.1; N, 4.7. Found: C, 40.5; H, 4.2; N, 4.7%.

3.4.2 Synthesis of (SpymXyS)HgBr₂

Acetonitrile (8 mL) was added to a mixture of HgBr₂ (0.081 g, 0.225 mmol) and SpymXyS (0.080 g, 0.247 mmol), resulting in the formation of an off-white solid and a pale yellow solution. After stirring for 24 h, the suspension was concentrated under reduced pressure to *ca.* 3 mL, treated with diethyl ether (10 mL), and the product was isolated by filtration and dried *in vacuo* for 18 h (0.120 g, 78%). Mp = 240-243 °C

(dec.). NMR data (in d_6 -acetone): ^1H δ 2.38 (s, 12 H, CH_3), 2.53 (quintet, $^3\text{J}_{\text{H-H}} = 6.0$, 2 H, CH_2), 3.90 (t, $^3\text{J}_{\text{H-H}} = 5.9$, 4 H, CH_2), 7.16-7.19 (m, 6 H, C_6H_3); ^{13}C δ 18.4 (q, $^1\text{J}_{\text{C-H}} = 128$, 4 C, CH_3), 21.9 (t, $^1\text{J}_{\text{C-H}} = 134$, 1 C, CH_2), 50.6 (t, $^1\text{J}_{\text{C-H}} = 143$, 2 C, CH_2), 129.8 (d, $^1\text{J}_{\text{C-H}} = 161$, 2 C, C_p in C_6H_3), 130.7 (d, $^1\text{J}_{\text{C-H}} = 157$, 4 C, C_m in C_6H_3), 135.8 (s, 2 C, C_o in C_6H_3), 143.4 (s, 4 C, C_{ipso} in C_6H_3), C=S not observed. IR data: 3023 (w), 2980 (w), 2931 (w), 1592 (w), 1536 (s), 1469 (m), 1442 (m), 1400 (m), 1378 (w), 1332 (s), 1305 (s), 1266 (w), 1243 (w), 1209 (m), 1186 (w), 1170 (w), 1163 (w), 1110 (w), 1077 (w), 1029 (w), 1001 (w), 982 (w), 917 (w), 885 (w), 835 (m), 782 (s), 766 (s), 739 (w), 669 (w). Anal. Calc. for $\text{C}_{20}\text{H}_{24}\text{Br}_2\text{HgN}_2\text{S}$: C, 35.1; H, 3.5; N, 4.1. Found: C, 35.5; H, 3.8; N, 4.3%.

3.4.3 Synthesis of (SpymXyS)HgI₂

Acetonitrile (8 mL) was added to a mixture of HgI_2 (0.102 g, 0.224 mmol) and SpymXyS (0.080 g, 0.247 mmol), resulting in the formation of an off-white solid and a pale yellow solution. After stirring for 24 h, the suspension was concentrated under reduced pressure to *ca.* 3 mL, treated with diethyl ether (10 mL), and the product was isolated by filtration and dried *in vacuo* for 18 h (0.109 g, 62%). Mp = 220-223 °C (dec.). NMR data (in d_6 -acetone): ^1H δ 2.39 (s, 12 H, CH_3), 2.53 (quintet, $^3\text{J}_{\text{H-H}} = 5.9$, 2 H, CH_2), 3.90 (t, $^3\text{J}_{\text{H-H}} = 5.9$, 4 H, CH_2), 7.18 (s, 6 H, C_6H_3); ^{13}C δ 18.7 (q, $^1\text{J}_{\text{C-H}} = 129$, 4 C, CH_3), 21.9 (t, $^1\text{J}_{\text{C-H}} = 128$, 1 C, CH_2), 50.4 (t, $^1\text{J}_{\text{C-H}} = 147$, 2 C, CH_2), 129.7 (d, $^1\text{J}_{\text{C-H}} = 160$, 2 C, C_p in C_6H_3), 130.8 (d, $^1\text{J}_{\text{C-H}} = 159$, 4 C, C_m in C_6H_3), 135.7 (s, 2 C, C_o in C_6H_3), 143.7 (s, 4 C, C_{ipso} in C_6H_3), C=S not observed. IR data: 3022 (w), 2934 (w), 2913 (w), 2879 (w), 1591 (w), 1522 (s), 1467 (m), 1442 (m), 1397 (m), 1377 (w), 1354 (w), 1329 (s), 1303 (s), 1264 (w), 1242 (w), 1209 (m), 1185 (w), 1164 (w), 1109 (w), 1078 (w), 1029 (w), 1001 (w),

984 (w), 910 (w), 885 (w), 839 (m), 810 (w), 781 (s), 768 (s), 740 (w), 669 (w). Anal. Calc. for $C_{20}H_{24}HgI_2N_2S$: C, 30.8; H, 3.1; N, 3.6. Found: C, 30.7; H, 3.1; N, 3.6%.

3.5 Synthesis of (SpymXySe)HgX₂

3.5.1 Synthesis of (SpymXySe)HgCl₂

Acetonitrile (10 mL) was added to a mixture of HgCl₂ (0.054 g, 0.199 mmol) and SpymXySe (0.080 g, 0.215 mmol) resulting in the formation of an off-white solid and a colorless solution. After stirring for 24 h, the suspension was concentrated under pressure to *ca.* 1 mL, treated with diethyl ether (10 mL), and the product was isolated by filtration and dried *in vacuo* for 24 h (0.065 g, 51%). Mp= 272-274 °C (dec.). NMR data (in d₆-acetone): ¹H δ 2.41 (s, 12 H, CH₃), 2.59 (quintet, ³J_{H-H} = 5.9, 2 H, CH₂), 3.98 (t, ³J_{H-H} = 5.9, 4 H, CH₂), 7.18-7.27 (m, 6 H, C₆H₃); ¹³C δ 18.4 (q, ¹J_{C-H} = 128, 4 C, CH₃), 21.5 (t, ¹J_{C-H} = 134, 1 C, CH₂), 50.8 (t, ¹J_{C-H} = 146, 2 C, CH₂), 130.3 (d, ¹J_{C-H} = 161, 2 C, C_p in C₆H₃), 130.8 (d, ¹J_{C-H} = 163, 4 C, C_m in C₆H₃), 135.6 (s, 2 C, C_o in C₆H₃), 144.4 (s, 4 C, C_{ipso} in C₆H₃), C=Se not observed. IR data: 2917 (w), 1592 (w), 1541 (s), 1469 (m), 1442 (w), 1401 (w), 1379 (w), 1324 (m), 1306 (s), 1267 (w), 1240 (w), 1210 (m), 1185 (w), 1168 (w), 1096 (w), 1077 (w), 1036 (w), 995 (w), 912 (w), 814 (w), 785 (s), 744 (w), 670 (w). Anal. Calc. for $C_{20}H_{24}Cl_2HgN_2Se$: C, 37.4; H, 3.8; N, 4.4. Found: C, 37.4; H, 3.7; N, 4.5%.

3.5.2 Synthesis of (SpymXySe)HgBr₂

Acetonitrile (10 mL) was added to a mixture of HgBr₂ (0.071 g, 0.197 mmol) and SpymXySe (0.081 g, 0.218 mmol), resulting in the formation of an off-white solid and a

colorless solution. After stirring for 24 h, the suspension was concentrated under pressure to *ca.* 1 mL, treated with diethyl ether (10 mL), and the product was isolated by filtration and dried *in vacuo* for 4 h (0.083 g, 58%). Mp= 276-278 °C (dec.). NMR data (in d_6 -acetone): ^1H δ 2.41 (s, 12 H, CH_3), 2.58 (quintet, $^3\text{J}_{\text{H-H}} = 5.8$, 2 H, CH_2), 3.96 (t, $^3\text{J}_{\text{H-H}} = 5.8$, 4 H, CH_2), 7.16-7.22 (m, 6 H, C_6H_3); ^{13}C δ 18.5 (q, $^1\text{J}_{\text{C-H}} = 126$, 4 C, CH_3), 21.5 (t, $^1\text{J}_{\text{C-H}} = 131$, 1 C, CH_2), 50.7 (t, $^1\text{J}_{\text{C-H}} = 145$, 2 C, CH_2), 130.3 (d, $^1\text{J}_{\text{C-H}} = 161$, 2 C, C_p in C_6H_3), 130.8 (d, $^1\text{J}_{\text{C-H}} = 160$, 4 C, C_m in C_6H_3), 135.5 (s, 2 C, C_o in C_6H_3), 144.4 (s, 4 C, C_{ipso} in C_6H_3), C=Se not observed. IR data: 3024 (w), 2916 (w), 1592 (w), 1540 (s), 1468 (m), 1440 (w), 1400 (w), 1378 (w), 1353 (w), 1326 (m), 1304 (s), 1264 (w), 1242 (w), 1208 (m), 1183 (w), 1163 (w), 1109 (w), 1096 (w), 1075 (w), 1030 (w), 997 (w), 981 (w), 908 (w), 885 (w), 812 (w), 779 (s), 767 (s), 738 (w), 669 (w). Anal. Calc. for $\text{C}_{20}\text{H}_{24}\text{Br}_2\text{HgN}_2\text{Se}$: C, 32.8; H, 3.3; N, 3.8. Found: C, 32.9; H, 3.3; N, 3.8%.

3.5.3 Synthesis of (SpymXySe)HgI₂

Acetonitrile (10 mL) was added to a mixture of HgI_2 (0.092 g, 0.202 mmol) and SpymXySe (0.080 g, 0.215 mmol), resulting in the formation of a pale yellow solid and a colorless solution. After stirring for 24 h, the suspension was concentrated under pressure to *ca.* 1 mL, treated with diethyl ether (10 mL), and the product was isolated by filtration and dried *in vacuo* for 4 h (0.118 g, 71%). Mp = 265-267 °C (dec.). NMR data (in d_6 -acetone): ^1H δ 2.40 (s, 12 H, CH_3), 2.56 (quintet, $^3\text{J}_{\text{H-H}} = 5.9$, 2 H, CH_2), 3.94 (t, $^3\text{J}_{\text{H-H}} = 5.9$, 4 H, CH_2), 7.19 (s, 6 H, C_6H_3); ^{13}C δ 18.8 (q, $^1\text{J}_{\text{C-H}} = 127$, 4 C, CH_3), 21.6 (t, $^1\text{J}_{\text{C-H}} = 133$, 1 C, CH_2), 50.6 (t, $^1\text{J}_{\text{C-H}} = 143$, 2 C, CH_2), 130.2 (d, $^1\text{J}_{\text{C-H}} = 161$, 2 C, C_p in C_6H_3), 130.9 (d, $^1\text{J}_{\text{C-H}} = 163$, 4 C, C_m in C_6H_3), 135.4 (s, 2 C, C_o in C_6H_3), 144.6 (s, 4 C, C_{ipso} in C_6H_3), C=Se not observed. IR data: 3023 (w), 2913 (w), 1592 (w), 1592 (w),

1533 (s), 1467 (s), 1439 (m), 1398 (m), 1377 (w), 1353 (w), 1323 (s), 1303 (s), 1263 (m), 1241 (m), 1208 (m), 1181 (w), 1163 (m), 1107 (w), 1096 (w), 1076 (w), 1029 (w), 996 (w), 981 (w), 909 (w), 885 (w), 813 (w), 777 (s), 767 (m), 744 (w), 738 (w), 669 (w).
 Anal. Calc. for $C_{20}H_{24}HgI_2N_2Se$: C, 29.1; H, 2.9; N, 3.4. Found: C, 29.3; H, 2.9; N, 3.5%.

3.6 Synthesis of (SpymMesS)HgX₂

3.6.1 Synthesis of (SpymMesS)HgCl₂

Acetonitrile (10 mL) was added to a mixture of HgCl₂ (0.059 g, 0.217 mmol) and SpymMesS (0.080 g, 0.227 mmol), resulting in the formation of a pale yellow solution. After stirring for 24 h, the solution was concentrated under reduced pressure to *ca.* 1 mL and treated with diethyl ether (10 mL), leading to the separation of the off-white product, which was isolated by filtration and dried *in vacuo* for 18 h (0.119, 88%). Mp = 202-204 °C (dec.). NMR data (in d₆-acetone): ¹H δ 2.21 (s, 6 H, CH₃), 2.32 (s, 12 H, CH₃), 2.50 (quintet, ³J_{H-H} = 5.9, 2 H, CH₂), 3.86 (t, ³J_{H-H} = 5.9, 4 H, CH₂), 6.96 (s, 4 H, C₆H₂); ¹³C δ 18.2 (q, ¹J_{C-H} = 128, 4 C, CH₃), 21.0 (q, ¹J_{C-H} = 128, 2 C, CH₃), 21.8 (t, ¹J_{C-H} = 129, 1 C, CH₂), 50.8 (t, ¹J_{C-H} = 150, 2 C, CH₂), 131.3 (d, ¹J_{C-H} = 159, 4 C, C_m in C₆H₂), 134.4 (s, 4 C, C_o in C₆H₂), 139.8 (s, 2 C, C_p in C₆H₂), 140.9 (s, 2 C, C_{ipso} in C₆H₂), C=S not observed. IR data: 2976 (w), 2917 (w), 1660 (m), 1607 (m), 1528 (vs), 1474 (s), 1443 (m), 1404 (m), 1379 (m), 1355 (w), 1330 (vs), 1312 (vs), 1303 (vs), 1258 (m), 1212 (s), 1148 (w), 1105 (w), 1086 (w), 1030 (m), 888 (w), 853 (s), 829 (m), 756 (w), 720 (w).
 Anal. Calc. for $C_{22}H_{28}Cl_2HgN_2S$: C, 42.3; H, 4.5; N, 4.5. Found: C, 42.0; H, 4.6; N, 4.7%.

3.6.2 Synthesis of [Hg(SpymMesS)₂][Hg₂Br₆]

Acetonitrile (10 mL) was added to a mixture of HgBr₂ (0.123 g, 0.341 mmol) and SpymMesS (0.088 g, 0.250 mmol), resulting in the formation of an off-white solid and a pale yellow solution. After stirring for 24 h, the suspension was concentrated under reduced pressure to *ca.* 1 mL and treated with diethyl ether (10 mL), leading to the separation of the off-white product, which was isolated by filtration and dried *in vacuo* for 18 h (0.194, 96%). Mp = 250-251 °C. NMR data (in d₆-acetone): ¹H δ 2.22 (s, 6 H, CH₃), 2.34 (s, 12 H, CH₃), 2.52 (quintet, ³J_{H-H} = 5.8, 2 H, CH₂), 3.91 (t, ³J_{H-H} = 5.8, 4 H, CH₂), 6.99 (s, 6 H, C₆H₂); ¹³C δ 18.3 (q, ¹J_{C-H} = 126, 4 C, CH₃), 21.0 (q, ¹J_{C-H} = 124, 2 C, CH₃), 22.1 (t, ¹J_{C-H} = 130, 1 C, CH₂), 50.3 (t, ¹J_{C-H} = 146, 2 C, CH₂), 130.4 (d, ¹J_{C-H} = 158, 4 C, C_m in C₆H₂), 135.4 (s, 4 C, C_o in C₆H₂), 139.0 (s, 2 C, C_p in C₆H₂), 141.6 (s, 2 C, C_{ipso} in C₆H₂), C=S not observed. IR data: 2921 (w), 1606 (w), 1524 (vs), 1473 (m), 1446 (m), 1401 (m), 1377 (w), 1352 (w), 1328 (vs), 1320 (m), 1310 (s), 1301 (s), 1258 (m), 1229 (w), 1209 (s), 1105 (w), 758 (w), 1029 (m), 946 (w), 887 (w), 850 (s), 841 (s), 782 (w), 726 (w). Anal. Calc. for C₄₄H₅₆Br₆Hg₃N₄S₂: C, 29.6; H, 3.2; N, 3.1. Found: C, 29.6; H, 3.0; N, 3.1%.

3.6.3 Synthesis of (SpymMesS)HgI₂

Acetonitrile (10 mL) was added to a mixture of HgI₂ (0.103 g, 0.227 mmol) and SpymMesS (0.088 g, 0.250 mmol), resulting in the formation of a pale yellow solid and a colorless solution. After stirring for 24 h, the suspension was concentrated under reduced pressure to *ca.* 1 and treated with diethyl ether (10 mL), leading to the separation of the off-white product, which was isolated by filtration and dried *in vacuo* for 18 h (0.141 g, 77%). Mp = 224-226 °C (dec.). NMR data (in d₆-acetone): ¹H δ 2.09 (s, 6 H, CH₃), 2.33

(s, 12 H, CH_3), 2.49 (quintet, $^3J_{H-H} = 5.9$, 2 H, CH_2), 3.89 (t, $^3J_{H-H} = 5.9$, 4 H, CH_2), 6.96 (s, 6 H, C_6H_2); ^{13}C δ 18.5 (q, $^1J_{C-H} = 127$, 4 C, CH_3), 21.1 (q, $^1J_{C-H} = 126$, 2 C, CH_3), 22.1 (t, 1 C, CH_2), 50.3 (t, $^1J_{C-H} = 144$, 2 C, CH_2), 131.2 (d, $^1J_{C-H} = 154$, 4 C, C_m in C_6H_2), 135.3 (s, 4 C, C_o in C_6H_2), 139.1 (s, 2 C, C_p in C_6H_2), 141.6 (s, 2 C, C_{ipso} in C_6H_2), $C=S$ not observed. IR data: 2965 (w), 2906 (w), 1607 (w), 1525 (vs), 1474 (m), 1442 (m), 1398 (m), 1374 (w), 1330 (vs), 1302 (vs), 1257 (m), 1233 (w), 1209 (s), 1102 (m), 1086 (m), 1030 (m), 882 (w), 852 (s), 834 (s), 802 (m), 718 (m). Anal. Calc. for $C_{22}H_{28}HgI_2N_2S$: C, 32.8; H, 3.5; N, 3.5. Found: C, 32.8; H, 3.5; N, 3.6%.

3.7 Synthesis of (SpymMesSe)HgX₂

3.7.1 Synthesis of (SpymMesSe)HgCl₂

Acetonitrile (10 mL) was added to a mixture of $HgCl_2$ (0.052 g, 0.192 mmol) and SpymMesSe (0.082 g, 0.205 mmol) resulting in the formation of a pale yellow solution, which was stirred for 24 h. Concentration of the solution under reduced pressure to *ca.* 1 mL and addition of diethyl ether (10 mL) led to the separation of the off-white product, which was isolated by filtration and dried *in vacuo* for 1 h (0.069 g, 54%). Mp = 280-282 °C (dec.). 1H NMR data (in d_6 -acetone): δ 2.20 (s, 6 H, CH_3), 2.33 (s, 12 H, CH_3), 2.53 (quintet, $^3J_{H-H} = 5.8$, 2 H, CH_2), 3.89 (t, $^3J_{H-H} = 5.8$, 4 H, CH_2), 6.97 (s, 4 H, C_6H_2). ^{13}C NMR data (in d_6 -DMSO): δ 17.5 (q, $^1J_{C-H} = 128$, 4 C, CH_3), 20.5 (t, $^1J_{C-H} = 132$, 1 C, CH_2), 20.6 (q, $^1J_{C-H} = 126$, 2 C, CH_3), 49.5 (t, $^1J_{C-H} = 146$, 2 C, CH_2), 130.1 (d, $^1J_{C-H} = 161$, 4 C, C_m in C_6H_2), 134.0 (s, 4 C, C_o in C_6H_2), 138.4 (s, 2 C, C_p in C_6H_2), 140.1 (s, 2 C, C_{ipso} in C_6H_2), $C=Se$ not observed. IR data: 2970 (w), 2914 (w), 1606 (m), 1532 (s), 1473 (m), 1444 (w), 1397 (m), 1376 (m), 1355 (w), 1325 (w), 1310 (s), 1300 (s), 1253

(m), 1211 (m), 1153 (w), 1105 (w), 1084 (w), 1028 (m), 998 (w), 952 (w), 907 (w), 899 (w), 888 (w), 861 (m), 847 (m), 812 (m), 754 (w), 717 (w). Anal. Calc. for $C_{22}H_{28}Cl_2HgN_2Se$: C, 39.4; H, 4.2; N, 4.2. Found: C, 39.4; H, 4.1; N, 4.2%.

3.7.2 Synthesis of (SpymMesSe)HgBr₂

Acetonitrile (10 mL) was added to a mixture of HgBr₂ (0.067 g, 0.186 mmol) and SpymMesSe (0.081 g, 0.203 mmol), resulting in the formation of an off-white solid and a colorless solution. The suspension was stirred for 24 h, concentrated under reduced pressure to *ca.* 1 mL, treated with diethyl ether (10 mL), and the product was isolated by filtration and dried *in vacuo* for 1 h (0.076 g, 54%). Mp = 278-280 °C (dec.). NMR data (in d₆-acetone): ¹H δ 2.19 (s, 6 H, CH₃), 2.33 (s, 12 H, CH₃), 2.52 (quintet, ³J_{H-H} = 5.8, 2 H, CH₂), 3.89 (t, ³J_{H-H} = 5.8, 4 H, CH₂), 6.97 (s, 4 H, C₆H₂); ¹³C δ 18.4 (q, ¹J_{C-H} = 129, 4 C, CH₃), 21.2 (q, ¹J_{C-H} = 129, 2 C, CH₃), 21.5 (t, ¹J_{C-H} = 137, 1 C, CH₂), 50.8 (t, ¹J_{C-H} = 145, 2 C, CH₂), 131.5 (d, ¹J_{C-H} = 160, 4 C, C_m in C₆H₂), 135.1 (s, 4 C, C_o in C₆H₂), 140.3 (s, 2 C, C_p in C₆H₂), 142.0 (s, 2 C, C_{ipso} in C₆H₂), C=Se not observed. IR data: 2970 (w), 2939 (w), 2913 (w), 2876 (w), 2732 (w), 1803 (w), 1762 (w), 1724 (w), 1606 (m), 1530 (s), 1473 (m), 1448 (w), 1397 (m), 1376 (m), 1355 (w), 1323 (w), 1308 (w), 1298 (s), 1251 (m), 1226 (w), 1211 (m), 1192 (w), 1154 (w), 1104 (w), 1085 (w), 1029 (m), 999 (w), 951 (w), 907 (w), 882 (w), 861 (m), 846 (m), 812 (w), 754 (w), 724 (w). Anal. Calc. for $C_{22}H_{28}Br_2HgN_2Se$: C, 34.8; H, 3.7; N, 3.7. Found: C, 34.8; H, 3.5; N, 3.6%.

3.7.3 Synthesis of (SpymMesSe)HgI₂

Acetonitrile (10 mL) was added to a mixture of HgI₂ (0.087 g, 0.191 mmol) and SpymMesSe (0.082 g, 0.205 mmol), resulting in the formation of a pale yellow solid and a colorless solution. The suspension was stirred for 24 h, concentrated under reduced pressure to *ca.* 1 mL, treated with diethyl ether (10 mL), and the product was isolated by filtration and dried *in vacuo* for 1 h (0.095 g, 58%). Mp = 280-282 °C (dec.). NMR data (in d₆-acetone): ¹H δ 2.18 (s, 6 H, CH₃), 2.34 (s, 12 H, CH₃), 2.52 (quintet, ³J_{H-H} = 5.8, 2 H, CH₂), 3.88 (t, ³J_{H-H} = 5.8, 4 H, CH₂), 6.96 (s, 4 H, C₆H₂); ¹³C δ 18.7 (q, ¹J_{C-H} = 126, 4 C, CH₃), 21.2 (q, ¹J_{C-H} = 126, 2 C, CH₃), 21.6 (t, ¹J_{C-H} = 125, 1 C, CH₂), 50.7 (t, ¹J_{C-H} = 147, 2 C, CH₂), 131.6 (d, ¹J_{C-H} = 157, 4 C, C_m in C₆H₂), 135.0 (s, 4 C, C_o in C₆H₂), 140.2 (s, 2 C, C_p in C₆H₂), 142.2 (s, 2 C, C_{ipso} in C₆H₂), C=Se not observed. IR data: 2912 (w), 2733 (w), 1607 (m), 1532 (s), 1473 (m), 1446 (m), 1397 (m), 1376 (m), 1355 (w), 1325 (w), 1301 (s), 1251 (m), 1231 (w), 1210 (m), 1193 (w), 1154 (w), 1105 (w), 1082 (w), 1031 (w), 1012 (w), 998 (w), 951 (w), 901 (w), 882 (w), 852 (m), 847 (m), 810 (m), 755 (w), 716 (w). Anal. Calc. for C₂₂H₂₈HgI₂N₂Se: C, 31.0; H, 3.3; N, 3.3. Found: C, 30.7; H, 3.2; N, 3.2%.

3.8 Synthesis of [Hg(SpymDippS)₂][Hg₂X₆]

3.8.1 Synthesis of [Hg(SpymDippS)₂][Hg₂Cl₆]

Acetonitrile (10 mL) was added to a mixture of HgCl₂ (0.068 g, 0.250 mmol) and SpymDippS (0.080 g, 0.183 mmol), resulting in the formation of a pale yellow solution. After stirring for 24 h, the solution was concentrated under reduced pressure to *ca.* 1 mL and treated with diethyl ether (10 mL), leading to the separation of the off-white product,

which was isolated by filtration and dried *in vacuo* for 18 h (0.055 g, 39%). Mp = 272-274 °C (dec.). ¹H NMR data (in d₆-acetone): δ 1.29 [d, ³J_{H-H} = 6.9, 12 H, CH(CH₃)₂], 1.35 [d, ³J_{H-H} = 6.9, 12 H, CH(CH₃)₂], 2.53 (quintet, ³J_{H-H} = 5.8, 2 H, CH₂), 3.17 [septet, ³J_{H-H} = 6.9, 4 H, CH(CH₃)₂], 3.88 (t, ³J_{H-H} = 5.8, 4 H, CH₂), 7.26-7.41 (m, 6 H, C₆H₃); ¹³C NMR data (in d₆-DMSO): δ 20.5 (t, ¹J_{C-H} = 131, 2 C, CH₂), 23.9 (q, ¹J_{C-H} = 127, 8 C, CH₃), 24.6 (q, ¹J_{C-H} = 127, 8 C, CH₃), 28.4 (d, ¹J_{C-H} = 128, 8 C, CH), 51.2 (t, ¹J_{C-H} = 144, 4 C, CH₂), 124.7 (d, ¹J_{C-H} = 160, 8 C, C_m in C₆H₃), 128.8 (d, ¹J_{C-H} = 160, 4 C, C_p in C₆H₃), 140.5 (s, 8 C, C_o in C₆H₃), 144.8 (s, 4 C, C_{ipso} in C₆H₃), C=S not observed. IR data: 2965 (s), 2923 (w), 2867 (m), 2844 (w), 1587 (m), 1552 (s), 1474 (w), 1460 (m), 1446 (w), 1408 (w), 1385 (w), 1363 (w), 1330 (s), 1313 (s), 1260 (w), 1216 (m), 1180 (w), 1101 (w), 1056 (vs), 1033 (vs), 1015 (m), 936 (w), 831 (w), 805 (vs), 760 (s), 724 (w). Anal. Calc. for C₅₆H₈₀Cl₆Hg₃N₄S₂: C, 39.9; H, 4.8; N, 3.3. Found: C, 39.1; H, 4.7; N, 3.3%.

3.8.2 Synthesis of [Hg(SpymDippS)₂][Hg₂Br₆]

Acetonitrile (10 mL) was added to a mixture of HgBr₂ (0.091 g, 0.252 mmol) and SpymDippS (0.080 g, 0.183 mmol), resulting in the formation of an off-white solid and a colorless solution. After stirring for 24 h, the suspension was concentrated under reduced pressure to *ca.* 1 mL, treated with diethyl ether (10 mL), and the product was isolated by filtration and dried *in vacuo* for 18 h (0.086 g, 52%). Mp = 262-264 °C (dec.). ¹H NMR data (in d₆-acetone): δ 1.31 [d, ³J_{H-H} = 6.9, 12 H, CH(CH₃)₂], 1.38 [d, ³J_{H-H} = 6.9, 12 H, CH(CH₃)₂], 2.57 (q, ³J_{H-H} = 5.7, 2 H, CH₂), 3.18 [septet, ³J_{H-H} = 6.9, 4 H, CH(CH₃)₂], 3.94 (t, ³J_{H-H} = 5.7, 4 H, CH₂), 7.31-7.47 (m, 6 H, C₆H₃); ¹³C NMR data (in d₆-DMSO): δ 20.7 (t, ¹J_{C-H} = 131, 2 C, CH₂), 24.0 (q, ¹J_{C-H} = 126, 8 C, CH₃), 24.6 (q, ¹J_{C-H} = 126, 8 C,

CH₃), 28.4 (d, ¹J_{C-H} = 128, 8 C, CH), 51.0 (t, ¹J_{C-H} = 143, 4 C, CH₂), 124.6 (d, ¹J_{C-H} = 155, 8 C, C_m in C₆H₃), 128.6 (d, ¹J_{C-H} = 165, 4 C, C_p in C₆H₃), 140.6 (s, 8 C, C_o in C₆H₃), 144.8 (s, 4 C, C_{ipso} in C₆H₃), C=S not observed. IR data: 2963 (s), 2924 (w), 2867 (m), 2844 (w), 1587 (m), 1548 (s), 1489 (w), 1459 (s), 1445 (m), 1405 (m), 1385 (w), 1363 (w), 1329 (vs), 1312 (vs), 1258 (m), 1215 (m), 1180 (m), 1148 (w), 1101 (w), 1055 (s), 1033 (s), 1016 (m), 935 (m), 883 (w), 830 (w), 805 (vs), 760 (s), 724 (w). Anal. Calc. for C₅₆H₈₀Br₆Hg₃N₄S₂: C, 34.4; H, 4.1; N, 2.9. Found: C, 34.9; H, 4.1; N, 3.7%.

3.8.3 Synthesis of [Hg(SpymDippS)₂][Hg₂I₆]

Acetonitrile (10 mL) was added to a mixture of HgI₂ (0.114 g, 0.250 mmol) and SpymDippS (0.080 g, 0.184 mmol), resulting in the formation of a pale yellow solid and a colorless solution. After stirring for 24 h, the suspension was concentrated under reduced pressure to *ca.* 1 mL, treated with diethyl ether (10 mL), and the product was isolated by filtration and dried *in vacuo* for 18 h (0.105 g, 56%). Mp = 238-240 °C (dec.). ¹H NMR data (in d₆-acetone): δ 1.31 [d, ³J_{H-H} = 6.9, 24 H, CH(CH₃)₂], 1.38 [d, ³J_{H-H} = 6.9, 24 H, CH(CH₃)₂], 2.56 (quintet, ³J_{H-H} = 5.6, 4 H, CH₂), 3.19 [septet, ³J_{H-H} = 6.9, 8 H, CH(CH₃)₂], 3.92 (t, ³J_{H-H} = 5.8, 8 H, CH₂), 7.30-7.47 (m, 12 H, C₆H₃); ¹³C NMR data (in d₆-DMSO): δ 20.9 (t, ¹J_{C-H} = 134, 2 C, CH₂), 24.0 (q, ¹J_{C-H} = 129, 8 C, CH₃), 24.5 (q, ¹J_{C-H} = 126, 8 C, CH₃), 28.3 (d, ¹J_{C-H} = 129, 8 C, CH), 50.5 (t, ¹J_{C-H} = 143, 4 C, CH₂), 124.1 (d, ¹J_{C-H} = 156, 8 C, C_m in C₆H₃), 127.9 (d, ¹J_{C-H} = 158, 4 C, C_p in C₆H₃), 141.4 (s, 8 C, C_o in C₆H₃), 144.9 (s, 4 C, C_{ipso} in C₆H₃), C=S not observed. IR data: 2961 (s), 2925 (m), 2866 (m), 1587 (m), 1544 (s), 1490 (m), 1448 (s), 1403 (m), 1386 (w), 1364 (w), 1326 (s), 1309 (vs), 1257 (m), 1209 (m), 1201 (m), 1180 (m), 1148 (w), 1101 (m), 1083 (w), 1055 (s), 1045 (m), 999 (w), 935 (m), 884 (w), 857 (w), 831 (w),

808 (s), 762 (m), 724 (w). Anal. Calc. for $C_{56}H_{80}Hg_3I_6N_4S_2$: C, 30.1; H, 3.6; N, 2.5. Found: C, 30.0; H, 3.6; N, 2.5%.

3.9 Synthesis of (SpymDippSe)HgX₂

3.9.1 Synthesis of [Hg(SpymDippSe)₂][Hg₂Cl₆]

Acetonitrile (10 mL) was added to a mixture of HgCl₂ (0.061 g, 0.225 mmol) and SpymDippSe (0.080 g, 0.165 mmol), resulting in the formation of a pale yellow solution. After stirring for 24 h, the solution was concentrated under reduced pressure to *ca.* 1 mL and treated with diethyl ether (10 mL), leading to the separation of the off-white product, which was isolated by filtration and dried *in vacuo* for 18 h (0.090 g, 67%). Mp = 288-290 °C (dec.). ¹H NMR data (in d₆-acetone): δ 1.33 [d, ³J_{H-H} = 6.9, 12 H, CH(CH₃)₂], 1.48 [d, ³J_{H-H} = 6.8, 12 H, CH(CH₃)₂], 2.10 (quintet, ³J_{H-H} = 2.3, 2 H, CH₂), 3.17 [septet, ³J_{H-H} = 6.8, 4 H, CH(CH₃)₂], 4.06 (t, ³J_{H-H} = 5.8, 4 H, CH₂), 7.40-7.58 (m, 6 H, C₆H₃); ¹³C NMR data (in d₆-DMSO): δ 19.8 (t, ¹J_{C-H} = 131, 2 C, CH₂), 23.8 (q, ¹J_{C-H} = 127, 8 C, CH₃), 24.9 (q, ¹J_{C-H} = 127, 8 C, CH₃), 28.5 (d, ¹J_{C-H} = 127, 8 C, CH), 51.8 (t, ¹J_{C-H} = 144, 4 C, CH₂), 125.5 (d, ¹J_{C-H} = 157, 8 C, C_m in C₆H₃), 130.2 (d, ¹J_{C-H} = 161, 4 C, C_p in C₆H₃), 140.5 (s, 8 C, C_o in C₆H₃), 144.5 (s, 4 C, C_{ipso} in C₆H₃), C=Se not observed. IR data: 2965 (s), 2924 (m), 2867 (m), 1587 (m), 1550 (vs), 1471 (sh), 1456 (s), 1401 (s), 1386 (m), 1363 (m), 1321 (vs), 1308 (vs), 1257 (m), 1218 (m), 1208 (m), 1180 (m), 1148 (w), 1102 (m), 1080 (w), 1056 (s), 1033 (w), 1022 (w), 995 (m), 934 (m), 883 (w), 805 (vs), 762 (m), 757 (m), 723 (w). Anal. Calc. for $C_{56}H_{80}Cl_6Hg_3N_4Se_2$: C, 37.8; H, 4.5; N, 3.2. Found: C, 38.1; H, 4.4; N, 3.3%.

3.9.2 Synthesis of [Hg(SpymDippSe)₂][Hg₂Br₆]

Acetonitrile (10 mL) was added to a mixture of HgBr₂ (0.081 g, 0.225 mmol) and SpymDippSe (0.082 g, 0.170 mmol), resulting in the formation of a colorless solution. After stirring for 24 h, the solution was concentrated under reduced pressure to *ca.* 1 mL and treated with diethyl ether (10 mL), leading to the separation of the off-white product, which was isolated by filtration and dried *in vacuo* for 18 h (0.097 g, 63%). Mp = 275-278°C (dec.). ¹H NMR data (in d₆-acetone): δ 1.33 [d, ³J_{H-H} = 6.8, 12 H, CH(CH₃)₂], 1.48 [d, ³J_{H-H} = 6.8, 12 H, CH(CH₃)₂], 2.14 (quintet, ³J_{H-H} = 2.2, 2 H, CH₂), 3.18 [septet, ³J_{H-H} = 6.8, 4 H, CH(CH₃)₂], 4.06 (t, ³J_{H-H} = 5.7, 4 H, CH₂), 7.41-7.57 (m, 6 H, C₆H₃); ¹³C NMR data (in d₆-DMSO): δ 19.8 (t, ¹J_{C-H} = 130, 2 C, CH₂), 23.9 (q, ¹J_{C-H} = 128, 8 C, CH₃), 24.9 (q, ¹J_{C-H} = 125, 8 C, CH₃), 28.4 (d, ¹J_{C-H} = 126, 8 C, CH), 51.7 (t, ¹J_{C-H} = 148, 4 C, CH₂), 125.5 (d, ¹J_{C-H} = 160, 8 C, C_m in C₆H₃), 130.1 (d, ¹J_{C-H} = 166, 4 C, C_p in C₆H₃), 140.6 (s, 8 C, C_o in C₆H₃), 144.5 (s, 4 C, C_{ipso} in C₆H₃), C=Se not observed. IR data: 2964 (s), 2924 (m), 2867 (m), 1587 (m), 1549 (vs), 1471 (sh), 1456 (s), 1401 (s), 1386 (m), 1363 (m), 1321 (vs), 1309 (vs), 1256 (m), 1218 (w), 1208 (m), 1179 (m), 1148 (w), 1102 (m), 1080 (w), 1056 (s), 1033 (w), 1022 (w), 995 (m), 956 (w), 934 (m), 883 (w), 805 (vs), 762 (m), 757 (m), 723 (w). Anal. Calc. for C₅₆H₈₀Br₆Hg₃N₄Se₂: C, 32.8; H, 3.9; N, 2.7. Found: C, 33.3; H, 3.9; N, 3.3%.

3.9.3 Synthesis of [Hg(SpymDippSe)₂][Hg₂I₆]

Acetonitrile (10 mL) was added to a mixture of HgI₂ (0.104 g, 0.229 mmol) and SpymDippSe (0.083 g, 0.172 mmol), resulting in the formation of a pale yellow solid and a colorless solution. After stirring for 24 h, the suspension was concentrated under reduced pressure to *ca.* 1 mL, treated with diethyl ether (10 mL), and the product was

isolated by filtration and dried *in vacuo* for 18 h (0.094, 53%). Mp = 229-231 °C (dec.). ¹H NMR data (in d₆-acetone): δ 1.33 [d, ³J_{H-H} = 6.9, 12 H, CH(CH₃)₂], 1.47 [d, ³J_{H-H} = 6.9, 12 H, CH(CH₃)₂], 2.12 (quintet, ³J_{H-H} = 2.21, 2 H, CH₂), 3.19 [septet, ³J_{H-H} = 6.8, 4 H, CH(CH₃)₂], 4.03 (t, ³J_{H-H} = 5.7, 4 H, CH₂), 7.40-7.56 (m, 6 H, C₆H₃); ¹³C NMR data (in d₆-DMSO): δ 19.9 (t, ¹J_{C-H} = 138, 2 C, CH₂), 23.9 (q, ¹J_{C-H} = 123, 8 C, CH₃), 24.8 (q, ¹J_{C-H} = 123, 8 C, CH₃), 28.4 (d, ¹J_{C-H} = 127, 8 C, CH), 51.5 (t, ¹J_{C-H} = 146, 4 C, CH₂), 125.3 (d, ¹J_{C-H} = 161, 8 C, C_m in C₆H₃), 129.9 (d, ¹J_{C-H} = 161, 4 C, C_p in C₆H₃), 141.0 (s, 8 C, C_o in C₆H₃), 144.5 (s, 4 C, C_{ipso} in C₆H₃), C=Se not observed. IR data: 2965 (s), 2924 (m), 2867 (m), 1587 (m), 1550 (vs), 1471 (sh), 1456 (s), 1401 (s), 1386 (w), 1363 (w), 1321 (vs), 1309 (vs), 1257 (m), 1217 (w), 1208 (m), 1179 (m), 1148 (w), 1102 (m), 1080 (w), 1056 (s), 1033 (w), 1022 (w), 995 (m), 977 (w), 957 (w), 934 (m), 912 (w), 884 (w), 813 (w), 805 (vs), 762 (m), 757 (m), 723 (w). Anal. Calc. for C₅₆H₈₀Hg₃I₆N₄Se₂: C, 28.9; H, 3.5; N, 2.4. Found: C, 29.0; H, 3.4; N, 2.5%.

3.10 Synthesis of (SpymXyS)AuX

3.10.1 Synthesis of (SpymXyS)AuCl

Dichloromethane (10 mL) was added to a mixture of (tth)AuCl (0.072 g, 0.225 mmol) and SpymXyS (0.081 g, 0.250 mmol), resulting in the formation of a pale yellow solution. After stirring for 16 h, the solution was concentrated under reduced pressure to *ca.* 1 mL and treated with pentane (10 mL), leading to the separation of the off-white product, which was isolated by filtration and dried *in vacuo* for 18 h (0.087 g, 69%). Mp = 288-290 °C (dec.). IR data: 2971 (w), 2948 (w), 2913 (w), 1591 (m), 1530 (vs), 1468 (s), 1442 (m), 1398 (s), 1373 (w), 1351 (w), 1332 (vs), 1308 (vs), 1269 (m), 1246 (w),

1223 (w), 1212 (s), 1190 (w), 1163 (w), 1112 (w), 1097 (w), 1078 (m), 1032 (w), 1023 (w), 1002 (w), 989 (w), 917 (w), 902 (w), 888 (w), 835 (m), 792 (m), 780 (vs), 739 (w), 700 (w), 677 (w), 663 (w). ESI-MS (in MeCN): $m/z = 844.72$, $[\text{Au}(\text{SpymXyS})_2]^+$; $m/z = 561.58$, $[(\text{SpymXyS})\text{Au}(\text{NCMe})]^+$. Anal. Calc. for $\text{C}_{20}\text{H}_{24}\text{AuClN}_2\text{S}$: C, 43.1; H, 4.3; N, 5.0. Found: C, 42.5; H, 4.4; N, 4.9%.

3.10.2 Synthesis of (SpymXyS)AuBr

Tetrahydrofuran (10 mL) was added to a mixture of (tht)AuBr (0.076 g, 0.208 mmol) and SpymXyS (0.078 g, 0.240 mmol), resulting in the formation of a pale yellow solution. After stirring for 16 h, the solution was concentrated under reduced pressure to *ca.* 1 mL and treated with pentane (10 mL), leading to the separation of the off-white product, which was isolated by filtration and dried *in vacuo* for 18 h (0.085 g, 68%). Mp = 290-292 °C (dec.). IR data: 2945 (w), 2911 (w), 1591 (w), 1529 (s), 1468 (m), 1441 (w), 1398 (m), 1373 (w), 1350 (w), 1331 (s), 1307 (s), 1268 (w), 1245 (w), 1223 (w), 1211 (m), 1189 (w), 1163 (w), 1097 (w), 1078 (m), 1023 (w), 1002 (w), 988 (w), 888 (w), 835 (m), 790 (m), 780 (vs), 747 (w), 676 (w). ESI-MS (in MeCN): $m/z = 844.60$, $[\text{Au}(\text{SpymXyS})_2]^+$; $m/z = 561.58$, $[(\text{SpymXyS})\text{Au}(\text{NCMe})]^+$. Anal. Calc. for $\text{C}_{20}\text{H}_{24}\text{AuBrN}_2\text{S}$: C, 40.0; H, 4.0; N, 4.7. Found: C, 40.2; H, 4.0; N, 4.6%.

3.11 Synthesis of (SpymXySe)AuX

3.11.1 Synthesis of (SpymXySe)AuCl

Dichloromethane (10 mL) was added to a mixture of (tht)AuCl (0.060 g, 0.187 mmol) and SpymXySe (0.079 g, 0.213 mmol), resulting in the formation of a pale yellow

solution. After stirring for 16 h, the solution was concentrated under reduced pressure to *ca.* 1 mL and treated with pentane (10 mL), leading to the separation of the off-white product, which was isolated by filtration and dried *in vacuo* for 18 h (0.100 g, 89%). Mp = 280-282 °C (dec.). IR data: 2933 (w), 2901 (w), 2840 (w), 1591 (w), 1537 (vs), 1469 (m), 1453 (w), 1438 (w), 1398 (m), 1372 (w), 1349 (w), 1326 (s), 1308 (s), 1268 (w), 1244 (w), 1222 (w), 1210 (m), 1187 (w), 1164 (w), 1110 (w), 1097 (w), 1076 (w), 1034 (w), 1021 (w), 1002 (w), 999 (w), 989 (w), 889 (w), 814 (w), 793 (m), 782 (vs), 739 (w), 677 (w). ESI-MS (in MeCN): $m/z = 940.54$, $[\text{Au}(\text{SpymXySe})_2]^+$. Anal. Calc. for $\text{C}_{20}\text{H}_{24}\text{AuClN}_2\text{Se}$: C, 39.8; H, 4.0; N, 4.6. Found: C, 39.2; H, 3.9; N, 4.5%.

3.11.2 Synthesis of (SpymXySe)AuBr

Dichloromethane (10 mL) was added to a mixture of (tht)AuBr (0.070 g, 0.192 mmol) and SpymXySe (0.080 g, 0.215 mmol), resulting in the formation of a pale yellow solution. After stirring for 16 h, the solution was concentrated under reduced pressure to *ca.* 1 mL and treated with pentane (10 mL), leading to the separation of the off-white product, which was isolated by filtration and dried *in vacuo* for 18 h (0.103 g, 83%). Mp = 284-286 °C (dec.). IR data: 2932 (w), 2906 (w), 1591 (w), 1535 (vs), 1469 (m), 1453 (w), 1438 (w), 1398 (m), 1372 (w), 1349 (w), 1325 (vs), 1307 (vs), 1267 (m), 1244 (w), 1222 (w), 1209 (m), 1186 (w), 1164 (w), 1110 (w), 1097 (w), 1076 (m), 1033 (w), 1021 (w), 999 (w), 988 (w), 908 (w), 888 (w), 814 (w), 792 (m), 781 (vs), 739 (w), 672 (w). ESI-MS (in MeCN): $m/z = 938.54$, $[\text{Au}(\text{SpymXySe})_2]^+$. Anal. Calc. for $\text{C}_{20}\text{H}_{24}\text{AuBrN}_2\text{Se}$: C, 37.1; H, 3.7; N, 4.3. Found: C, 36.9; H, 3.6; N, 4.3%.

3.12 Synthesis of (SpymMesS)AuX

3.12.1 Synthesis of (SpymMesS)AuCl

Dichloromethane (10 mL) was added to a mixture of (tht)AuCl (0.067 g, 0.209 mmol) and SpymMesS (0.084 g, 0.238 mmol), resulting in the formation of a pale yellow solution. After stirring for 16 h, the solution was concentrated under reduced pressure to *ca.* 1 mL and treated with pentane (10 mL), leading to the separation of the off-white product, which was isolated by filtration and dried *in vacuo* for 18 h (0.090 g, 75%). Mp = 262-263 °C (dec.). IR data: 2972 (w), 2941 (w), 2914 (w), 2860 (w), 1608 (w), 1532 (s), 1480 (m), 1450 (w), 1401 (m), 1373 (w), 1354 (w), 1331 (vs), 1304 (s), 1258 (w), 1232 (w), 1211 (s), 1155 (w), 1106 (w), 1089 (w), 1035 (w), 1013 (w), 948 (w), 898 (w), 853 (m), 831 (m), 801 (w), 761 (w), 725 (m), 677 (w). ESI-MS (in MeCN): $m/z = 900.72$, $[\text{Au}(\text{SpymMesS})_2]^+$; $m/z = 589.52$, $[(\text{SpymMesS})\text{Au}(\text{NCMe})]^+$. Anal. Calc. for $\text{C}_{22}\text{H}_{28}\text{AuClN}_2\text{S}$: C, 45.2; H, 4.8; N, 4.8. Found: C, 45.4; H, 4.9; N, 4.8%.

3.12.2 Synthesis of (SpymMesS)AuBr

Dichloromethane (10 mL) was added to a mixture of (tht)AuBr (0.074 g, 0.203 mmol) and SpymMesS (0.081 g, 0.230 mmol), resulting in the formation of a pale orange solution. After stirring for 16 h, the solution was concentrated under reduced pressure to *ca.* 1 mL and treated with pentane (10 mL), leading to the separation of the off-white product, which was isolated by filtration and dried *in vacuo* for 18 h (0.078 g, 63%). Mp = 288-290 °C (dec.). IR data: 2972 (w), 2941 (w), 2910 (w), 2855 (w), 1658 (w), 1608 (w), 1532 (s), 1479 (m), 1450 (w), 1438 (w), 1400 (m), 1373 (w), 1352 (w), 1330 (vs), 1304 (s), 1257 (w), 1231 (w), 1211 (s), 1153 (w), 1106 (w), 1031 (w), 1035 (w), 950 (w),

898 (w), 853 (s), 832 (m), 725 (m) 676 (w). ESI-MS (in MeCN): $m/z = 900.72$, $[\text{Au}(\text{SpymMesS})_2]^+$; $m/z = 589.46$, $[(\text{SpymMesS})\text{Au}(\text{NCMe})]^+$. Anal. Calc. for $\text{C}_{22}\text{H}_{28}\text{AuBrN}_2\text{S}$: C, 42.0; H, 4.5; N, 4.5. Found: C, 42.2; H, 4.5; N, 4.4%.

3.13 Synthesis of (SpymMesSe)AuX

3.13.1 Synthesis of (SpymMesSe)AuCl

Dichloromethane (10 mL) was added to a mixture of (tht)AuCl (0.061 g, 0.190 mmol) and SpymMesSe (0.080 g, 0.200 mmol), resulting in the formation of a pale orange solution. After stirring for 16 h, the solution was concentrated under reduced pressure to *ca.* 1 mL and treated with pentane (10 mL), leading to the separation of the off-white product, which was isolated by filtration and dried *in vacuo* for 18 h (0.101, 84%). Mp = 242-244 °C (dec.). IR data: 2956 (w), 2914 (w), 2845 (w), 1608 (w), 1536 (s), 1477 (m), 1448 (m), 1399 (w), 1373 (w), 1350 (w), 1325 (s), 1315 (s), 1304 (s), 1255 (w), 1228 (w), 1210 (s), 1142 (w), 1106 (w), 1087 (w), 1033 (w), 892 (w), 852 (s), 805 (w), 722 (w). ESI-MS (in MeCN): $m/z = 996.60$, $[\text{Au}(\text{SpymMesSe})_2]^+$; $m/z = 795.41$, $[\text{Au}_2(\text{SpymMesSe})_3]^{2+}$; $m/z = 637.15$, $[(\text{SpymMesSe})\text{Au}(\text{NCMe})]^+$. Anal. Calc. for $\text{C}_{22}\text{H}_{28}\text{AuClN}_2\text{Se}$: C, 41.8; H, 4.5; N, 4.4. Found: C, 41.5; H, 4.4; N, 4.3%.

3.13.2 Synthesis of (SpymMesSe)AuBr

Dichloromethane (10 mL) was added to a mixture of (tht)AuBr (0.064 g, 0.175 mmol) and SpymMesSe (0.081 g, 0.203 mmol), resulting in the formation of a pale orange solution. After stirring for 16 h, the solution was concentrated under reduced pressure to *ca.* 1 mL and treated with pentane (10 mL), leading to the separation of the off-white

product, which was isolated by filtration and dried *in vacuo* for 18 h (0.082, 69%). Mp = 285-286 °C (dec.). IR data: 2969 (w), 2939 (w), 2912 (w), 2860 (w), 1608 (m), 1538 (s), 1497 (m), 1478 (m), 1447 (m), 1400 (m), 1373 (m), 1351 (w), 1325 (s), 1304 (vs), 1255 (m), 1231 (w), 1210 (s), 1152 (w), 1107 (w), 1087 (w), 1031 (w), 1012 (w), 999 (w), 986 (w), 952 (w), 896 (w), 852 (s), 810 (w), 737 (w), 722 (m), 703 (w), 655 (w). ESI-MS (in MeCN): $m/z = 996.60$, $[\text{Au}(\text{SpymMesSe})_2]^+$. Anal. Calc. for $\text{C}_{22}\text{H}_{28}\text{AuBrN}_2\text{Se}$: C, 39.1; H, 4.2; N, 4.1. Found: C, 39.2; H, 4.2; N, 4.0%.

3.14 Synthesis of (SpymDippS)AuX

3.14.1 Synthesis of (SpymDippS)AuCl

Dichloromethane (10 mL) was added to a mixture of (tht)AuCl (0.051 g, 0.159 mmol) and SpymDippS (0.080 g, 0.183 mmol), resulting in the formation of a pale yellow solution. After stirring for 16 h, the solution was concentrated under reduced pressure to *ca.* 1 mL and treated with pentane (10 mL), leading to the separation of the off-white product, which was isolated by filtration and dried *in vacuo* for 18 h (0.096, 90%). Mp = 240-242 °C (dec.). IR data: 2959 (m), 2927 (m), 2866 (m), 1590 (w), 1515 (s), 1490 (m), 1450 (m), 1397 (m), 1321 (vs), 1258 (w), 1209 (m), 1201 (m), 1179 (w), 1101 (w), 1086 (w), 1056 (m), 1017 (w), 1003 (w), 968 (w), 937 (w), 886 (w), 842 (m), 801 (s), 755 (m) 736 (m), 705 (w). ESI-MS (in MeCN): $m/z = 1068.85$, $[\text{Au}(\text{SpymDippS})_2]^+$; $m/z = 673.65$, $[(\text{SpymDippS})\text{Au}(\text{NCMe})]^+$. Anal. Calc. for $\text{C}_{28}\text{H}_{40}\text{AuClN}_2\text{S}$: C, 50.3; H, 6.0; N, 4.2. Found: C, 50.9; H, 6.3; N, 4.2%.

3.14.2 Synthesis of (SpymDippS)AuBr

Dichloromethane (10 mL) was added to a mixture of (tht)AuBr (0.060 g, 0.164 mmol) and SpymDippS (0.080 g, 0.183 mmol), resulting in the formation of a pale yellow solution. After stirring for 16 h, the solution was concentrated under reduced pressure to *ca.* 1 mL and treated with pentane (10 mL), leading to the separation of the off-white product, which was isolated by filtration and dried *in vacuo* for 18 h (0.093, 82%). Mp = 285-287 °C (dec.). IR data: 2960 (m), 2925 (m), 2866 (m), 1591 (w), 1512 (s), 1449 (m), 1397 (m), 1385 (w), 1322 (vs), 1307 (m), 1258 (w), 1209 (m), 1179 (w), 1110 (w), 1086 (w), 1057 (w), 1003 (w), 936 (w), 885 (w), 840 (m), 797 (m), 752 (m), 727 (w), 675 (w), 660 (w). ESI-MS (in MeCN): $m/z = 1068.79$, $[\text{Au}(\text{SpymDippS})_2]^+$; $m/z = 673.65$, $[(\text{SpymDippS})\text{Au}(\text{NCMe})]^+$. Anal. Calc. for $\text{C}_{28}\text{H}_{40}\text{AuBrN}_2\text{S}$: C, 47.1; H, 5.7; N, 3.9. Found: C, 47.3; H, 5.8; N, 4.1%.

3.15 Synthesis of (SpymDippSe)AuX

3.15.1 Synthesis of (SpymDippSe)AuCl

Dichloromethane (10 mL) was added to a mixture of (tht)AuCl (0.047 g, 0.147 mmol) and SpymDippSe (0.080 g, 0.165 mmol), resulting in the formation of a pale yellow solution. After stirring for 16 h, the solution was concentrated under reduced pressure to *ca.* 1 mL and treated with pentane (10 mL), leading to the separation of the off-white product, which was isolated by filtration and dried *in vacuo* for 18 h (0.081, 79%). Mp = 234-236 °C (dec.). IR data: 3062 (w), 2962 (m), 2926 (m), 2867 (m), 1589 (w), 1521 (vs), 1455 (m), 1398 (w), 1384 (w), 1363 (w), 1308 (vs), 1256 (m), 1207 (m), 1179 (w), 1147 (w), 1103 (w), 1082 (w), 1057 (m), 999 (w), 936 (w), 884 (w), 799 (s), 753 (s), 725

(w). ESI-MS (in MeCN): $m/z = 1162.67$, $[\text{Au}(\text{SpymDippSe})_2]^+$; $m/z = 721.53$, $[(\text{SpymDippSe})\text{Au}(\text{NCMe})]^+$. Anal. Calc. for $\text{C}_{28}\text{H}_{40}\text{AuClN}_2\text{Se}$: C, 47.0; H, 5.6; N, 3.9. Found: C, 47.1; H, 5.6; N, 3.9%.

3.15.2 Synthesis of $(\text{SpymDippSe})\text{AuBr}$

Dichloromethane (10 mL) was added to a mixture of $(\text{tht})\text{AuBr}$ (0.056 g, 0.153 mmol) and SpymDippSe (0.080 g, 0.165 mmol), resulting in the formation of a pale yellow solution. After stirring for 16 h, the solution was concentrated under reduced pressure to *ca.* 1 mL and treated with pentane (10 mL), leading to the separation of the off-white product, which was isolated by filtration and dried *in vacuo* for 18 h (0.084, 77%). $\text{Mp} = 285\text{-}286\text{ }^\circ\text{C}$ (dec.). IR data: 3063 (w), 2961 (m), 2925 (w), 2866 (m), 1589 (w), 1520 (vs), 1452 (m), 1398 (w), 1384 (w), 1364 (w), 1314 (vs), 1306 (vs), 1256 (w), 1207 (m), 1177 (w), 1145 (w), 1103 (w), 1082 (w), 1056 (m), 998 (w), 936 (w), 798 (s), 752 (s), 725 (w), 703 (w), 659 (w). ESI-MS (in MeCN): $m/z = 1164.67$, $[\text{Au}(\text{SpymDippSe})_2]^+$; $m/z = 721.53$, $[(\text{SpymDippSe})\text{Au}(\text{NCMe})]^+$. Anal. Calc. for $\text{C}_{28}\text{H}_{40}\text{AuBrN}_2\text{Se}$: C, 44.2; H, 5.3; N, 3.7. Found: C, 43.9; H, 5.3; N, 3.5%.

CHAPTER 4: CONCLUSIONS AND FUTURE WORK

4.1 Conclusions

In summary, the synthesis of six-membered N-heterocyclic chalcogenone ligands has been developed from previously accomplished synthesis published in the literature. As discussed in section 1.4, the C=S and C=Se bond length exhibited in the SpymArE ligands is consistent with the resonance forms shown in Figure 1.3. This characteristic of the ligand supports our claim of increased stability seen in this class of chalcogenone ligand as it is observed in both the NHT and NHSe ligands as well as this zwitterionic resonance upon coordination with a metal complex.¹⁴ To further understand the stability of these ligands, iodine adducts were prepared for each of the ligands yielding air-stable compounds and interestingly an iodonium species. Further work into the reactivity of these compounds is needed to determine their similarities and differences to other iodonium reagents, particularly Barluenga's reagent.^{40,41}

The coordination of the SpymArE ligands to mercury(II) halides has been completed, including full characterization. This has yielded the unexpected result of varying crystal geometries with respect to the mercury center. As discussed in section 2.3., these geometries being trigonal planar and linear two-coordinate. The linear two-coordinate mercury(II) species are unprecedented, however rare with NHT ligands and

previously unknown for NHSe ligands of any type. The completion of the SpymArE mercury(II) halide set also shed light on how sterically demanding these ligands are with respect to the aromatic substituent as the data supports that as the steric demand of a ligand increases, the favorability of the linear two-coordinate geometry increases. This trend is exemplified by the SpymDippE ligands, as they are the most sterically demanding of the six-membered ligand set, and each of the mercury(II) halides with these ligands has a linear two-coordinate geometry.

The copper(I) and gold(I) complexes are isoelectronic to the mercury(II) compounds as they are each closed-shell d^{10} metals. These complexes of copper(I) and gold(I) with the SpymArE ligands are each linear two-coordinate with almost all of these being neutral compounds. As discussed in section 2.4, there is a solution state equilibrium present for the gold(I) complexes leading to multiple signals present in the NMR and observed in the ESI-MS.

When comparing the six-membered SpymArE ligands versus the saturated five-membered SIrE ligands, it can be said that they show similar chalcogen–metal bond distances for the closed shell d^{10} discussed. The major difference between the metal complexes of these ligands being the varying coordination geometries of the SpymArE ligands, trigonal planar and linear, as opposed to the more uniform structures of the SIrE metal complexes. This is observed throughout the mercury(II) halide complexes as each of the SIrE mercury complexes is trigonal planar, while only eleven of the total 18 structures of SpymArE mercury complexes are trigonal planar.

4.2 Future Work

The ease of synthesis for each of the SpymArE ligands as a result of previous reported NHC preparation makes the expansion of this project into other N-substituents facile and worth investigating. As very little coordination chemistry has been done with six-membered NHT and NHSe ligands, each metal complex prepared with a new ligand would be novel. Potential new six-membered NHT and NHSe ligands are shown in Figure 4.1. The synthesis of some both the isopropyl and t-butyl derivatives are known and the synthesis of the adamantyl ligand should be able to be to prepare.

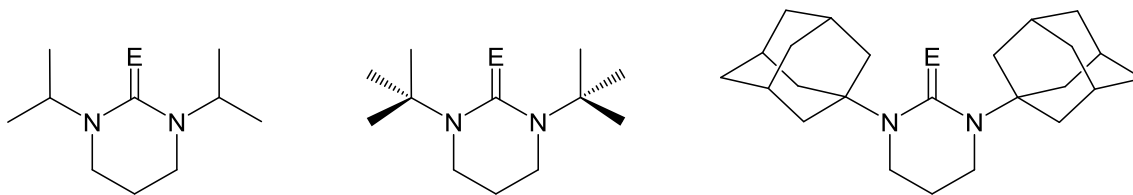


Figure 4.1: Proposed new Six-membered NHT and NHSe ligands.

Within the field of NHCs, the solubility of metal complexes in aqueous environments has expanded as it opens new avenues of green chemistry, catalysis, and further biological applications.⁶² The primary method for increasing water solubility in NHC metal complexes has been through water-soluble functionalization. These functional groups include but not limited to sulfonate, ammonium, and carboxylate functional groups (Figure 4.2).

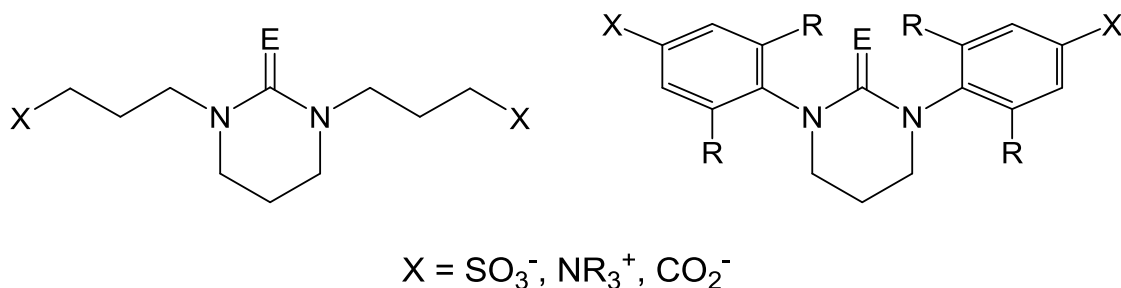
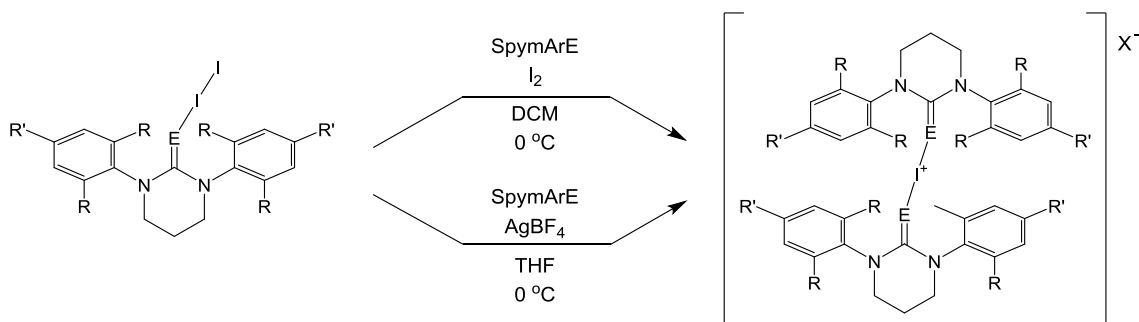


Figure 4.2: Proposed water soluble Six-membered NHT and NHSe ligands.

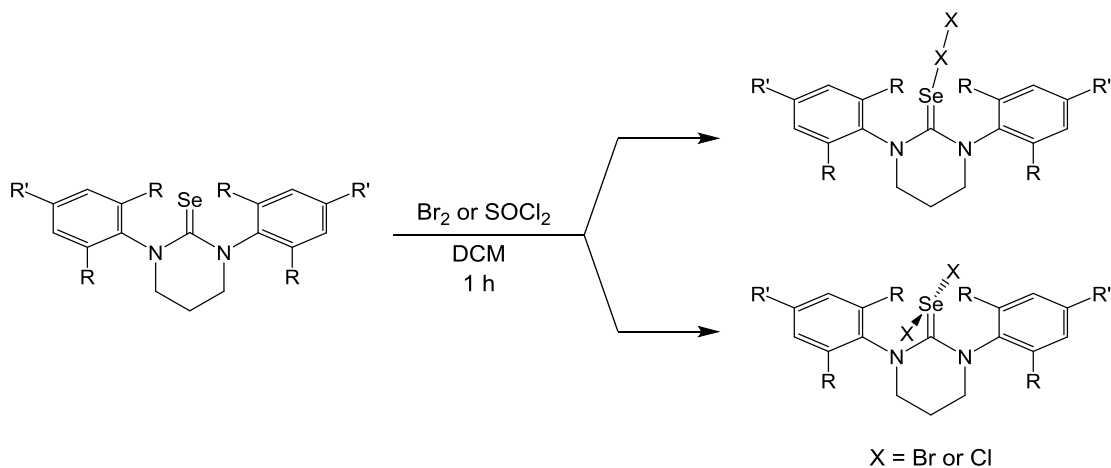
Following the accidental synthesis of the $[(\text{SpymXyS})_2\text{I}]^+$, the rational synthesis of other $[(\text{SpymArE})_2\text{I}]^+$ compounds would be an interesting goal to achieve. The method used in the preparation of iodonium salts by Hadjilidas *et al.* and Manjare *et al.* and has been proposed for each of the SpymArE ligands (Scheme 4.1).^{39,63} These methods, using excess I_2 or AgBF_4 to abstract an iodine, could potentially yield iodonium complexes for each of the SpymArE ligands.

Scheme 4.1: Proposed Synthesis of SpymArE Iodonium Salts



To date, the only halogen compounds to be fully characterized of the SpymArE ligands are the iodine adducts. Both the bromine and chlorine derivatives have been successfully prepared for the SIrSe ligands and the synthesis for these compounds is shown in Scheme 4.2. Unlike the iodine adducts of SpymArE, the bromine and chlorine derivatives are predicted to favor the T-shaped geometry shown in Scheme 4.1.

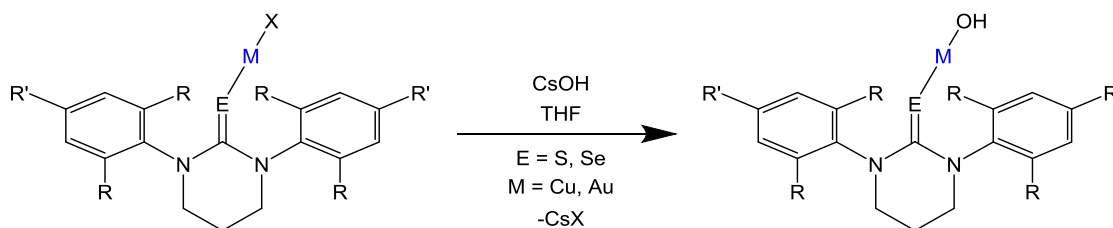
Scheme 4.2: Proposed Synthesis of Bromine and Chlorine Compounds



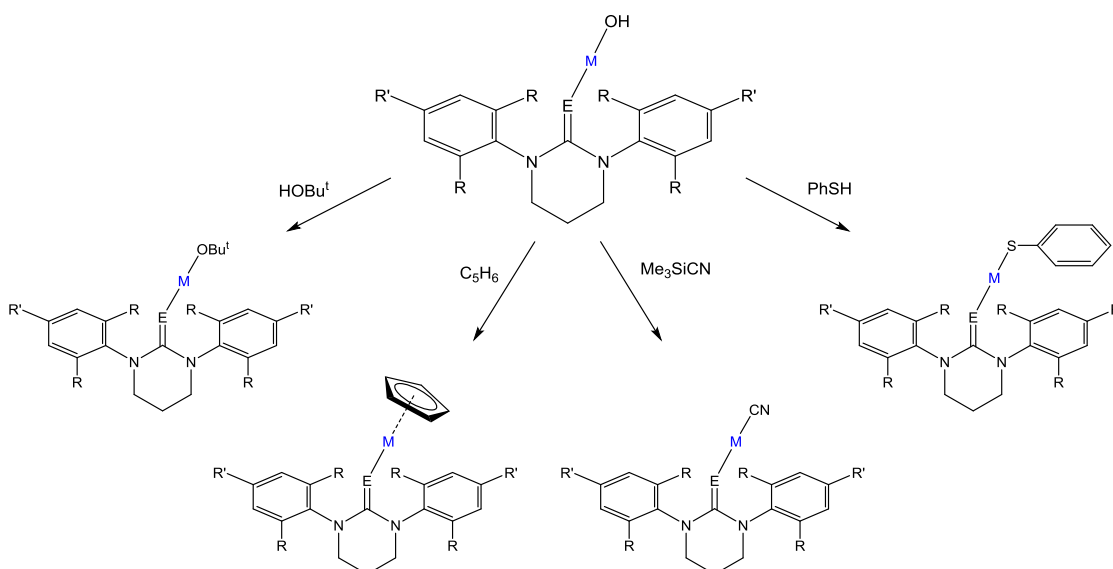
Unlike the mercury(II) and gold(I) complexes, the copper(I) complexes are incomplete. The synthesis of analytically pure compounds proved less facile than the mercury(II) and gold(I) complexes as a result of the air- and moisture-sensitivity of these compounds. Further work is needed to complete the copper(I) halide complexes.

Both the copper(I) and gold(I) complexes could be used as synthetic precursors for copper(I) and gold(I) hydroxide complexes (Scheme 4.3). These would be highly reactive due to the soft-hard acid-base bonding of the metal and hydroxide as well as the electron deficiency of this 13 electron complex. Copper(I) and gold(I) NHC hydroxide synthons have been successfully prepared by Nolan *et al* and used to synthesize a wide variety of organometallic compounds.⁶⁴⁻⁶⁷ Scheme 4.4 illustrates some of the potential copper(I) and gold(I) compounds that could be prepared following the synthetic procedure proposed by Nolan *et al.*⁶⁶

Scheme 4.3: Proposed Synthesis of Copper(I) and Gold(I) Hydroxide Complexes



Scheme 4.4: Proposed Synthesis of Copper(I) and Gold(I) Complexes

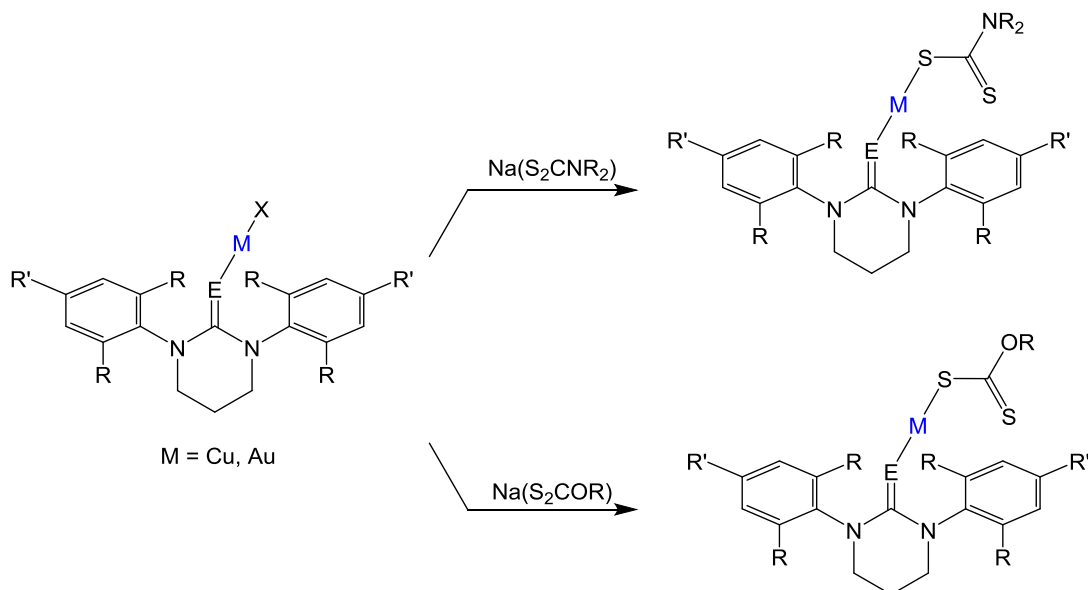


The biological activity for copper(I) and gold(I) complexes containing NHT ligands is known and has been patented by Che.⁶⁸ This should therefore be further looked into for all of the NHT copper(I) and gold(I) complexes contained in this work and especially for the NHSe complexes as there has been less work done with these selenium donor ligands.

Further reactivity studies involving dithiocarbamates and xanthates (Scheme 4.5) for both the copper(I) and gold(I) halides will also be explored. Dithiocarbamates have been shown to possess anticancer properties in gold(I) NHC^{28,69,70} and gold(I)

phosphine⁷¹ complexes. These analogues would also provide further insight into the comparison of similar complexes with chalcogenones versus NHCs or phosphines.

Scheme 4.5: Proposed Synthesis of Dithiocarbamate and Xanthate Metal Complexes



As mentioned in section 1.3, expanded ring NHC chemistry is growing and includes NHCs with rings greater than five atoms.⁷² While this work focuses on six-membered NHT and NHSe ligands, seven-membered NHT and NHSe ligands would be an interesting next step as there are a number of seven-membered NHC ligands in the literature.⁷⁻¹⁰ The increased ring size of these ligands is reported to increase catalytic activity in some NHC-complex-catalyzed reactions in comparison to six-membered NHCs due to the enhanced steric demand of the ligands.⁸ The proposed seven-membered chalcogenone ligands are shown in Figure 4.3 and compared to the SpymArE ligands.

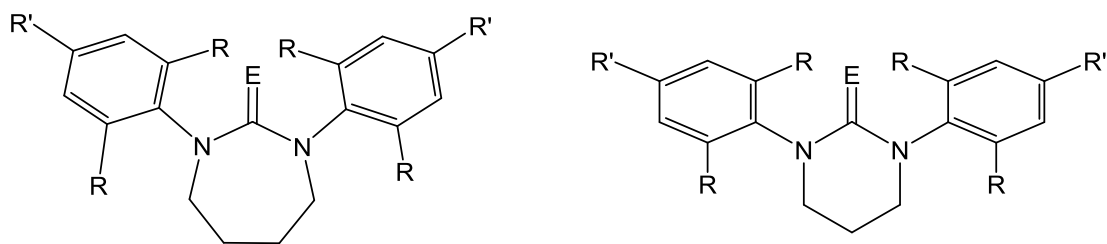


Figure 4.3: Proposed seven-membered chalcogenone ligands compared to SpymArE.

REFERENCES

- (1) de Fremont, P.; Marion, N.; Nolan, S. P. *Coord. Chem. Rev.* **2009**, *253*, 862–892.
- (2) Tomioka, H.; Watanabe, T.; Hattori, M.; Nomura, N.; Hirai, K. *J. Am. Chem. Soc.* **2002**, *124*, 474–482.
- (3) Öfele, K. *J. Organomet. Chem.* **1968**, *12*, 42–43.
- (4) Wanzlick, H. W.; Schönherr, H. J. *Angew. Chem. Int. Ed. Engl.* **1968**, *7*, 141–142.
- (5) Arduengo, A. J.; Kline, M.; Harlow, R. L. *J. Am. Chem. Soc.* **1991**, *113*, 361–363.
- (6) Hopkinson, M. N.; Richter, C.; Schedler, M.; Glorius, F. *Nature* **2014**, *510*, 485–496.
- (7) Male, L.; Hursthouse, M.; Cavell, K. J.; Dervisi, A. *Organometallics* **2008**, *27*, 3279–3289.
- (8) Iglesias, M.; Beetstra, D. J.; Cavell, K. J.; Dervisi, A.; Fallis, I. A.; Kariuki, B.; Harrington, R. W.; Clegg, W.; Horton, P. N.; Coles, S. J.; Hursthouse, M. B. *Eur. J. Inorg. Chem.* **2010**, *1*, 1604–1607.
- (9) Binobaid, A.; Iglesias, M.; Beetstra, D.; Dervisi, A.; Fallis, I.; Cavell, K. J. *Eur. J. Inorg. Chem.* **2010**, *34*, 5426–5431.
- (10) Dunsford, J. J.; Cavell, K. J.; Kariuki, B. M. *Organometallics* **2012**, *31*, 4118–4121.
- (11) Liske, A.; Verlinden, K.; Buhl, H.; Schaper, K.; Ganter, C. *Organometallics* **2013**, *32*, 5269–5272.
- (12) Raper, E. S. *Coord. Chem. Rev.* **1985**, *61*, 115–184.
- (13) Akrivos, P. D. *Coord. Chem. Rev.* **2001**, *213*, 181–210.

- (14) Stadelman, B. S.; Brumaghim, J. L. In *ACS Symposium Series*; 2013; Vol. 1152, pp 33–70.
- (15) Han, L.; Wu, B.; Xu, Y.; Wu, M.; Gong, Y.; Lou, B.; Chen, B.; Hong, M. *Inorg. Chim Acta.* **2005**, 358, 2005–2013.
- (16) Lobana, T. S.; Sultana, R.; Castineiras, A.; Butcher, R. J. *Inorg. Chim Acta.* **2009**, 362, 5265–5270.
- (17) Majhi, P. K.; Schnakenburg, G.; Streubel, R. *Dalton Trans.* **2014**, 43, 16673–16679.
- (18) Xu, Y.; Kool, E. T. *J. Am. Chem. Soc.* **2000**, 122, 9040–9041.
- (19) Tamilselvi, A.; Mugesh, G. *Bioorganic Med. Chem. Lett.* **2010**, 20, 3692–3697.
- (20) Dias, H. W.; Truter, M. R. *Acta Crystallogr.* **1964**, 17, 937–943.
- (21) Hagemann, H.; Ley, K. *Angew. Chem. Int. Ed. Engl.* **1972**, 11, 1012–1013.
- (22) Yang, D.; Chen, Y.; Zhu, N. *Org. Lett.* **2004**, 6, 1577–1580.
- (23) Matsumura, T.; Nakada, M. *Tetrahedron Lett.* **2014**, 55, 1412–1415.
- (24) Warner, J. S. *Org. Chem.* **1963**, 28, 1642–1644.
- (25) Hartwig, L.; Truter, M. R. *J. Chem. Soc. A* **1968**, 1879–1886.
- (26) Isab, A. A.; Hussain, M. S. *Transition Met. Chem.* **1986**, 11, 298–301.
- (27) Altaf, M.; Isab, A. A. U.S. Patent 9 481 699 B1, 2016.
- (28) Altaf, M.; Monim-ul-Mehboob, M.; Seliman, A. A. A.; Isab, A. A.; Dhuna, V.; Bhatia, G.; Dhuna, K. *J. Organomet. Chem.* **2014**, 765, 68–79.

- (29) Ahmad, S.; Isab, A.; Al-arfaj, A. R.; Arnold, A. P. *Polyhedron* **2002**, *21*, 2099–2105.
- (30) Ahmad, S.; Isab, A. A.; Arnold, A. P. *J. Coord. Chem* **2003**, *56*, 539–544.
- (31) Kuhn, K. M.; Grubbs, R. H. *Org. Lett.* **2008**, *10*, 2075–2077.
- (32) Paas, M.; Wibbeling, B.; Fröhlich, R.; Hahn, F. E. *Eur. J. Inorg. Chem.* **2006**, *2006*, 158–162.
- (33) Vummaleti, S. V. C.; Nelson, D. J.; Poater, A.; Gómez-Suárez, A.; Cordes, D. B.; Slawin, A. M. Z.; Nolan, S. P.; Cavallo, L. *Chem. Sci.* **2015**, *6*, 1895–1904.
- (34) Boyle, P. D.; Godfrey, S. M. *Coord. Chem. Rev.* **2001**, *223*, 265–299.
- (35) Jeske, J.; du Mont, W.-W.; Jones, P. G. *Chem. Eur. J.* **1995**, *5*, 385.
- (36) Cristiani, F.; Devillanova, A.; Isaia, F.; Lippolis, V.; Demartin, F. *Polyhedron* **1995**, *14*, 2937–2943.
- (37) Demartin, F.; Devillanova, F. A.; Isaia, F.; Lippolis, V.; Verani, G. *Inorg. Chim. Acta.* **1997**, *255*, 203–205.
- (38) Perkins, C. W.; Martin, J. C.; Arduengo, A. J.; Lau, W.; Alegria, A.; Kochi, J. K. *J. Am. Chem. Soc.* **1980**, *102*, 7753–7759.
- (39) Corban, G. J.; Hadjikakou, S. K.; Hadjiliadis, N.; Kubicki, M.; Tiekink, E. R. T.; Butler, I. S.; Drougas, E.; Kosmas, A. M. *Inorg. Chem.* **2005**, *44*, 8617–8627.
- (40) Barluenga, J.; González, J. M.; Campos, P. J.; Asensio, G. *Angew. Chem. Int. Ed. Engl.* **1985**, *24*, 319–320.
- (41) Chalker, J. M.; Thompson, Amber, L.; Davis, B. G. *Org. Synth.* **2010**, *87*, 288–298.
- (42) Clarkson, T. W.; Magos, L. *Crit. Rev. Toxicol.* **2006**, *36*, 609–662.

- (43) Mutter, J.; Naumann, J.; Guethlin, C. *Crit. Rev. Toxicol.* **2007**, *37*, 537–549.
- (44) Sugiura, Y.; Tamai, Y.; Tanaka, H. *Bioinorg. Chem.* **1978**, *9*, 167–180.
- (45) George, G. N.; Pickering, I. J.; Madden, S.; Prince, R. C.; Yu, E. Y.; Denton, M. B.; Younis, H. S.; Aposhian, H. V. *Chem. Res. Toxicol.* **2000**, *13*, 1135–1142.
- (46) Isaia, F.; Aragoni, M. C.; Arca, M.; Caltagirone, C.; Castellano, C.; Demartin, F.; Garau, A.; Lippolis, V.; Pintus, A. *Dalton Trans.* **2011**, *40*, 4505–4513.
- (47) Lobana, T. S.; Sandhu, A. K.; Jassal, A. K.; Hundal, G.; Mahajan, R. K.; Jasinski, J. P.; Butcher, R. J. *Polyhedron* **2015**, *87*, 17–27.
- (48) Lu, W.; Barber, P. S.; Kelley, S. P.; Rogers, R. D. *Dalton Trans.* **2013**, *42*, 12908–12916.
- (49) Popovic, Z.; Matkovic-Calogovic, D.; Soldin, Z.; Pavlovic, G.; Davidovic, N.; Vikić-Topic, D. *Inorg. Chim. Acta.* **1999**, *294*, 35–46.
- (50) Popović, Z.; Matković-Čalogović, D.; Pavlović, G.; Soldin, Z.; Giester, G.; Rajić, M.; Vikić-Topić, D. *Croat. Chem. Acta* **2001**, *74*, 359–380.
- (51) Melnick, J. G.; Yurkerwich, K.; Parkin, G. *Inorg. Chem.* **2009**, *48*, 6763–6772.
- (52) Cristiani, F.; Demartin, F.; Devillanova, F. A.; Diaz, A.; Isaia, F.; Verani, G. *J. Coord. Chem* **1990**, *21*, 137–146.
- (53) Gardinier, J. R.; Gabbai, F. P. *Dalton Trans.* **2000**, 2861–2865.
- (54) Hwang, H. J.; Berry, S. M.; Nilges, M. J.; Lu, Y. *J. Am. Chem. Soc.* **2005**, *127*, 7274–7275.
- (55) Wilson, T. D.; Yu, Y.; Lu, Y. *Coord. Chem. Rev.* **2013**, *257*, 260–276.
- (56) Uson, R.; Laguna, A. *Inorg. Synth.* **1989**, *26*, 85–91.

- (57) Nelson, D. J.; Nahra, F.; Patrick, S. R.; Cordes, D. B.; Slawin, A. M. Z.; Nolan, S. P. *Organometallics* **2014**, *33*, 3640–3645.
- (58) Herrero-Gómez, E.; Nieto-Oberhuber, C.; López, S.; Benet-Buchholz, J.; Echavarren, A. M. *Angew. Chem. Int. Ed. Engl.* **2006**, *45*, 5455–5459.
- (59) Perez-Galan, P.; Delpont, N.; Herrero-Gomez, E.; Maseras, F.; Echavarren, A. M. *Chem. Eur. J.* **2010**, *16*, 5324–5332.
- (60) Fulmer, G. R.; Miller, A. J. M.; Sherden, N. H.; Gottlieb, H. E.; Nudelman, A.; Stoltz, B. M.; Bercaw, J. E.; Goldberg, K. I. *Organometallics* **2010**, *29*, 2176–2179.
- (61) Mayr, M.; Wurst, K.; Ongania, K.-H.; Buchmeiser, M. R. *Chem. - A Eur. J.* **2004**, *10*, 1256–1266.
- (62) Schaper, L. A.; Hock, S. J.; Herrmann, W. A.; Kuhn, F. E. *Angew. Chem. Int. Ed. Engl.* **2013**, *52*, 270–289.
- (63) Manjare, S. T.; Singh, H. B.; Butcher, R. J. *Eur. J. Inorg. Chem.* **2013**, 2161–2166.
- (64) Bantu, B.; Wang, D.; Wurst, K.; Buchmeiser, M. R. *Tetrahedron* **2005**, *61*, 12145–12152.
- (65) Bertrand, B.; Stefan, L.; Pirrotta, M.; Monchaud, D.; Bodio, E.; Richard, P.; Le Gendre, P.; Warmerdam, E.; de Jager, M. H.; Groothuis, G. M. M.; Picquet, M.; Casini, A. *Inorg. Chem.* **2014**, *53*, 2296–2303.
- (66) Fortman, G. C.; Slawin, A. M. Z.; Nolan, S. P. *Organometallics* **2010**, *29*, 3966–3972.
- (67) Gaillard, S.; Slawin, A. M. Z.; Nolan, S. P. *Chem. Commun.* **2010**, *46*, 2742–2744.
- (68) Che, C. M. U.S. Patent 8 722 897 B2, 2014.
- (69) Oliver, K.; White, A. J. P.; Hogarth, G.; Wilton-Ely, J. D. E. T. *Dalton Trans.* **2011**, *40*, 5852–5864.

- (70) Sun, R. W. ai Y.; Zhang, M.; Li, D.; Zhang, Z. F.; Cai, H.; Li, M.; Xian, Y. J.; Ng, S. W. eng; Wong, A. S. T. *Chem. Eur. J.* **2015**, *21*, 18534–18538.
- (71) Jamaludin, N. S.; Goh, Z. J.; Cheah, Y. K.; Ang, K. P.; Sim, J. H.; Khoo, C. H.; Fairuz, Z. A.; Halim, S. N. B. A.; Ng, S. W.; Seng, H. L.; Tiekink, E. R. T. *Eur. J. Med. Chem.* **2013**, *67*, 127–141.
- (72) Yang, L.; Wei, D.; Mai, W.; Mao, P. *Chin. J. Org. Chem.* **2013**, *33*, 943–953.

APPENDIX A: CRYSTAL DATA FOR SpymXyS

Empirical formula	C ₂₀ H ₂₄ N ₂ S	
Formula weight	324.47	
Temperature	200(2) K	
Wavelength	1.54178 Å	
Crystal system, space group	Monoclinic, <i>P</i> 2 ₁ / <i>n</i> (No. 11)	
Unit cell dimensions	a = 12.9086(19) Å	α = 90°.
	b = 7.3709(10) Å	β = 94.062(6)°.
	c = 18.691(3) Å	γ = 90°.
Volume	1774.0(4) Å ³	
Z, Calculated density	4, 1.215 Mg/m ³	
Absorption coefficient	1.608 mm ⁻¹	
Crystal size	0.20 x 0.20 x 0.20 mm ³	
Crystal color / habit	colorless / block	
Theta range for data collection	4.03 to 70.31°.	
Reflections collected / unique	23186 / 3344 [R(int) = 0.0383]	
Completeness to theta = 25.25°	99.4 %	
Absorption correction	multi-scan / sadabs	
Max. and min. transmission	0.7393 and 0.7393	
Refinement method	Full-matrix least-squares on F ²	
Goodness-of-fit on F ²	1.032	
Final R indices [I > 2σ(I)]	R1 = 0.0388, wR2 = 0.1108	
R indices (all data)	R1 = 0.0430, wR2 = 0.1154	
Largest diff. peak and hole	0.202 and -0.276 e.Å ⁻³	

APPENDIX B: CRYSTAL DATA FOR SpymXySe

Empirical formula	C ₂₀ H ₂₄ N ₂ Se	
Formula weight	371.37	
Temperature	200(2) K	
Wavelength	0.71073 Å	
Crystal system, space group	Monoclinic, <i>P</i> 2 ₁ / <i>n</i> (No. 11)	
Unit cell dimensions	a = 8.3395(13) Å	$\alpha = 90^\circ$.
	b = 16.445(3) Å	$\beta = 98.634(5)^\circ$.
	c = 13.390(2) Å	$\gamma = 90^\circ$.
Volume	1815.5(5) Å ³	
Z, Calculated density	4, 1.359 Mg/m ³	
Absorption coefficient	2.070 mm ⁻¹	
Crystal size	0.20 x 0.18 x 0.15 mm ³	
Crystal color / habit	colorless / block	
Theta range for data collection	3.08 to 25.67°.	
Reflections collected / unique	23186 / 3344 [R(int) = 0.0383]	
Completeness to theta = 25.25°	99.4 %	
Absorption correction	multi-scan / sadabs	
Max. and min. transmission	0.7465 and 0.6823	
Refinement method	Full-matrix least-squares on F ²	
Goodness-of-fit on F ²	1.006	
Final R indices [I > 2sigma(I)]	R1 = 0.0248, wR2 = 0.0583	
R indices (all data)	R1 = 0.0346, wR2 = 0.0628	
Largest diff. peak and hole	0.258 and -0.335 e.Å ⁻³	

APPENDIX C: CRYSTAL DATA FOR SpymMesS

Empirical formula	C ₂₂ H ₂₈ N ₂ S	
Formula weight	352.52	
Temperature	200(2) K	
Wavelength	0.71073 Å	
Crystal system, space group	Orthorhombic, <i>Pbcn</i> (No. 60)	
Unit cell dimensions	a = 15.641(2) Å	α = 90°.
	b = 16.445(3) Å	β = 90°.
	c = 13.390(2) Å	γ = 90°.
Volume	1965.4(5) Å ³	
Z, Calculated density	4, 1.191 Mg/m ³	
Absorption coefficient	0.171 mm ⁻¹	
Crystal size	0.25 x 0.20 x 0.18 mm ³	
Crystal color / habit	colorless / block	
Theta range for data collection	3.65 to 25.72°.	
Reflections collected / unique	54779/ 1874 [R(int) = 0.0497]	
Completeness to theta = 25.25°	99.6 %	
Absorption correction	multi-scan / sadabs	
Max. and min. transmission	0.9698 and 0.9584	
Refinement method	Full-matrix least-squares on F ²	
Goodness-of-fit on F ²	1.023	
Final R indices [I>2sigma(I)]	R1 = 0.0363, wR2 = 0.1055	
R indices (all data)	R1 = 0.0433, wR2 = 0.1135	
Largest diff. peak and hole	0.186 and -0.185 e.Å ⁻³	

APPENDIX D: CRYSTAL DATA FOR SpymMesSe

Empirical formula	C ₂₂ H ₂₈ N ₂ Se	
Formula weight	399.42	
Temperature	200(2) K	
Wavelength	1.54178 Å	
Crystal system, space group	Orthorhombic, <i>Pbcn</i> (No. 60)	
Unit cell dimensions	a = 15.598(2) Å	α = 90°.
	b = 7.9457(12) Å	β = 90°.
	c = 16.054(2) Å	γ = 90°.
Volume	1989.7(5) Å ³	
Z, Calculated density	4, 1.333 Mg/m ³	
Absorption coefficient	2.582 mm ⁻¹	
Crystal size	0.29 x 0.20 x 0.20 mm ³	
Crystal color / habit	colorless / block	
Theta range for data collection	6.25 to 70.13°.	
Reflections collected / unique	54779/ 1874 [R(int) = 0.0497]	
Completeness to theta = 25.25°	99.6 %	
Absorption correction	multi-scan / sadabs	
Max. and min. transmission	0.6262 and 0.5214	
Refinement method	Full-matrix least-squares on F ²	
Goodness-of-fit on F ²	1.050	
Final R indices [I>2sigma(I)]	R1 = 0.0270, wR2 = 0.0800	
R indices (all data)	R1 = 0.0290, wR2 = 0.0820	
Largest diff. peak and hole	0.260 and -0.544 e.Å ⁻³	

APPENDIX E: CRYSTAL DATA FOR (SpymMesS)I₂

Empirical formula	C ₂₂ H ₂₈ I ₂ N ₂ S	
Formula weight	606.32	
Temperature	200(2) K	
Wavelength	0.71073 Å	
Crystal system, space group	Triclinic, $P\bar{1}$ (No. 2)	
Unit cell dimensions	a = 7.6891(11) Å	$\alpha = 83.037(5)^\circ$.
	b = 8.2888(13) Å	$\beta = 86.716(5)^\circ$.
	c = 18.868(3) Å	$\gamma = 81.224(5)^\circ$.
Volume	1178.8(3) Å ³	
Z, Calculated density	2, 1.708 Mg/m ³	
Absorption coefficient	2.766 mm ⁻¹	
Crystal size	0.20 x 0.18 x 0.16 mm ³	
Crystal color / habit	red / block	
Theta range for data collection	3.12 to 25.46°.	
Reflections collected / unique	25720/ 4323 [R(int) = 0.0328]	
Completeness to theta = 25.25°	99.6 %	
Absorption correction	multi-scan / sadabs	
Max. and min. transmission	0.6659 and 0.6077	
Refinement method	Full-matrix least-squares on F ²	
Goodness-of-fit on F ²	1.014	
Final R indices [I > 2sigma(I)]	R1 = 0.0211, wR2 = 0.0513	
R indices (all data)	R1 = 0.0268, wR2 = 0.0562	
Largest diff. peak and hole	0.444 and -0.588 e.Å ⁻³	

APPENDIX F: CRYSTAL DATA FOR (SpymDippS)I₂

Empirical formula	C ₂₈ H ₄₀ I ₂ N ₂ S	
Formula weight	690.48	
Temperature	200(2) K	
Wavelength	0.71073 Å	
Crystal system, space group	Orthorhombic, <i>Fdd2</i> (No. 43)	
Unit cell dimensions	a = 32.326(7) Å	α = 90°
	b = 33.873(7) Å	β = 90°
	c = 10.764(2) Å	γ = 90°
Volume	11786(4) Å ³	
Z, Calculated density	16, 1.557 Mg/m ³	
Absorption coefficient	2.223 mm ⁻¹	
Crystal size	0.35 x 0.12 x 0.10 mm ³	
Crystal color / habit	orange-brown/ block	
Theta range for data collection	2.793 to 25.721°	
Reflections collected / unique	70772/ 5607 [R(int) = 0.0593]	
Completeness to theta = 25.25°	99.8 %	
Absorption correction	multi-scan / sadabs	
Max. and min. transmission	0.6659 and 0.6077	
Refinement method	Full-matrix least-squares on F ²	
Goodness-of-fit on F ²	1.003	
Final R indices [I > 2σ(I)]	R1 = 0.0257, wR2 = 0.0429	
R indices (all data)	R1 = 0.0338, wR2 = 0.0456	
Largest diff. peak and hole	0.408 and -0.333 e.Å ⁻³	

APPENDIX G: CRYSTAL DATA FOR (SpymXySe)I₂

Empirical formula	C ₂₀ H ₂₄ I ₂ N ₂ Se	
Formula weight	625.17	
Temperature	200(2) K	
Wavelength	0.71073 Å	
Crystal system, space group	Monoclinic, <i>P</i> 2 ₁ / <i>n</i> (No. 11)	
Unit cell dimensions	a = 8.2103(5) Å	α = 90°.
	b = 11.5150(8) Å	β = 97.927(2)°.
	c = 23.0290(16) Å	γ = 90°.
Volume	2156.4(2) Å ³	
Z, Calculated density	4, 1.926 Mg/m ³	
Absorption coefficient	4.610 mm ⁻¹	
Crystal size	0.25 x 0.15 x 0.10 mm ³	
Crystal color / habit	red/ block	
Theta range for data collection	3.10 to 25.38°.	
Reflections collected / unique	46806/ 3942 [R(int) = 0.0347]	
Completeness to theta = 25.25°	99.7 %	
Absorption correction	multi-scan / sadabs	
Max. and min. transmission	0.6557 and 0.3919	
Refinement method	Full-matrix least-squares on F ²	
Goodness-of-fit on F ²	1.094	
Final R indices [I > 2σ(I)]	R1 = 0.0275, wR2 = 0.0596	
R indices (all data)	R1 = 0.0362, wR2 = 0.0654	
Largest diff. peak and hole	0.970 and -0.728 e.Å ⁻³	

APPENDIX H: CRYSTAL DATA FOR (SpymMesSe)I₂

Empirical formula	C ₂₂ H ₂₈ I ₂ N ₂ Se	
Formula weight	625.17	
Temperature	200(2) K	
Wavelength	0.71073 Å	
Crystal system, space group	Triclinic, $P\bar{1}$ (No. 2)	
Unit cell dimensions	a = 7.7778(5) Å	$\alpha = 83.519(3)^\circ$.
	b = 8.2299(6) Å	$\beta = 86.419(3)^\circ$.
	c = 18.9104(15) Å	$\gamma = 81.224(3)^\circ$.
Volume	1187.39(15) Å ³	
Z, Calculated density	2, 1.827 Mg/m ³	
Absorption coefficient	4.191 mm ⁻¹	
Crystal size	0.18 x 0.15 x 0.10 mm ³	
Crystal color / habit	red/ block	
Theta range for data collection	3.15 to 25.74°.	
Reflections collected / unique	35252/ 4508 [R(int) = 0.0473]	
Completeness to theta = 25.25°	99.8 %	
Absorption correction	multi-scan / sadabs	
Max. and min. transmission	0.6793 and 0.5192	
Refinement method	Full-matrix least-squares on F ²	
Goodness-of-fit on F ²	1.065	
Final R indices [I > 2sigma(I)]	R1 = 0.0217, wR2 = 0.0437	
R indices (all data)	R1 = 0.0334, wR2 = 0.0487	
Largest diff. peak and hole	0.536 and -0.577 e.Å ⁻³	

APPENDIX I: CRYSTAL DATA FOR (SpymDippSe)I₂

Empirical formula	C ₂₈ H ₄₀ I ₂ N ₂ Se	
Formula weight	737.38	
Temperature	200(2) K	
Wavelength	0.71073 Å	
Crystal system, space group	Orthorhombic, <i>Fdd2</i> (No. 43)	
Unit cell dimensions	a = 32.401(5) Å	α = 90°.
	b = 33.843(5) Å	β = 90°.
	c = 10.8165(15) Å	γ = 90°.
Volume	11861(3) Å ³	
Z, Calculated density	16, 1.652 Mg/m ³	
Absorption coefficient	3.367 mm ⁻¹	
Crystal size	0.34 x 0.06 x 0.04 mm ³	
Crystal color / habit	red/ block	
Theta range for data collection	3.22 to 25.48°.	
Reflections collected / unique	47707/ 5481 [R(int) = 0.0528]	
Completeness to theta = 25.25°	99.7 %	
Absorption correction	multi-scan / sadabs	
Max. and min. transmission	0.8771 and 0.3940	
Refinement method	Full-matrix least-squares on F ²	
Goodness-of-fit on F ²	1.010	
Final R indices [I > 2σ(I)]	R1 = 0.0212, wR2 = 0.0437	
R indices (all data)	R1 = 0.0284, wR2 = 0.0465	
Largest diff. peak and hole	0.454 and -0.337 e.Å ⁻³	

APPENDIX J: CRYSTAL DATA FOR [(SpymXyS)₂I][I₃]

Empirical formula	C ₄₀ H ₄₈ I ₄ N ₄ S ₂	
Formula weight	1156.54	
Temperature	200(2) K	
Wavelength	0.71073 Å	
Crystal system, space group	Triclinic, $P\bar{1}$ (No. 2)	
Unit cell dimensions	a = 11.8310(11) Å	$\alpha = 88.969(3)^\circ$.
	b = 12.0083(11) Å	$\beta = 73.747(3)^\circ$.
	c = 16.1731(12) Å	$\gamma = 81.548(3)^\circ$.
Volume	2181.3(3) Å ³	
Z, Calculated density	2, 1.761 Mg/m ³	
Absorption coefficient	2.985 mm ⁻¹	
Crystal size	0.20 x 0.18 x 0.10 mm ³	
Crystal color / habit	red/ block	
Theta range for data collection	3.10 to 25.42°.	
Reflections collected / unique	74178/ 8037 [R(int) = 0.0328]	
Completeness to theta = 25.25°	99.8 %	
Absorption correction	multi-scan / sadabs	
Max. and min. transmission	0.7545 and 0.5867	
Refinement method	Full-matrix least-squares on F ²	
Goodness-of-fit on F ²	1.088	
Final R indices [I > 2sigma(I)]	R1 = 0.0223, wR2 = 0.0471	
R indices (all data)	R1 = 0.0314, wR2 = 0.0527	
Largest diff. peak and hole	0.730 and -0.653 e.Å ⁻³	

APPENDIX K: CRYSTAL DATA FOR [(SpymXyS)₂HgCl][HgCl₃]

Empirical formula	C ₄₀ H ₄₈ Cl ₄ Hg ₂ N ₄ S ₂
Formula weight	1191.92
Temperature	200(2) K
Wavelength	0.71073 Å
Crystal system, space group	Orthorhombic, <i>P</i> 2 ₁ 2 ₁ 2 ₁ (No. 19)
Unit cell dimensions	a = 8.3784(6) Å α = 90°. b = 18.6452(15) Å β = 90°. c = 27.298(2) Å γ = 90°.
Volume	4264.4(6) Å ³
Z, Calculated density	4, 1.857 Mg/m ³
Absorption coefficient	7.574 mm ⁻¹
Crystal size	0.20 x 0.20 x 0.14 mm ³
Crystal color / habit	colorless/ block
Theta range for data collection	3.05 to 25.39°.
Reflections collected / unique	112882/ 7806 [R(int) = 0.0752]
Completeness to theta = 25.25°	99.7 %
Absorption correction	multi-scan / sadabs
Max. and min. transmission	0.4169 and 0.3127
Refinement method	Full-matrix least-squares on F ²
Goodness-of-fit on F ²	1.059
Final R indices [I > 2σ(I)]	R1 = 0.0255, wR2 = 0.0444
R indices (all data)	R1 = 0.0386, wR2 = 0.0486
Largest diff. peak and hole	0.644 and -0.689 e.Å ⁻³

APPENDIX L: CRYSTAL DATA FOR (SpymXyS)HgBr₂

Empirical formula	C ₂₀ H ₂₄ Br ₂ HgN ₂ S	
Formula weight	684.88	
Temperature	200(2) K	
Wavelength	0.71073 Å	
Crystal system, space group	Monoclinic, C2/c (No. 15)	
Unit cell dimensions	a = 17.348(3) Å	α = 90°.
	b = 8.5572(13) Å	β = 90.554(5)°.
	c = 29.590(4) Å	γ = 90°.
Volume	4392.5(12) Å ³	
Z, Calculated density	8, 2.071 Mg/m ³	
Absorption coefficient	10.749 mm ⁻¹	
Crystal size	0.20 x 0.18 x 0.12 mm ³	
Crystal color / habit	colorless/ block	
Theta range for data collection	3.36 to 25.77°.	
Reflections collected / unique	94160/ 4192 [R(int) = 0.0498]	
Completeness to theta = 25.25°	99.7 %	
Absorption correction	multi-scan / sadabs	
Max. and min. transmission	0.3587 and 0.2224	
Refinement method	Full-matrix least-squares on F ²	
Goodness-of-fit on F ²	1.089	
Final R indices [I > 2σ(I)]	R1 = 0.0273, wR2 = 0.0628	
R indices (all data)	R1 = 0.0345, wR2 = 0.0654	
Largest diff. peak and hole	0.530 and -1.083 e.Å ⁻³	

APPENDIX M: CRYSTAL DATA FOR (SpymXyS)HgI₂

Empirical formula	C ₂₀ H ₂₄ HgI ₂ N ₂ S	
Formula weight	778.86	
Temperature	200(2) K	
Wavelength	0.71073 Å	
Crystal system, space group	Monoclinic, C2 (No. 5)	
Unit cell dimensions	a = 18.291(2) Å	α = 90°.
	b = 8.5355(10) Å	β = 114.123(3)°.
	c = 16.5271(16) Å	γ = 90°.
Volume	2354.9(4) Å ³	
Z, Calculated density	4, 2.197 Mg/m ³	
Absorption coefficient	9.253 mm ⁻¹	
Crystal size	0.20 x 0.20 x 0.19 mm ³	
Crystal color / habit	pale yellow / block	
Theta range for data collection	3.22 to 25.76°.	
Reflections collected / unique	58630/ 4461 [R(int) = 0.0381]	
Completeness to theta = 25.25°	99.6 %	
Absorption correction	multi-scan / sadabs	
Max. and min. transmission	0.2723 and 0.2591	
Refinement method	Full-matrix least-squares on F ²	
Goodness-of-fit on F ²	1.043	
Final R indices [I > 2σ(I)]	R1 = 0.0143, wR2 = 0.0311	
R indices (all data)	R1 = 0.0153, wR2 = 0.0313	
Largest diff. peak and hole	0.563 and -0.647 e.Å ⁻³	

APPENDIX N: CRYSTAL DATA FOR (SpymXySe)HgCl₂

Empirical formula	C ₂₀ H ₂₄ Cl ₂ HgN ₂ Se	
Formula weight	642.86	
Temperature	200(2) K	
Wavelength	0.71073 Å	
Crystal system, space group	Triclinic, $P\bar{1}$ (No. 2)	
Unit cell dimensions	a = 8.4660(7) Å	$\alpha = 79.709(2)^\circ$.
	b = 9.4961(7) Å	$\beta = 89.393(3)^\circ$.
	c = 14.7337(10) Å	$\gamma = 68.318(2)^\circ$.
Volume	1081.00(14) Å ³	
Z, Calculated density	2, 1.975 Mg/m ³	
Absorption coefficient	9.056 mm ⁻¹	
Crystal size	0.20 x 0.20 x 0.20 mm ³	
Crystal color / habit	pale yellow / block	
Theta range for data collection	3.31 to 25.71°.	
Reflections collected / unique	31348/ 4107 [R(int) = 0.0290]	
Completeness to theta = 25.25°	99.5 %	
Absorption correction	multi-scan / sadabs	
Max. and min. transmission	0.2646 and 0.2646	
Refinement method	Full-matrix least-squares on F ²	
Goodness-of-fit on F ²	1.082	
Final R indices [I > 2sigma(I)]	R1 = 0.0159, wR2 = 0.0373	
R indices (all data)	R1 = 0.0172, wR2 = 0.0379	
Largest diff. peak and hole	0.728 and -0.562 e.Å ⁻³	

APPENDIX O: CRYSTAL DATA FOR (SpymXySe)HgBr₂

Empirical formula	C ₂₀ H ₂₄ Br ₂ HgN ₂ Se	
Formula weight	731.78	
Temperature	200(2) K	
Wavelength	0.71073 Å	
Crystal system, space group	Monoclinic, C2/c (No. 15)	
Unit cell dimensions	a = 17.591(2) Å	α = 90°.
	b = 8.4772(10) Å	β = 90.901(4)°.
	c = 29.792(3) Å	γ = 90°.
Volume	4442.1(9) Å ³	
Z, Calculated density	8, 2.188 Mg/m ³	
Absorption coefficient	12.173 mm ⁻¹	
Crystal size	0.22 x 0.20 x 0.18 mm ³	
Crystal color / habit	pale yellow / block	
Theta range for data collection	3.01 to 25.74°.	
Reflections collected / unique	48423/ 4220 [R(int) = 0.0449]	
Completeness to theta = 25.00°	99.7 %	
Absorption correction	multi-scan / sadabs	
Max. and min. transmission	0.2179 and 0.1748	
Refinement method	Full-matrix least-squares on F ²	
Goodness-of-fit on F ²	1.055	
Final R indices [I > 2σ(I)]	R1 = 0.0317, wR2 = 0.0789	
R indices (all data)	R1 = 0.0388, wR2 = 0.0830	
Largest diff. peak and hole	0.539 and -1.199 e.Å ⁻³	

APPENDIX P: CRYSTAL DATA FOR (SpymXySe)HgI₂

Empirical formula	C ₂₀ H ₂₄ HgI ₂ N ₂ Se	
Formula weight	825.76	
Temperature	200(2) K	
Wavelength	0.71073 Å	
Crystal system, space group	Monoclinic, C2 (No. 5)	
Unit cell dimensions	a = 18.273(2) Å	α = 90°.
	b = 8.5111(11) Å	β = 117.773(4)°.
	c = 16.9790(19) Å	γ = 90°.
Volume	2336.4(5) Å ³	
Z, Calculated density	4, 2.348 Mg/m ³	
Absorption coefficient	10.795 mm ⁻¹	
Crystal size	0.18 x 0.06 x 0.04 mm ³	
Crystal color / habit	yellow / block	
Theta range for data collection	3.28 to 25.75°.	
Reflections collected / unique	28362/ 4432 [R(int) = 0.0438]	
Completeness to theta = 25.25°	99.6 %	
Absorption correction	multi-scan / sadabs	
Max. and min. transmission	0.6720 and 0.2468	
Refinement method	Full-matrix least-squares on F ²	
Goodness-of-fit on F ²	1.002	
Final R indices [I > 2σ(I)]	R1 = 0.0208, wR2 = 0.0443	
R indices (all data)	R1 = 0.0238, wR2 = 0.0455	
Largest diff. peak and hole	0.681 and -0.907 e.Å ⁻³	

APPENDIX Q: CRYSTAL DATA FOR [(SpymMesS)₂HgCl][HgCl₃]

Empirical formula	C ₄₄ H ₅₆ Cl ₄ Hg ₂ N ₄ S ₂
Formula weight	1248.03
Temperature	200(2) K
Wavelength	0.71073 Å
Crystal system, space group	Monoclinic, <i>P</i> ₂ ₁ / <i>c</i> (No. 14)
Unit cell dimensions	a = 15.5639(15) Å α = 90°. b = 21.3923(17) Å β = 108.375(3)°. c = 14.8571(13) Å γ = 90°.
Volume	4694.4(7) Å ³
Z, Calculated density	4, 1.766 Mg/m ³
Absorption coefficient	6.884 mm ⁻¹
Crystal size	0.18 x 0.15 x 0.14 mm ³
Crystal color / habit	colorless / block
Theta range for data collection	2.84 to 25.43°.
Reflections collected / unique	108364/ 8617 [R(int) = 0.0368]
Completeness to theta = 25.25°	99.8 %
Absorption correction	multi-scan / sadabs
Max. and min. transmission	0.4457 and 0.3704
Refinement method	Full-matrix least-squares on F ²
Goodness-of-fit on F ²	1.052
Final R indices [I > 2σ(I)]	R1 = 0.0310, wR2 = 0.0772
R indices (all data)	R1 = 0.0383, wR2 = 0.0824
Largest diff. peak and hole	3.030 and -1.863 e.Å ⁻³

APPENDIX R: CRYSTAL DATA FOR [Hg(SpymMesS)₂][Hg₂Br₆]

Empirical formula	C ₄₄ H ₅₆ Br ₆ Hg ₃ N ₄ S ₂	
Formula weight	1786.28	
Temperature	200(2) K	
Wavelength	0.71073 Å	
Crystal system, space group	Triclinic, $P\bar{1}$ (No. 2)	
Unit cell dimensions	a = 10.4994(5) Å	$\alpha = 74.9400(10)^\circ$.
	b = 11.3798(4) Å	$\beta = 81.878(2)^\circ$.
	c = 11.4318(5) Å	$\gamma = 84.3110(10)^\circ$.
Volume	1302.96(10) Å ³	
Z, Calculated density	1, 2.277 Mg/m ³	
Absorption coefficient	13.529 mm ⁻¹	
Crystal size	0.18 x 0.15 x 0.12 mm ³	
Crystal color / habit	colorless / block	
Theta range for data collection	2.86 to 25.71°.	
Reflections collected / unique	20760/ 4937 [R(int) = 0.0252]	
Completeness to theta = 25.25°	99.7 %	
Absorption correction	multi-scan / sadabs	
Max. and min. transmission	0.2936 and 0.1944	
Refinement method	Full-matrix least-squares on F ²	
Goodness-of-fit on F ²	1.037	
Final R indices [I > 2sigma(I)]	R1 = 0.0288, wR2 = 0.0664	
R indices (all data)	R1 = 0.0383, wR2 = 0.0716	
Largest diff. peak and hole	3.339 and -1.788 e.Å ⁻³	

APPENDIX S: CRYSTAL DATA FOR (SpymMesS)HgI₂

Empirical formula	C ₂₂ H ₂₈ HgI ₂ N ₂ S	
Formula weight	806.91	
Temperature	200(2) K	
Wavelength	0.71073 Å	
Crystal system, space group	Monoclinic, C2/c (No. 15)	
Unit cell dimensions	a = 17.757(4) Å	α = 90°.
	b = 8.432(2) Å	β = 92.310(7)°.
	c = 33.425(9) Å	γ = 90°.
Volume	5001(2) Å ³	
Z, Calculated density	8, 2.144 Mg/m ³	
Absorption coefficient	8.719 mm ⁻¹	
Crystal size	0.18 x 0.18 x 0.18 mm ³	
Crystal color / habit	colorless/ block	
Theta range for data collection	2.92 to 25.75°.	
Reflections collected / unique	40798/ 4741 [R(int) = 0.0364]	
Completeness to theta = 25.25°	99.8 %	
Absorption correction	multi-scan / sadabs	
Max. and min. transmission	0.3029 and 0.3029	
Refinement method	Full-matrix least-squares on F ²	
Goodness-of-fit on F ²	1.032	
Final R indices [I > 2σ(I)]	R1 = 0.0347, wR2 = 0.1138	
R indices (all data)	R1 = 0.0431, wR2 = 0.1194	
Largest diff. peak and hole	0.587 and -2.199 e.Å ⁻³	

APPENDIX T: CRYSTAL DATA FOR [(SpymMesSe)₂HgCl][HgCl₃]

Empirical formula	C ₄₄ H ₅₆ Cl ₄ Hg ₂ N ₄ Se ₂	
Formula weight	1341.83	
Temperature	200(2) K	
Wavelength	0.71073 Å	
Crystal system, space group	Monoclinic, <i>P</i> ₂ ₁ / <i>c</i> (No. 14)	
Unit cell dimensions	a = 15.610(2) Å	α = 90°.
	b = 21.508(3) Å	β = 107.540(4)°.
	c = 14.768(2) Å	γ = 90°.
Volume	4727.7(12) Å ³	
Z, Calculated density	4, 1.885 Mg/m ³	
Absorption coefficient	8.287 mm ⁻¹	
Crystal size	0.21 x 0.18 x 0.18 mm ³	
Crystal color / habit	pale yellow / block	
Theta range for data collection	3.15 to 25.43°.	
Reflections collected / unique	88676/ 8680 [R(int) = 0.0389]	
Completeness to theta = 25.25°	99.7 %	
Absorption correction	multi-scan / sadabs	
Max. and min. transmission	0.3170 and 0.2750	
Refinement method	Full-matrix least-squares on F ²	
Goodness-of-fit on F ²	1.012	
Final R indices [I > 2σ(I)]	R1 = 0.0220, wR2 = 0.0513	
R indices (all data)	R1 = 0.0314, wR2 = 0.0560	
Largest diff. peak and hole	0.652 and -0.812 e.Å ⁻³	

APPENDIX U: CRYSTAL DATA FOR (SpymMesSe)HgBr₂

Empirical formula	C ₂₂ H ₂₈ Br ₂ HgN ₂ S	
Formula weight	759.83	
Temperature	200(2) K	
Wavelength	0.71073 Å	
Crystal system, space group	Monoclinic, <i>P</i> ₂ ₁ / <i>c</i> (No. 14)	
Unit cell dimensions	a = 8.5034(18) Å	α = 90°.
	b = 21.320(4) Å	β = 97.013(7)°.
	c = 13.385(3) Å	γ = 90°.
Volume	2408.5(9) Å ³	
Z, Calculated density	4, 2.095 Mg/m ³	
Absorption coefficient	17.146 mm ⁻¹	
Crystal size	0.20 x 0.18 x 0.10 mm ³	
Crystal color / habit	colorless/ block	
Theta range for data collection	3.92 to 25.43°.	
Reflections collected / unique	30358/ 4395 [R(int) = 0.0483]	
Completeness to theta = 25.25°	99.3 %	
Absorption correction	multi-scan / sadabs	
Max. and min. transmission	0.2789 and 0.1308	
Refinement method	Full-matrix least-squares on F ²	
Goodness-of-fit on F ²	1.031	
Final R indices [I > 2σ(I)]	R1 = 0.0369, wR2 = 0.1105	
R indices (all data)	R1 = 0.0378, wR2 = 0.1121	
Largest diff. peak and hole	1.958 and -0.858 e.Å ⁻³	

APPENDIX V: CRYSTAL DATA FOR (SpymMesSe)HgI₂

Empirical formula	C ₂₂ H ₂₈ HgI ₂ N ₂ S	
Formula weight	853.81	
Temperature	200(2) K	
Wavelength	1.54178 Å	
Crystal system, space group	Monoclinic, C2/c (No. 15)	
Unit cell dimensions	a = 18.101(3) Å	α = 90°.
	b = 8.3479(17) Å	β = 91.077(7)°.
	c = 33.500(7) Å	γ = 90°.
Volume	5061.1(17) Å ³	
Z, Calculated density	8, 2.241 Mg/m ³	
Absorption coefficient	31.778 mm ⁻¹	
Crystal size	0.18 x 0.14 x 0.09 mm ³	
Crystal color / habit	colorless/ block	
Theta range for data collection	2.638 to 25.43°.	
Reflections collected / unique	26386/ 4571 [R(int) = 0.0701]	
Completeness to theta = 25.25°	98.9 %	
Absorption correction	None	
Max. and min. transmission	0.2789 and 0.1308	
Refinement method	Full-matrix least-squares on F ²	
Goodness-of-fit on F ²	1.059	
Final R indices [I > 2σ(I)]	R1 = 0.0460, wR2 = 0.1243	
R indices (all data)	R1 = 0.0524, wR2 = 0.1306	
Largest diff. peak and hole	1.586 and -1.434 e.Å ⁻³	

APPENDIX W: CRYSTAL DATA FOR [Hg(SpymDippS)₂][Hg₂Cl₆](C₃H₆O)₂(C₆H₆)

Empirical formula	C ₆₈ H ₉₈ Cl ₆ Hg ₃ N ₂ O ₂ S ₂	
Formula weight	1882.09	
Temperature	200(2) K	
Wavelength	0.71073 Å	
Crystal system, space group	Triclinic, $P\bar{1}$ (No. 2)	
Unit cell dimensions	a = 10.844(2) Å	$\alpha = 66.442(6)^\circ$.
	b = 13.975(3) Å	$\beta = 68.493(6)^\circ$.
	c = 14.786(3) Å	$\gamma = 88.706(6)^\circ$.
Volume	1890.8(6) Å ³	
Z, Calculated density	1, 1.653 Mg/m ³	
Absorption coefficient	6.385 mm ⁻¹	
Crystal size	0.20 x 0.18 x 0.15 mm ³	
Crystal color / habit	colorless/ block	
Theta range for data collection	2.730 to 25.768°.	
Reflections collected / unique	62911/ 7207 [R(int) = 0.0477]	
Completeness to theta = 25.25°	99.8 %	
Absorption correction	multi-scan / sadabs	
Max. and min. transmission	0.2789 and 0.1308	
Refinement method	Full-matrix least-squares on F ²	
Goodness-of-fit on F ²	1.074	
Final R indices [I > 2sigma(I)]	R1 = 0.0240, wR2 = 0.0500	
R indices (all data)	R1 = 0.0344, wR2 = 0.0548	
Largest diff. peak and hole	0.967 and -0.636 e.Å ⁻³	

APPENDIX X: CRYSTAL DATA FOR [Hg(SpymDippS)₂][Hg₂Br₆](C₃H₆O)₂

Empirical formula	C ₆₂ H ₉₂ Cl ₆ Hg ₃ N ₂ O ₂ S ₂
Formula weight	2070.75
Temperature	200(2) K
Wavelength	0.71073 Å
Crystal system, space group	Monoclinic, <i>P</i> 2 ₁ / <i>n</i> (No. 11)
Unit cell dimensions	a = 10.8048(13) Å α = 90°. b = 16.6544(19) Å β = 104.118(4)°. c = 20.745(2) Å γ = 90°.
Volume	3620.3(7) Å ³
Z, Calculated density	2, 1.900 Mg/m ³
Absorption coefficient	9.755 mm ⁻¹
Crystal size	0.19 x 0.15 x 0.14 mm ³
Crystal color / habit	colorless/ block
Theta range for data collection	3.12 to 25.48°.
Reflections collected / unique	119271/ 6638 [R(int) = 0.0731]
Completeness to theta = 25.25°	99.8 %
Absorption correction	multi-scan / sadabs
Max. and min. transmission	0.3421 and 0.2587
Refinement method	Full-matrix least-squares on F ²
Goodness-of-fit on F ²	1.099
Final R indices [I > 2σ(I)]	R1 = 0.0397, wR2 = 0.1029
R indices (all data)	R1 = 0.0495, wR2 = 0.1130
Largest diff. peak and hole	2.219 and -2.036 e.Å ⁻³

APPENDIX Y: CRYSTAL DATA FOR [Hg(SpymDippS)₂][Hg₂I₆](C₃H₆O)₂

Empirical formula	C ₆₂ H ₉₂ I ₆ Hg ₃ N ₂ O ₂ S ₂	
Formula weight	2352.69	
Temperature	200(2) K	
Wavelength	0.71073 Å	
Crystal system, space group	Monoclinic, <i>P</i> 2 ₁ / <i>n</i> (No. 11)	
Unit cell dimensions	a = 10.9463(9) Å	α = 90°.
	b = 16.9962(14) Å	β = 104.798(2)°.
	c = 21.0877(17) Å	γ = 90°.
Volume	3793.1(5) Å ³	
Z, Calculated density	2, 2.060 Mg/m ³	
Absorption coefficient	8.592 mm ⁻¹	
Crystal size	0.19 x 0.18 x 0.17 mm ³	
Crystal color / habit	pale yellow / block	
Theta range for data collection	3.07 to 25.40°.	
Reflections collected / unique	127887/ 6957 [R(int) = 0.0500]	
Completeness to theta = 25.25°	99.6 %	
Absorption correction	multi-scan / sadabs	
Max. and min. transmission	0.3229 and 0.2921	
Refinement method	Full-matrix least-squares on F ²	
Goodness-of-fit on F ²	1.098	
Final R indices [I > 2σ(I)]	R1 = 0.0390, wR2 = 0.1078	
R indices (all data)	R1 = 0.0463, wR2 = 0.1119	
Largest diff. peak and hole	1.902 and -2.095 e.Å ⁻³	

APPENDIX Z: CRYSTAL DATA FOR [Hg(SpymDippSe)₂][Hg₂Cl₆](C₃H₆O)₂

Empirical formula	C ₆₂ H ₉₂ I ₆ Hg ₃ N ₂ O ₂ S ₂	
Formula weight	1897.79	
Temperature	200(2) K	
Wavelength	0.71073 Å	
Crystal system, space group	Triclinic, $P\bar{1}$ (No. 2)	
Unit cell dimensions	a = 10.8100(13) Å	$\alpha = 73.382(5)^\circ$.
	b = 11.2186(13) Å	$\beta = 84.276(5)^\circ$.
	c = 15.215(2) Å	$\gamma = 87.981(4)^\circ$.
Volume	1759.3(4) Å ³	
Z, Calculated density	1, 1.791 Mg/m ³	
Absorption coefficient	7.833 mm ⁻¹	
Crystal size	0.19 x 0.15 x 0.10 mm ³	
Crystal color / habit	colorless / block	
Theta range for data collection	3.20 to 25.78°.	
Reflections collected / unique	59368/ 6715 [R(int) = 0.0415]	
Completeness to theta = 25.25°	99.8 %	
Absorption correction	multi-scan / sadabs	
Max. and min. transmission	0.5080 and 0.3176	
Refinement method	Full-matrix least-squares on F ²	
Goodness-of-fit on F ²	1.001	
Final R indices [I > 2sigma(I)]	R1 = 0.0170, wR2 = 0.0383	
R indices (all data)	R1 = 0.0236, wR2 = 0.0408	
Largest diff. peak and hole	0.484 and -0.482 e.Å ⁻³	

APPENDIX AA: CRYSTAL DATA FOR [Hg(SpymDippSe)₂][Hg₂Br₆](C₄H₈O)₂

Empirical formula	C ₆₄ H ₉₆ I ₆ Hg ₃ N ₂ O ₂ S ₂	
Formula weight	2192.60	
Temperature	200(2) K	
Wavelength	0.71073 Å	
Crystal system, space group	Monoclinic, <i>P</i> 2 ₁ / <i>n</i> (No. 11)	
Unit cell dimensions	a = 11.2588(7) Å	α = 90°.
	b = 20.9431(11) Å	β = 98.413(2)°.
	c = 15.7313(10) Å	γ = 90°.
Volume	3669.4(4) Å ³	
Z, Calculated density	2, 1.984 Mg/m ³	
Absorption coefficient	10.561 mm ⁻¹	
Crystal size	0.10 x 0.10 x 0.08 mm ³	
Crystal color / habit	colorless / block	
Theta range for data collection	3.12 to 25.41°.	
Reflections collected / unique	88432/ 6741 [R(int) = 0.0483]	
Completeness to theta = 25.25°	99.8 %	
Absorption correction	multi-scan / sadabs	
Max. and min. transmission	0.4854 and 0.4182	
Refinement method	Full-matrix least-squares on F ²	
Goodness-of-fit on F ²	1.076	
Final R indices [I > 2σ(I)]	R1 = 0.0444, wR2 = 0.1264	
R indices (all data)	R1 = 0.0591, wR2 = 0.1425	
Largest diff. peak and hole	1.665 and -3.579 e.Å ⁻³	

APPENDIX AB: CRYSTAL DATA FOR [Hg(SpymDippSe)₂][Hg₂I₆](C₃H₆O)₂

Empirical formula	C ₆₂ H ₉₄ I ₆ Hg ₃ N ₂ O ₂ S ₂
Formula weight	2446.49
Temperature	200(2) K
Wavelength	0.71073 Å
Crystal system, space group	Monoclinic, <i>P</i> ₂ ₁ / <i>c</i> (No. 14)
Unit cell dimensions	a = 10.9130(13) Å α = 90°. b = 16.941(2) Å β = 104.792(3)°. c = 21.304(3) Å γ = 90°.
Volume	3807.9(8) Å ³
Z, Calculated density	2, 2.134 Mg/m ³
Absorption coefficient	9.460 mm ⁻¹
Crystal size	0.21 x 0.20 x 0.18 mm ³
Crystal color / habit	colorless / block
Theta range for data collection	3.08 to 25.78°.
Reflections collected / unique	120318/ 7266 [R(int) = 0.0387]
Completeness to theta = 25.25°	99.8 %
Absorption correction	multi-scan / sadabs
Max. and min. transmission	0.2808 and 0.2413
Refinement method	Full-matrix least-squares on F ²
Goodness-of-fit on F ²	1.042
Final R indices [I > 2σ(I)]	R1 = 0.0318, wR2 = 0.0855
R indices (all data)	R1 = 0.0374, wR2 = 0.0906
Largest diff. peak and hole	1.100 and -3.331 e.Å ⁻³

APPENDIX AC: CRYSTAL DATA FOR (SpymXyS)CuI

Empirical formula	C ₂₀ H ₂₄ CuIN ₂ S	
Formula weight	514.91	
Temperature	200(2) K	
Wavelength	0.71073 Å	
Crystal system, space group	Monoclinic, C2/c (No. 15)	
Unit cell dimensions	a = 31.380(3) Å	α = 90°.
	b = 8.3520(9) Å	β = 99.560(4)°.
	c = 15.9174(16) Å	γ = 90°.
Volume	4113.8(7) Å ³	
Z, Calculated density	8, 1.663 Mg/m ³	
Absorption coefficient	2.669 mm ⁻¹	
Crystal size	0.20 x 0.18 x 0.10 mm ³	
Crystal color / habit	colorless / block	
Theta range for data collection	3.10 to 25.76°.	
Reflections collected / unique	47201/ 3919 [R(int) = 0.0354]	
Completeness to theta = 25.25°	99.7 %	
Absorption correction	multi-scan / sadabs	
Max. and min. transmission	0.7762 and 0.6173	
Refinement method	Full-matrix least-squares on F ²	
Goodness-of-fit on F ²	1.012	
Final R indices [I > 2σ(I)]	R1 = 0.0225, wR2 = 0.0610	
R indices (all data)	R1 = 0.0285, wR2 = 0.0659	
Largest diff. peak and hole	0.546 and -0.849 e.Å ⁻³	

APPENDIX AD: CRYSTAL DATA FOR (SpymMesS)CuI

Empirical formula	C ₂₂ H ₂₈ CuIN ₂ S	
Formula weight	542.96	
Temperature	200(2) K	
Wavelength	0.71073 Å	
Crystal system, space group	Triclinic, $P\bar{1}$ (No. 2)	
Unit cell dimensions	a = 7.5279(5) Å	$\alpha = 83.059(2)^\circ$.
	b = 8.1151(4) Å	$\beta = 87.267(3)^\circ$.
	c = 18.6993(12) Å	$\gamma = 81.177(2)^\circ$.
Volume	1120.05(12) Å ³	
Z, Calculated density	2, 1.610 Mg/m ³	
Absorption coefficient	2.456 mm ⁻¹	
Crystal size	0.20 x 0.19 x 0.18 mm ³	
Crystal color / habit	pale yellow / block	
Theta range for data collection	3.17 to 25.39°.	
Reflections collected / unique	29066/ 4102 [R(int) = 0.0369]	
Completeness to theta = 25.25°	99.8 %	
Absorption correction	multi-scan / sadabs	
Max. and min. transmission	0.6662 and 0.6394	
Refinement method	Full-matrix least-squares on F ²	
Goodness-of-fit on F ²	1.083	
Final R indices [I > 2sigma(I)]	R1 = 0.0360, wR2 = 0.0985	
R indices (all data)	R1 = 0.0441, wR2 = 0.1033	
Largest diff. peak and hole	0.509 and -0.741 e.Å ⁻³	

APPENDIX AE: CRYSTAL DATA FOR (SpymMesSe)CuI

Empirical formula	C ₂₂ H ₂₈ CuIN ₂ Se	
Formula weight	589.86	
Temperature	200(2) K	
Wavelength	0.71073 Å	
Crystal system, space group	Triclinic, $P\bar{1}$ (No. 2)	
Unit cell dimensions	a = 7.6197(9) Å	$\alpha = 82.685(4)^\circ$.
	b = 8.1190(9) Å	$\beta = 86.997(4)^\circ$.
	c = 18.703(2) Å	$\gamma = 81.270(4)^\circ$.
Volume	1133.7(2) Å ³	
Z, Calculated density	2, 1.728 Mg/m ³	
Absorption coefficient	3.939 mm ⁻¹	
Crystal size	0.22 x 0.18 x 0.10 mm ³	
Crystal color / habit	colorless / block	
Theta range for data collection	2.89 to 25.75°.	
Reflections collected / unique	39882/ 4321 [R(int) = 0.0599]	
Completeness to theta = 25.25°	99.7 %	
Absorption correction	multi-scan / sadabs	
Max. and min. transmission	0.6941 and 0.4778	
Refinement method	Full-matrix least-squares on F ²	
Goodness-of-fit on F ²	1.080	
Final R indices [I > 2sigma(I)]	R1 = 0.0256, wR2 = 0.0649	
R indices (all data)	R1 = 0.0287, wR2 = 0.0673	
Largest diff. peak and hole	0.396 and -0.894 e.Å ⁻³	

APPENDIX AF: CRYSTAL DATA FOR (SpymXyS)AuCl

Empirical formula	C ₂₀ H ₂₄ AuClN ₂ S	
Formula weight	556.89	
Temperature	200(2) K	
Wavelength	0.71073 Å	
Crystal system, space group	Monoclinic, <i>P</i> 2 ₁ / <i>n</i> (No. 11)	
Unit cell dimensions	a = 7.8960(9) Å	α = 90°.
	b = 11.9572(17) Å	β = 98.911(4)°.
	c = 20.930(3) Å	γ = 90°.
Volume	1952.2(4) Å ³	
Z, Calculated density	4, 1.895 Mg/m ³	
Absorption coefficient	7.785 mm ⁻¹	
Crystal size	0.25 x 0.08 x 0.05 mm ³	
Crystal color / habit	colorless / block	
Theta range for data collection	2.930 to 25.721°.	
Reflections collected / unique	57579/ 3715 [R(int) = 0.0346]	
Completeness to theta = 25.25°	99.9 %	
Absorption correction	multi-scan / sadabs	
Max. and min. transmission	0.6662 and 0.4778	
Refinement method	Full-matrix least-squares on F ²	
Goodness-of-fit on F ²	1.038	
Final R indices [I > 2σ(I)]	R1 = 0.0184, wR2 = 0.0398	
R indices (all data)	R1 = 0.0237, wR2 = 0.0439	
Largest diff. peak and hole	1.219 and -0.850 e.Å ⁻³	

APPENDIX AG: CRYSTAL DATA FOR (SpymXyS)AuBr

Empirical formula	C ₂₀ H ₂₄ AuBrN ₂ S	
Formula weight	601.35	
Temperature	200(2) K	
Wavelength	0.71073 Å	
Crystal system, space group	Monoclinic, <i>P</i> ₂ ₁ / <i>n</i> (No. 11)	
Unit cell dimensions	a = 7.9825(10) Å	α = 90°.
	b = 11.9961(14) Å	β = 99.173(4)°.
	c = 21.161(2) Å	γ = 90°.
Volume	2000.4(4) Å ³	
Z, Calculated density	4, 1.997 Mg/m ³	
Absorption coefficient	9.461 mm ⁻¹	
Crystal size	0.22 x 0.08 x 0.05 mm ³	
Crystal color / habit	colorless / block	
Theta range for data collection	2.904 to 25.712°.	
Reflections collected / unique	56569/ 3802 [R(int) = 0.0533]	
Completeness to theta = 25.25°	99.7 %	
Absorption correction	multi-scan / sadabs	
Max. and min. transmission	0.6941 and 0.6394	
Refinement method	Full-matrix least-squares on F ²	
Goodness-of-fit on F ²	1.057	
Final R indices [I > 2σ(I)]	R1 = 0.0292, wR2 = 0.0783	
R indices (all data)	R1 = 0.0337, wR2 = 0.0814	
Largest diff. peak and hole	1.309 and -1.043 e.Å ⁻³	

APPENDIX AH: CRYSTAL DATA FOR (SpymXySe)AuBr

Empirical formula	C ₂₀ H ₂₄ AuBrN ₂ Se	
Formula weight	648.25	
Temperature	200(2) K	
Wavelength	0.71073 Å	
Crystal system, space group	Monoclinic, <i>P</i> ₂ ₁ / <i>n</i> (No. 11)	
Unit cell dimensions	a = 8.0368(13) Å	α = 90°.
	b = 11.9414(19) Å	β = 99.228(5)°.
	c = 21.317(4) Å	γ = 90°.
Volume	2019.3(6) Å ³	
Z, Calculated density	4, 2.132 Mg/m ³	
Absorption coefficient	11.072 mm ⁻¹	
Crystal size	0.18 x 0.08 x 0.04 mm ³	
Crystal color / habit	colorless / block	
Theta range for data collection	3.08 to 25.45°.	
Reflections collected / unique	4196/ 4196 [R(int) = 0.0000]	
Completeness to theta = 25.25°	99.7 %	
Absorption correction	multi-scan / sadabs	
Max. and min. transmission	0.6657 and 0.2405	
Refinement method	Full-matrix least-squares on F ²	
Goodness-of-fit on F ²	1.035	
Final R indices [I > 2σ(I)]	R1 = 0.0475, wR2 = 0.1167	
R indices (all data)	R1 = 0.0709, wR2 = 0.1340	
Largest diff. peak and hole	0.894 and -1.143 e.Å ⁻³	

APPENDIX AI: CRYSTAL DATA FOR (SpymMesS)AuCl

Empirical formula	C ₂₂ H ₂₈ AuClN ₂ S	
Formula weight	584.94	
Temperature	200(2) K	
Wavelength	0.71073 Å	
Crystal system, space group	Triclinic, $P\bar{1}$ (No. 2)	
Unit cell dimensions	a = 7.3726(8) Å	$\alpha = 83.110(5)^\circ$.
	b = 7.9904(10) Å	$\beta = 87.014(4)^\circ$.
	c = 18.946(3) Å	$\gamma = 80.492(4)^\circ$.
Volume	1092.2(2) Å ³	
Z, Calculated density	2, 1.779 Mg/m ³	
Absorption coefficient	6.962 mm ⁻¹	
Crystal size	0.21 x 0.15 x 0.09 mm ³	
Crystal color / habit	colorless / block	
Theta range for data collection	3.19 to 25.39°.	
Reflections collected / unique	32608/ 3983 [R(int) = 0.0422]	
Completeness to theta = 25.25°	99.7 %	
Absorption correction	multi-scan / sadabs	
Max. and min. transmission	0.5730 and 0.3226	
Refinement method	Full-matrix least-squares on F ²	
Goodness-of-fit on F ²	1.002	
Final R indices [I > 2sigma(I)]	R1 = 0.0163, wR2 = 0.0392	
R indices (all data)	R1 = 0.0185, wR2 = 0.0402	
Largest diff. peak and hole	0.481 and -0.418 e.Å ⁻³	

APPENDIX AJ: CRYSTAL DATA FOR (SpymMesS)AuBr

Empirical formula	C ₂₂ H ₂₈ AuBrN ₂ S	
Formula weight	629.40	
Temperature	200(2) K	
Wavelength	0.71073 Å	
Crystal system, space group	Triclinic, $P\bar{1}$ (No. 2)	
Unit cell dimensions	a = 7.4387(12) Å	$\alpha = 83.034(5)^\circ$.
	b = 8.0411(13) Å	$\beta = 87.058(6)^\circ$.
	c = 18.873(3) Å	$\gamma = 80.649(6)^\circ$.
Volume	1105.1(3) Å ³	
Z, Calculated density	2, 1.891 Mg/m ³	
Absorption coefficient	8.568 mm ⁻¹	
Crystal size	0.25 x 0.06 x 0.05 mm ³	
Crystal color / habit	colorless / block	
Theta range for data collection	3.18 to 25.41°.	
Reflections collected / unique	32218/ 4036 [R(int) = 0.0364]	
Completeness to theta = 25.25°	99.8 %	
Absorption correction	multi-scan / sadabs	
Max. and min. transmission	0.6740 and 0.2232	
Refinement method	Full-matrix least-squares on F ²	
Goodness-of-fit on F ²	1.008	
Final R indices [I > 2sigma(I)]	R1 = 0.0208, wR2 = 0.0527	
R indices (all data)	R1 = 0.0235, wR2 = 0.0542	
Largest diff. peak and hole	1.685 and -0.791 e.Å ⁻³	

APPENDIX AK: CRYSTAL DATA FOR (SpymMesSe)AuCl

Empirical formula	C ₂₂ H ₂₈ AuClN ₂ Se	
Formula weight	631.84	
Temperature	200(2) K	
Wavelength	0.71073 Å	
Crystal system, space group	Triclinic, $P\bar{1}$ (No. 2)	
Unit cell dimensions	a = 7.4622(9) Å	$\alpha = 83.013(4)^\circ$.
	b = 7.9933(9) Å	$\beta = 86.810(5)^\circ$.
	c = 18.934(3) Å	$\gamma = 80.197(5)^\circ$.
Volume	1103.9(2) Å ³	
Z, Calculated density	2, 1.901 Mg/m ³	
Absorption coefficient	8.442 mm ⁻¹	
Crystal size	0.35 x 0.06 x 0.04 mm ³	
Crystal color / habit	colorless / block	
Theta range for data collection	2.93 to 25.39°.	
Reflections collected / unique	35014/ 4037 [R(int) = 0.0374]	
Completeness to theta = 25.25°	99.8 %	
Absorption correction	multi-scan / sadabs	
Max. and min. transmission	0.7288 and 0.1561	
Refinement method	Full-matrix least-squares on F ²	
Goodness-of-fit on F ²	1.030	
Final R indices [I > 2sigma(I)]	R1 = 0.0175, wR2 = 0.0406	
R indices (all data)	R1 = 0.0206, wR2 = 0.0423	
Largest diff. peak and hole	0.639 and -0.656 e.Å ⁻³	

APPENDIX AL: CRYSTAL DATA FOR (SpymMesSe)AuBr

Empirical formula	C ₂₂ H ₂₈ AuBrN ₂ Se	
Formula weight	676.30	
Temperature	200(2) K	
Wavelength	0.71073 Å	
Crystal system, space group	Triclinic, $P\bar{1}$ (No. 2)	
Unit cell dimensions	a = 7.5296(10) Å	$\alpha = 82.995(5)^\circ$.
	b = 8.0537(10) Å	$\beta = 86.755(5)^\circ$.
	c = 18.884(3) Å	$\gamma = 80.489(4)^\circ$.
Volume	1120.2(3) Å ³	
Z, Calculated density	2, 2.005 Mg/m ³	
Absorption coefficient	9.984 mm ⁻¹	
Crystal size	0.20 x 0.18 x 0.15 mm ³	
Crystal color / habit	colorless / block	
Theta range for data collection	3.18 to 25.41°.	
Reflections collected / unique	27738/ 4096 [R(int) = 0.0316]	
Completeness to theta = 25.25°	99.6 %	
Absorption correction	multi-scan / sadabs	
Max. and min. transmission	0.3159 and 0.2401	
Refinement method	Full-matrix least-squares on F ²	
Goodness-of-fit on F ²	1.087	
Final R indices [I > 2sigma(I)]	R1 = 0.0314, wR2 = 0.0945	
R indices (all data)	R1 = 0.0340, wR2 = 0.0963	
Largest diff. peak and hole	0.893 and -1.718 e.Å ⁻³	

APPENDIX AM: CRYSTAL DATA FOR (SpymDippS)AuCl(C₃H₆O)₂

Empirical formula	C ₆₂ H ₉₂ Au ₂ Cl ₂ N ₄ O ₂ S ₂	
Formula weight	1454.42	
Temperature	200(0) K	
Wavelength	0.71073 Å	
Crystal system, space group	Triclinic, $P\bar{1}$ (No. 2)	
Unit cell dimensions	a = 11.4650(7) Å	$\alpha = 104.894(3)^\circ$.
	b = 12.5640(9) Å	$\beta = 96.050(3)^\circ$.
	c = 12.7930(9) Å	$\gamma = 99.674(2)^\circ$.
Volume	1734.1(2) Å ³	
Z, Calculated density	1, 1.393 Mg/m ³	
Absorption coefficient	4.402 mm ⁻¹	
Crystal size	0.20 × 0.19 × 0.18 mm ³	
Crystal color / habit	colorless / block	
Theta range for data collection	5.8 to 25.4°.	
Reflections collected / unique	48833/ 6362 [R(int) = 0.0301]	
Completeness to theta = 25.25°	99.6 %	
Absorption correction	multi-scan / sadabs	
Max. and min. transmission	0.3159 and 0.2401	
Refinement method	Full-matrix least-squares on F ²	
Goodness-of-fit on F ²	1.072	
Final R indices [I > 2σ(I)]	R1 = 0.0292, wR2 = 0.0733	
R indices (all data)	R1 = 0.0332, wR2 = 0.0788	
Largest diff. peak and hole	2.24 and -1.68 e.Å ⁻³	

APPENDIX AN: CRYSTAL DATA FOR (SpymDippS)AuBr(C₃H₆O)

Empirical formula	C ₃₁ H ₄₆ AuBrN ₂ OS	
Formula weight	771.63	
Temperature	200(2) K	
Wavelength	0.71073 Å	
Crystal system, space group	Monoclinic, <i>P</i> 2 ₁ (No. 4)	
Unit cell dimensions	a = 10.7945(12) Å	α = 90°.
	b = 14.6666(19) Å	β = 99.904(4)°.
	c = 20.751(3) Å	γ = 90°.
Volume	3236.2(7) Å ³	
Z, Calculated density	4, 1.584 Mg/m ³	
Absorption coefficient	5.870 mm ⁻¹	
Crystal size	0.18 x 0.10 x 0.07 mm ³	
Crystal color / habit	colorless / block	
Theta range for data collection	2.99 to 25.82°.	
Reflections collected / unique	89596/ 11953 [R(int) = 0.0439]	
Completeness to theta = 25.25°	99.8 %	
Absorption correction	multi-scan / sadabs	
Max. and min. transmission	0.6841 and 0.4180	
Refinement method	Full-matrix least-squares on F ²	
Goodness-of-fit on F ²	1.070	
Final R indices [I > 2σ(I)]	R1 = 0.0187, wR2 = 0.0391	
R indices (all data)	R1 = 0.0220, wR2 = 0.0408	
Largest diff. peak and hole	0.481 and -0.714 e.Å ⁻³	

APPENDIX AO: CRYSTAL DATA FOR (SpymDippSe)AuCl

Empirical formula	C ₂₈ H ₄₀ AuClN ₂ Se	
Formula weight	716.00	
Temperature	200(0) K	
Wavelength	0.71073 Å	
Crystal system, space group	Orthorhombic, <i>Pna</i> 2 ₁ (No. 33)	
Unit cell dimensions	a = 18.7981(16) Å	α = 90°.
	b = 12.4559(9) Å	β = 90°.
	c = 12.4528(11) Å	γ = 90°.
Volume	2915.8(4) Å ³	
Z, Calculated density	4, 1.631 Mg/m ³	
Absorption coefficient	6.403 mm ⁻¹	
Crystal size	0.25 x 0.20 x 0.03 mm ³	
Crystal color / habit	colorless / block	
Theta range for data collection	3.17 to 25.37°.	
Reflections collected / unique	59846/ 5328 [R(int) = 0.0654]	
Completeness to theta = 25.25°	99.8 %	
Absorption correction	multi-scan / sadabs	
Max. and min. transmission	0.8311 and 0.2974	
Refinement method	Full-matrix least-squares on F ²	
Goodness-of-fit on F ²	1.028	
Final R indices [I > 2σ(I)]	R1 = 0.0241, wR2 = 0.0593	
R indices (all data)	R1 = 0.0310, wR2 = 0.0635	
Largest diff. peak and hole	0.677 and -0.600 e.Å ⁻³	

APPENDIX AP: CRYSTAL DATA FOR (SpymDippSe)AuBr

Empirical formula	$C_{56}H_{80}Au_2Br_2N_4Se_2$	
Formula weight	1520.91	
Temperature	200(0) K	
Wavelength	0.71073 Å	
Crystal system, space group	Monoclinic, $P2_1/c$ (No. 14)	
Unit cell dimensions	$a = 15.888(3)$ Å	$\alpha = 90^\circ$.
	$b = 12.124(2)$ Å	$\beta = 114.206(5)^\circ$.
	$c = 16.954(3)$ Å	$\gamma = 90^\circ$.
Volume	$2978.8(9)$ Å ³	
Z, Calculated density	2, 1.696 Mg/m ³	
Absorption coefficient	7.519 mm ⁻¹	
Crystal size	0.22 x 0.20 x 0.15 mm ³	
Crystal color / habit	colorless / block	
Theta range for data collection	2.81 to 25.74°.	
Reflections collected / unique	98321/ 5686 [R(int) = 0.0450]	
Completeness to theta = 25.25°	99.9 %	
Absorption correction	multi-scan / sadabs	
Max. and min. transmission	0.8311 and 0.2974	
Refinement method	Full-matrix least-squares on F ²	
Goodness-of-fit on F ²	1.000	
Final R indices [I>2sigma(I)]	R1 = 0.0315, wR2 = 0.0920	
R indices (all data)	R1 = 0.0463, wR2 = 0.1109	
Largest diff. peak and hole	1.347 and -1.778 e.Å ⁻³	